ONTOGENESIS OF CORNEAL SURFACE ULTRASTRUCTURE IN NOCTURNAL LEPIDOPTERA

By G. GEMNE
Department of Physiology, Karolinska Institutet, S-104 01 Stockholm

(*Communicated by Sir Bernard Katz, Sec.R.S.—Received 27 November* 1970—*Revised* 12 *February* 1971)

[Plates 36 to 53]

CONTENTS

The morphogenesis of epicorneal structures in nocturnal Lepidoptera was studied with light and electron microscopy. During the first 4–5 days after pupation, microvilli (with their tips hexagonally distributed) arose gradually from the corneagenous cell surface. At the time of onset of moulting (about 5 days after pupation), patches of lamellar elements appeared distal to the tips of the microvilli. There was one patch for each microvillus from which the patch was separated by a narrow cleft. The cleft was traversed by a few thin bridges which seemed to originate in the microvillus. The bridges were interpreted to be extracellular continuations of intramicrovillar filaments and to insert on the proximal surface of the patch.

At about 5½ days after pupation, the patches were seen to be composed of two outer electron-dense lines and a less distinct, inner and thicker dense line. The patches bulged markedly, their concavity turned towards the microvillar tip. A number of discrete bridges extended between the microvillus and

Vol. 262. B. 843. (Price £2.00; U.S. $5.20) 26 [Published 20 August 1971

the base of the patch, which now appeared as a low dome. The bases of the domes later coalesced to form a continuous lamellar 'membrane' system (*epicorneal lamina*, ECL), and the concavity of the domes increased, forming successively deeper lamina evaginations (LE) which strictly retained their spatial relationship to the tips of the microvilli (MV) throughout the ontogenesis.

Growth of the ECL evaginations to form an array of successively higher cupoles—and, finally, the complete nipple anlage—was suggested to take place by addition of new material at all points of the LE surface within the palisade of MV/LE bridges. The latter were proposed to act as structures of constraint preventing the ECL to buckle randomly and causing the evaginations to develop in a regular fashion.

The results were compared with those described in reports on the morphogenesis of the body cuticle of insects. It was proposed that different types of corneal surface protuberances (corneal nipples of various heights; low protrusions in regular or irregular arrangement) as well as some types of surface sculpturing in the body cuticle of insects may be produced on the basis of the same mechanism as the one described for the formation of the full-sized nipples of nocturnal Lepidoptera.

Introduction

The corneal surface of some nocturnal Lepidoptera was found by Bernhard & Miller (1962) to carry an orderly array of protuberances ('corneal nipples') which in their highest ('full-sized') form (figure 2, plate 36) have an amplitude of about 250 nm. They are hexagonally distributed over the entire facet surface with a centre-to-centre distance between their bases of approximately 200 nm (figures 3, 4, plates 36, 37). In model microwave experiments, spectrophotometric measurements, and mathematical calculations it was shown (Bernhard, Miller & Møller 1963, 1965; Miller, Møller & Bernhard 1966) that the array of full-sized nipples functions as an impedance transformer, equalizing by gradual transition the refractive index of air to that of the cornea. By this action, the reflexion of light from the cornea is decreased; the concomitant increase in light transmission into the eye operates over a broad range of wavelengths. Since the height of the nipples is smaller than the wavelengths of visible light, the nipple array does not interfere with the image-forming capacity of the eye.

Nipples and other types of corneal surface protuberances occur in a wide variety of heights, irregularly or regularly arranged, as shown in a survey of the insect class with respect to corneal surface topography (Bernhard, Gemne & Sällström 1970). The fact that a simple, regular pattern of the corneal surface is common to many insect groups—especially in the most advanced orders—raised the question about the morphogenesis of the corneal surface in insects with different types of corneal protuberances. Together with preliminary studies (Gemne 1966*a*, *b*), this paper presents the results of an investigation into the development of the corneal ultrastructure of the compound eye. The material may be compared with the formation

---

Description of plate 36

Figure 2. Electron micrograph of a perpendicular section through the cornea of the compound eye of an adult *Deilephila elpenor*, showing 'full-sized nipples' with an average height of about 225 nm (range among the nipples shown, 200 to 250 nm). The distance between the tips can only be estimated (about 220 nm) since the nipples were deformed by the sectioning. Their baselines cannot be determined with any certainty, and therefore also the average amplitude value given is very approximate. Furthermore, the nipples may partially melt in the electron beam. In this particular case, however, such an effect may have been prevented since the nipples were selected from a row located in a fold of the section. (This picture should be compared with figure 33, plate 50, which shows a more reliable image of the shape and arrangement of the nipple array.) × 78500.

Figure 3. Electron micrograph of a freeze-etching replica of the compound eye of a 13-day-old pupa of *Philosamia cynthia ricini*. The fracture has passed obliquely through the cornea. The picture shows a small part of one ommatidium with the array of nipples (top) on the thin developing cornea. Most of the corneagenous cell microvilli (MV) are seen in cross-section. Their interspacing averages about 190 nm. A small area of the cytoplasm of one crystalline cone cell is seen at bottom left. (ER, endoplasmic reticulum.) The direction of platinum evaporation is from 5 to 11 o'clock. × 25700.

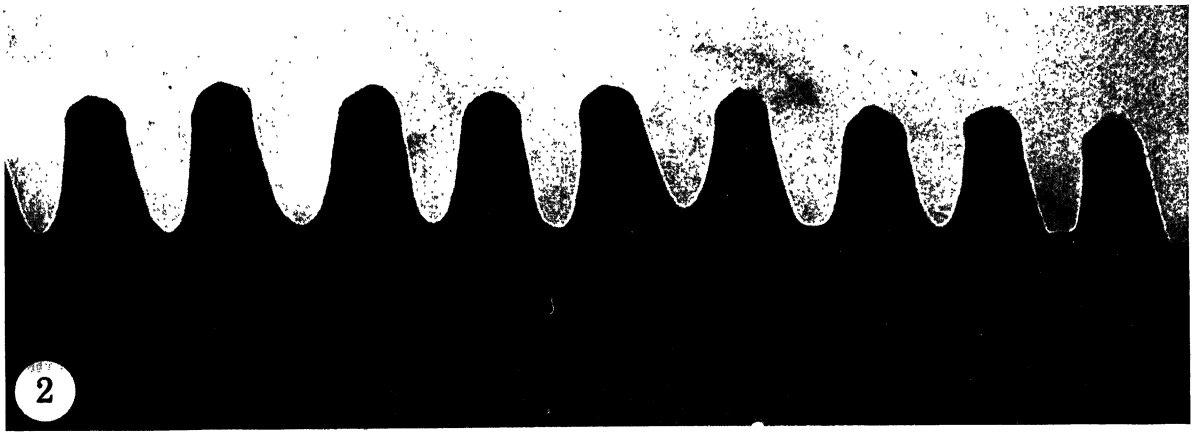

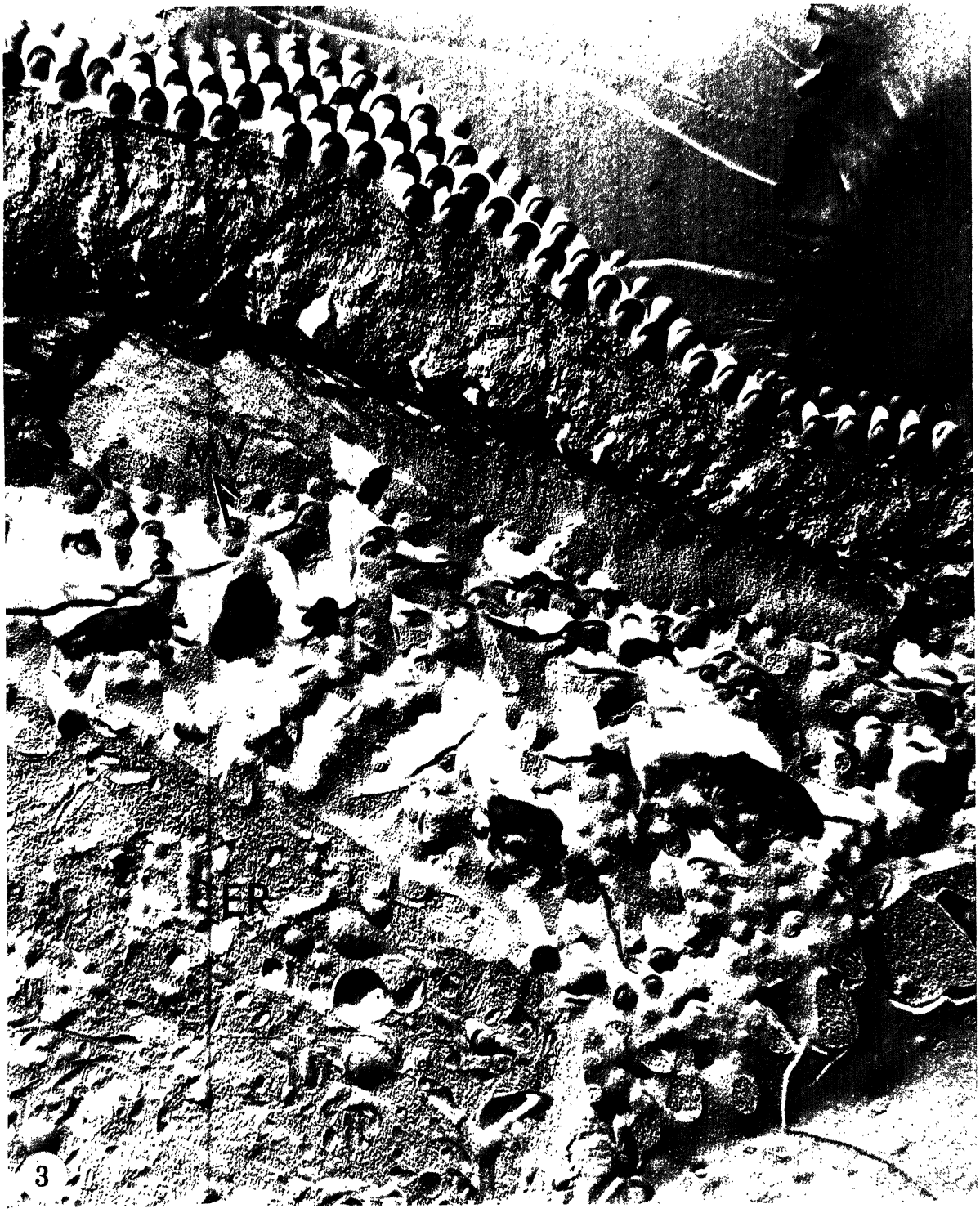

FIGURES 2 and 3. For legends see facing page

(*Facing p.* 344)

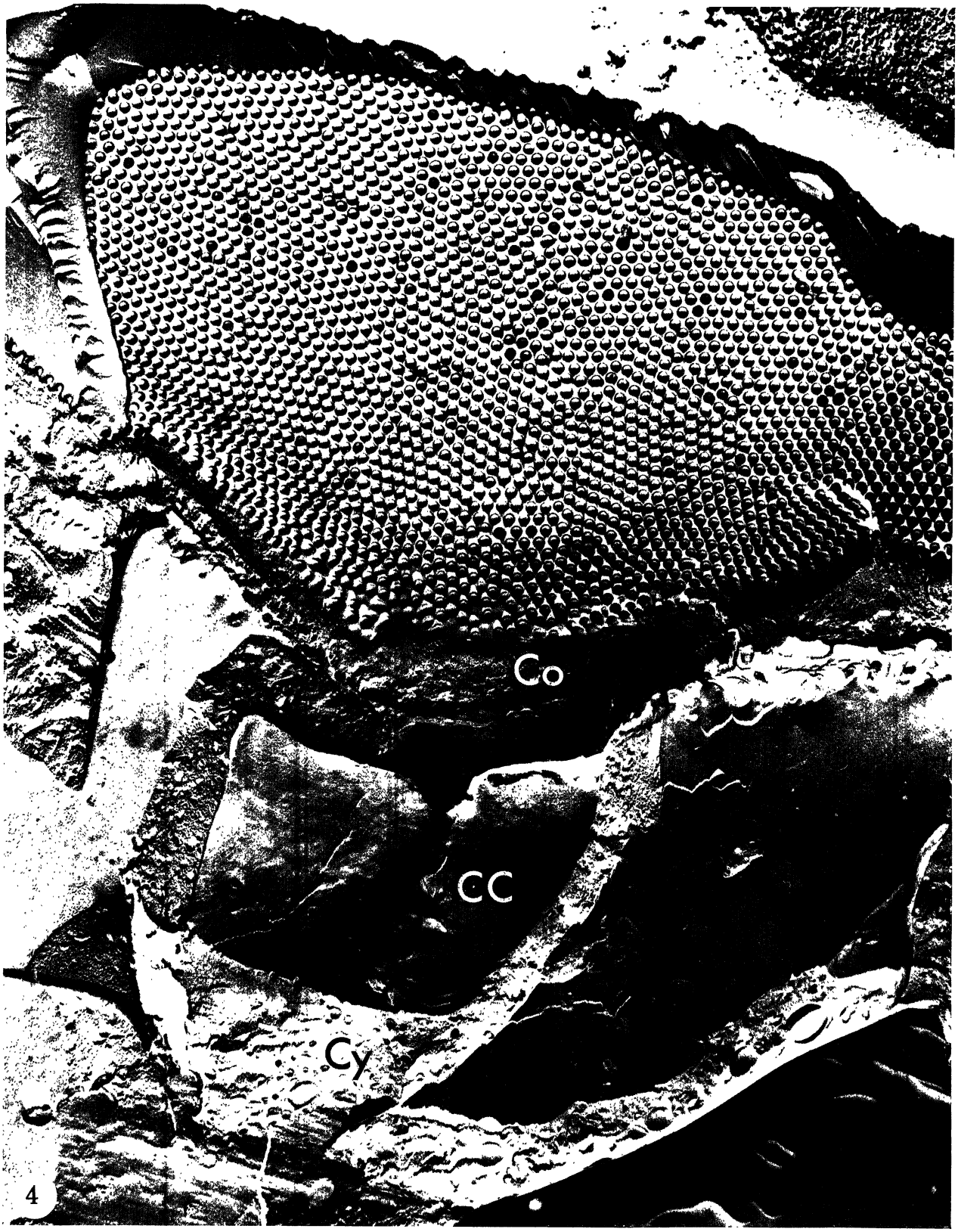

FIGURE 4. Electron micrograph of the same freeze-etching replica as in figure 3. The fracture has passed tangential to part of the corneal surface. The nipple array has been exposed and is seen in a bird's-eye view. The distance between the nipple tips averages about 195 nm. There are about 40 nipples per μm^2, giving a total of about 30000 on one facet, the diameter of which is about 30 μm. The arrangement of the nipples is only roughly hexagonal, the imperfections being due to the fact that the cornea is convex. (CC, crystalline cone; Co, cornea; Cy, cytoplasm of crystalline cone cell.) The direction of platinum evaporation is from 5 to 11 o'clock. × 13400.

of the fine structure of the body epicuticle studied by several authors (Locke 1966, 1967, 1969; Rinterknecht & Levi 1966; Filshie & Waterhouse 1969; Noirot & Noirot-Timothée 1969; Delachambre 1970).

In the preliminary work (Gemne 1966*a*, *b*), on *Deilephila elpenor* (Lepidoptera: Sphingidae), it was shown that an extracellular lamina forms distal to the corneagenous cell microvilli at an early stage of the pharate adult and evaginates above the tip of each microvillus. In its final form—which was shown to be completed before the onset of deposition of the material of the cornea proper—the evaginated lamina constitutes the nipple array anlage. The substance of the corneal lamellae, secreted from the surface cells of the eye epidermis, pushes up the nipple anlage so that in the adult moth it composes the most external layer of the corneal surface. Perry (1968), investigating the development of bristles and ommatidia in *Drosophila* eyes, reported observations on the corneal formation which confirmed the results on *Deilephila*. The present investigation extends the initial work, now including other nocturnal Lepidoptera as well. Attention has been focused on the interaction between membranes and other substances involved in the epicorneal morphogenesis. A discussion of the work on corneal topography, including phylogenetic and functional aspects, in relation to epicorneal morphogenesis has been published elsewhere (Gemne 1970).

Material

Pupae of *Manduca sexta* (*Protoparce sexta* Johanns.), the tobacco hornworm moth (Sphingidae), were investigated. Control observations were also made on four other Lepidoptera, viz. *Celerio euphorbiae*, the spurge hawk moth (Sphingidae); *Deilephila elpenor*, the elephant hawk moth (Sphingidae); *Philosamia cynthia ricini*, the Eri silk moth (Saturnidae); and *Sphinx ligustri*, the privet hawk moth (Sphingidae).

The pupae were obtained from the United States Department of Agriculture Tobacco Research Station in Oxford, North Carolina (*Manduca*) or from Great Britain (*Celerio*, *Deilephila*, *Philosamia* and *Sphinx*). All pupae were reared in heating cabinets at a temperature of 25 to 28 °C and a relative air humidity of about 80 %. In one case (*Philosamia*), the starting material was larvae of different ages. The larvae were reared in plastic trays at room temperature (20 to 24 °C) on lilac leaves that were renewed each day. After coccoon spinning and pupation, the pupae were transferred to the rearing cabinets.

Dissection, fixation and embedding of *Manduca* pupae for the purpose of identifying successive stages of development was performed in Stockholm and at the Oxford Tobacco Research Station, making use of the station's facilities for continuous rearing under well-controlled conditions (Hoffman, Lawson & Yamamoto 1966; Baumhover 1968). Stocks of diapausing *Manduca* pupae from larvae fed on tobacco plants were subsequently shipped to Stockholm. There they were reared in the laboratory for preparation at well-timed intervals. All diapausing pupae (making up most of the material) were stored at about 12 °C and 50 to 70 % relative air humidity. *Manduca* pupae from larvae reared on an artificial diet containing tobacco leaf extract were obtained from the Oxford Tobacco Research Station for use in this study. *Manduca* specimens reared on tobacco leaves at the United States Department of Agriculture, Entomological Research Station, Beltsville, Maryland, and at the Department of Entomology, University of Kentucky, Lexington, U.S.A. were also used in the investigation.

The selection of the material was influenced by such factors as the size of the pupa and the eye, the hardness of the pupal cuticle, the availability of a large number of specimens, and rearing

conditions. As mentioned above, the bulk of the material of the present work consists of *Manduca* pupae, which proved to be advantageous in many respects, especially in rearing properties and viability. The description in this article applies to the whole of the material studied. No significant differences (at light or electron microscopic levels) were found in the ontogenetic characteristics in the other species as compared to those in *Manduca*.

Methods

Techniques

The specimens were most commonly prefixed in a 5 % solution of phosphate-buffered glutaraldehyde (pH about 7.2), purified by shaking with active charcoal. The fixation time was usually 4 h at room temperature. After rinsing for several hours in phosphate buffer, postfixation was carried out in 1 % or 2 % s-collidine- or phosphate-buffered OsO_4 for 0.5 to 2 h at 0 to 4 °C. (For buffer osmolality, see below.)

A mixture of 5 % phosphate-buffered glutaraldehyde and 1 % thiotepa, a mustard gas derivative (Tifosyl®, Astra Co., Södertälje, Sweden) was tested as a prefixative. For reasons of availability, thiotepa was chosen as a substitute for tris(1-aziridinyl)phosphine oxide, which was used by Williams & Luft (1968) with the argument that this substance would assist in the cross-linking, stabilizing and fixing effect of the glutaraldehyde. Tifosyl® is very similar to tris(1-aziridinyl)phosphine oxide, with sulphur substituted for oxygen. The use of thiotepa gave no superior results as regards the ultrastructure of the present material. The only significant difference observed in comparison to material prefixed in glutaraldehyde alone was an enhanced 'density' of the cytoplasmic matrix and, possibly, a better preservation of some thin filaments.

The addition of 10 mM $CaCl_2$ to the osmium tetroxide (Palade & Bruns 1968) in some cases enabled membranes to be better visualized.

Epon 812, Araldite (Durcupan®, Fluka AG, Switzerland) and Vestopal W were used as embedding media. Vestopal consistently gave superior results. The Vestopal embedding procedure was that of Ryter & Kellenberger (1958), or with equally good results the rapid method of Estes & Apicella (1969). Thin sectioning was performed with an LKB Ultrotome I, using glass knives.

Thin sections of Vestopal-embedded specimens were stained in a saturated, aqueous solution of uranyl acetate at 50 °C, followed by lead citrate (Reynolds 1963), each for about 10 s.

Description of plate 38

Figure 5. Light micrographs showing the main characteristics of early developmental stages of the optic imaginal disk of Lepidoptera pupae.

A, *Manduca sexta*, including the anterior, sharply demarcated zone of transition to the extraocular region (Eo). In this area, the eye anlage epidermis consists of an approximately 50 μm thick epithelium with indications of ommatidial cell grouping (each group about 20 μm in width). This is the typical picure of the eye anlage in the diapausing pupa as well as from pupation and up to about 4 days (stage P0). The nuclei of the crystalline cone cells (Cn) can be recognized. Nerve fibre bundles (N) can be seen below the basal lamina that separates the epidermis from the haemocoel (Hc). Phase contrast. Toluidine-blue. × 740.

B, *C*, *Philosamia cynthia ricini*. *B*, stage P1. In the interior parts of the eye anlage, the ommatidial cell grouping is more conspicuous than in the preceding stage, whereas the transition zone (included in figure 6*A*) shows stage P0 features. The epithelium is about 65 μm thick. In *C* (stage P1 to II), the crystalline cone substance is clearly seen as discrete clumps (Cs). The nerve bundles (consisting of 8 or 9 axons and their investing cells) which pass through the basal lamina are approximately 4 μm in diameter. (R, retinular cells.) Phase contrast. Toluidine-blue. *B*, × 800; *C*, × 1120.

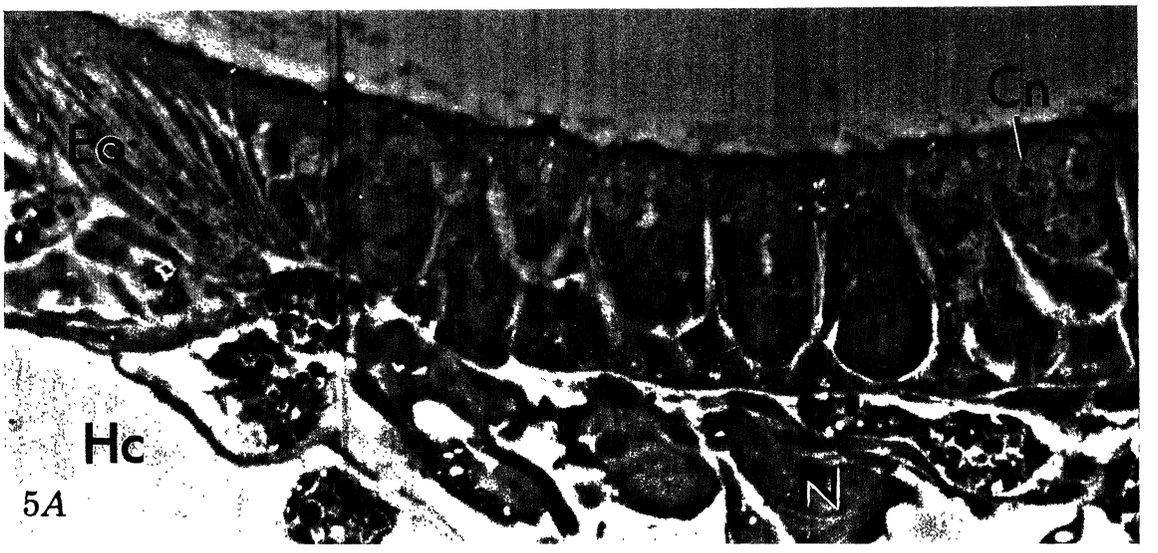

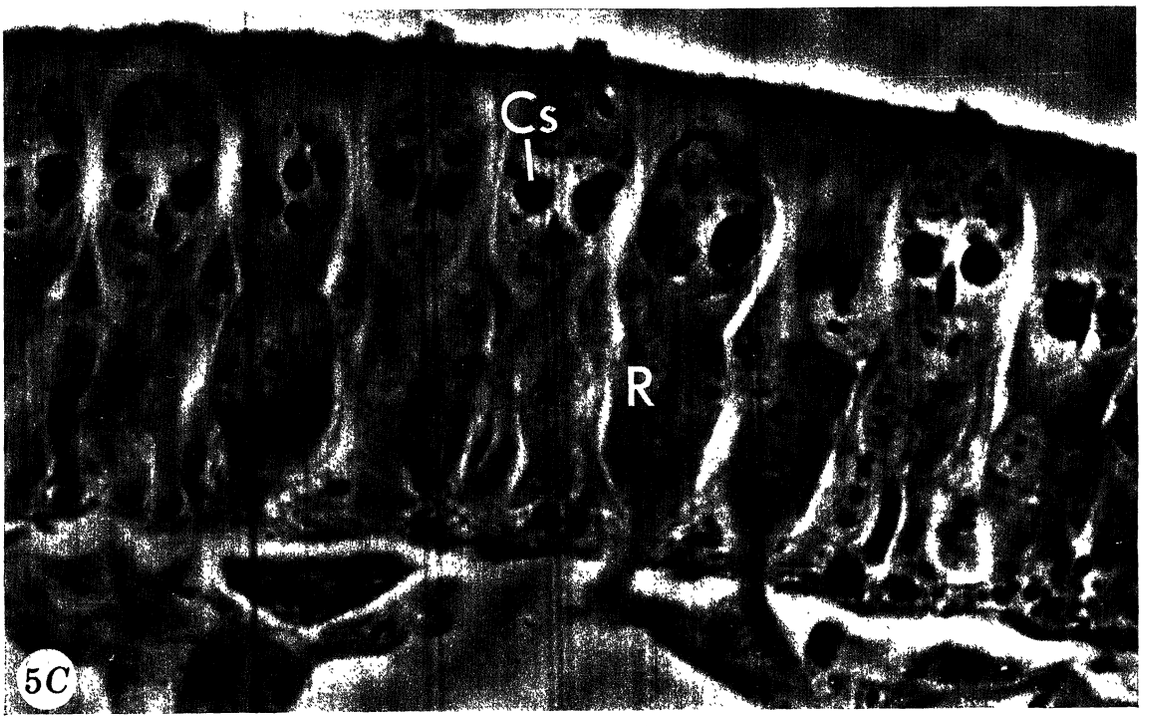

FIGURE 5. For legend see facing page

(*Facing p.* 346)

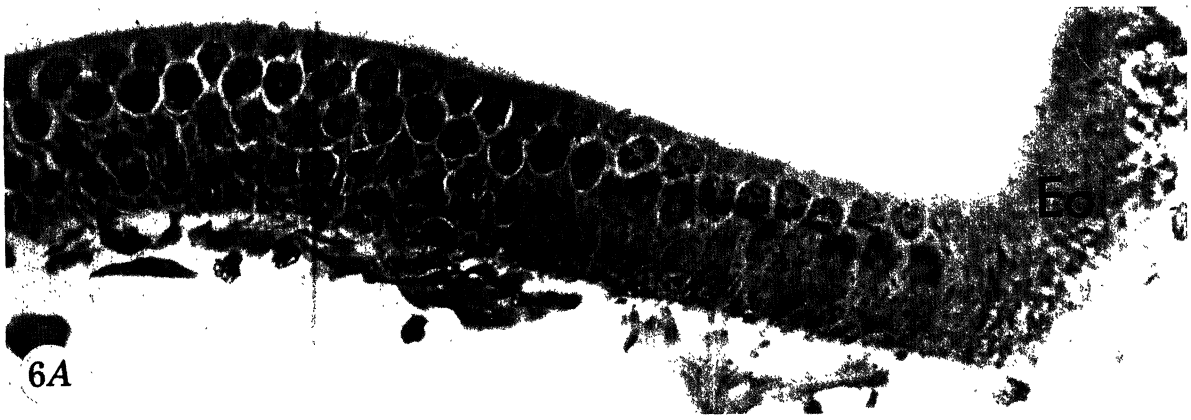

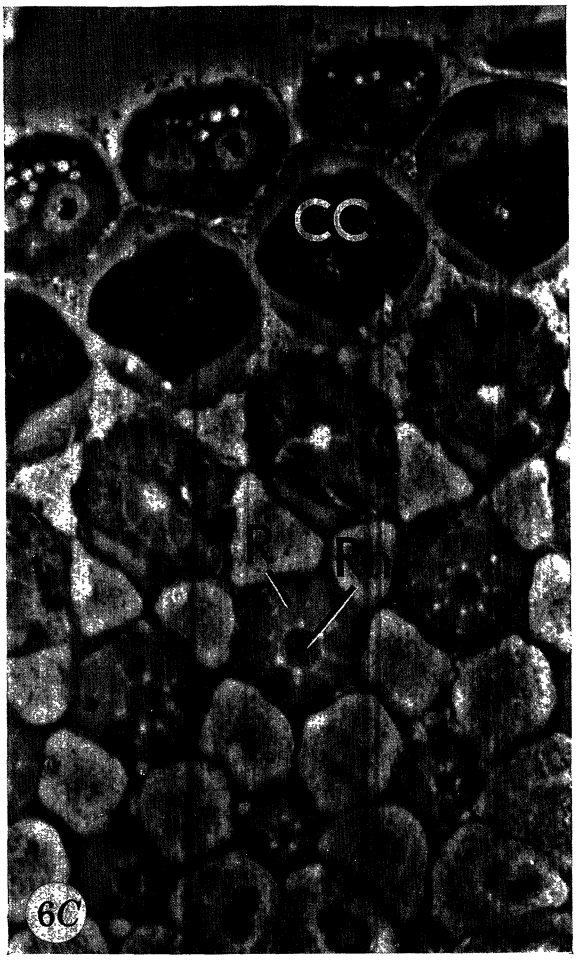

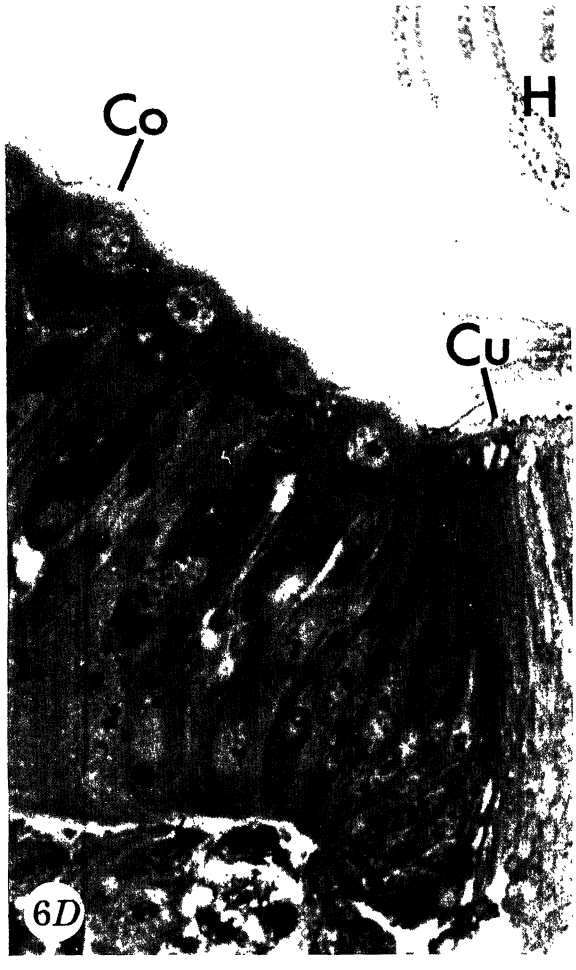

FIGURE 6. For legend see facing page

For Epon and Araldite sections, a saturated uranyl acetate solution in methanol/ethanol (Locke 1966) or a methanol solution of uranyl acetate (Stempak & Ward 1964) sometimes had to be used. These two methods produced an undesired coarseness which was further accentuated by the phase image granularity associated with defocusing (Haydon 1968).

Replicas were obtained of specimens fixed in 5 % phosphate-buffered glutaraldehyde, treated with a 20 % glycerol solution for 1 to 12 h, rapidly frozen in Freon 22 and liquid nitrogen and fractured in a plane orientated obliquely or perpendicularly to the surface of the eye anlage. A Balzers BA 360M freeze-etching apparatus was used and the technique employed was essentially that of Moor & Mühlethaler (1963).

Light microscopy of 0.5 to 1 μm thick sections stained in a 1 % toluidine-blue solution in 1 % borax was used for observation and orientation of the specimens prior to electron microscopy. The sections were examined and photographed in a Zeiss Photomikroskop using phase or interference contrast (Nomarski) techniques.

Thin sections and freeze-etching replicas were examined with a Zeiss EM 9A electron microscope equipped with the accessories allowing magnification to 60000 times. Electron micrographs were made on Agfa-Gevaert Scientia 23D56 film, fine-grain developed in Refinal.

Osmolalities of pupal haemolymph and buffer solutions

In preliminary experiments, a number of different NaCl concentrations in the buffer solution were used to test the possible effect of variations in osmolality on the general appearance of the eye anlage and the preservation of its ultrastructure. The osmolalities of pupal haemolymph and of different phosphate buffer solutions were therefore determined; the methods used were those of freezing-point depression and vapour pressure. The results are given in table 1A, B and in the diagram of figure 1.

As can be seen from table 1A, the osmolality values of non-diapausing *Manduca* pupae tended to be lower than those of diapausing pupae. In non-diapausing pupae, the lowest value was 270 mosmol; the highest, 301 mosmol. The lowest value for the osmolality of haemolymph of pupae still in diapause was about 281 mosmol, while the highest was 368 mosmol. The total mean for non-diapausing pupae was 285 mosmol; that of diapausing pupae, 326 mosmol.

Description of plate 39

Figure 6. Light micrographs showing the main characteristics of different developmental stages of the optic imaginal disk of Lepidoptera pupae.

A, *Philosamia cynthia ricini* (stage PI to II). Oblique section including the zone of transition to the extraocular region (Eo). The transition zone has the characteristics of stage P0, whereas the interior parts have reached a somewhat more advanced stage of development (stage PI). Phase contrast. Toluidine-blue. × 315.

B, *Manduca sexta* (stage PII). Perpendicular section including the anterior zone of transition to the extraocular region. There is a difference in degree of differentiation between the ommatidia close to the zone of transition and those of the more interior parts of the eye anlage, where the crystalline cone substance has formed one rounded body in each ommatidium. The epithelium is about 75 μm thick. (H, head hairs; CC, crystalline cone.) Phase contrast. Toluidine-blue. × 240.

C, *Manduca sexta* (stage PIII). Oblique section showing the eye surface and the corneagenous cells (top left), the crystalline cones (CC), and the retinular cell rosettes (R) with the developing rhabdom (Rh). Phase contrast. Toluidine-blue × 800.

D, *Manduca sexta* (stage PIV). Perpendicular section including the sharply demarcated zone of transition to the extraocular body cuticle (Cu). The thin cornea (Co) is seen as a strongly refractile line at the rim of the ommatidium, which is about 30 μm wide. A cluster of undifferentiated ommatidial cells is seen in the deeper portion of the epithelium adjacent to the extraocular region (bottom right). Phase contrast. Toluidine-blue. × 915.

The lower osmolality of non-diapausing pupae is consistent with the relative increase in water content of haemolymph in the pharate adult (Fyhn & Saether 1970).

The phosphate concentrations of all buffers tested were those given by Karlsson & Schultz (1965), viz. 12.32 g of anhydrous Na_2HPO_4, and 1.57 g of anhydrous NaH_2PO_4 in 1000 ml of distilled water. (This formula originates from Dr G. Millonig; cf. Karlsson & Schultz 1965, footnote to page 164.)

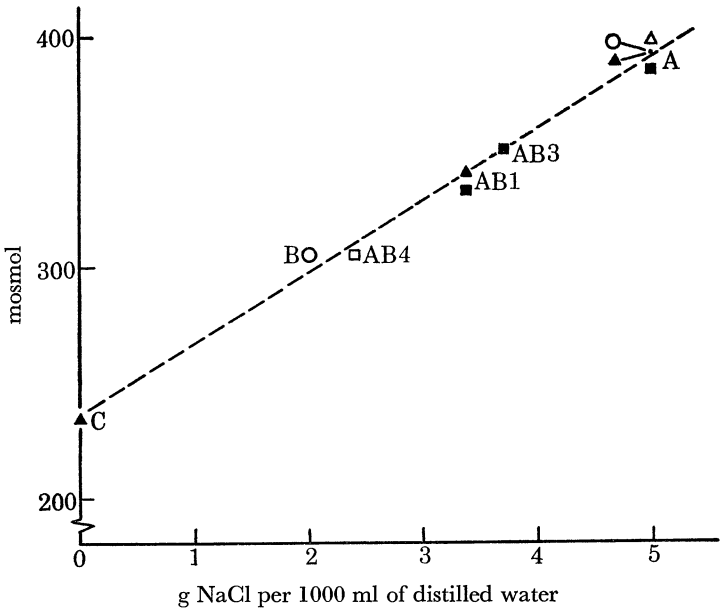

FIGURE 1. Osmolality of phosphate buffers with various concentrations of NaCl (average values). Symbols: △, vapour pressure osmometer ('VPI'); ▲, vapour pressure osmometer ('VPII'); □, freezing-point depression osmometer ('FI'); ■, freezing-point depression osmometer ('FII'); ○, determination of freezing-point depression according to Beckmann ('FIII').

The osmolality values obtained for the 'basic' buffer with the above-mentioned composition (here called 'Millonig C') and those of buffers, where various amounts of NaCl had been added, are given in table 1B. The osmolality values have been plotted against the NaCl concentrations (see the diagram in figure 1). The broken line has been drawn arbitrarily in order to illustrate the possible relation between the two parameters.

The effects of lower NaCl concentration (buffers with osmolality about 300 mosmol, i.e. close to isotonicity with the pupa haemolymph) were inconsistent. No improvement over the

DESCRIPTION OF PLATE 40

FIGURE 7. Light micrograph of a perpendicular section through the *Manduca* eye anlage at stage PIII to IV, showing the groups of ommatidial cells. Vacuoles, nuclei, and other organelles are seen distal to the heart-shaped crystalline cones. The groups of retinular cells with conspicuous nuclei are seen to be in contact with the proximal end of the cones. Bundles of retinular cell axons pass through the basal lamina joining other bundles in the hemocoel. Phase interference contrast (Nomarski). × 1220.

FIGURE 8. Electron micrograph of a perpendicular section through the optic imaginal disk of a diapausing *Deilephila elpenor* pupa. Below the inner layer of the pupal endocuticle (PC), in contact with the epidermis, the plasma membrane of the distal surface of two epidermal (corneagenous) cells (CoC) is indentated to form blunt, irregular processes (Pr). × 47500.

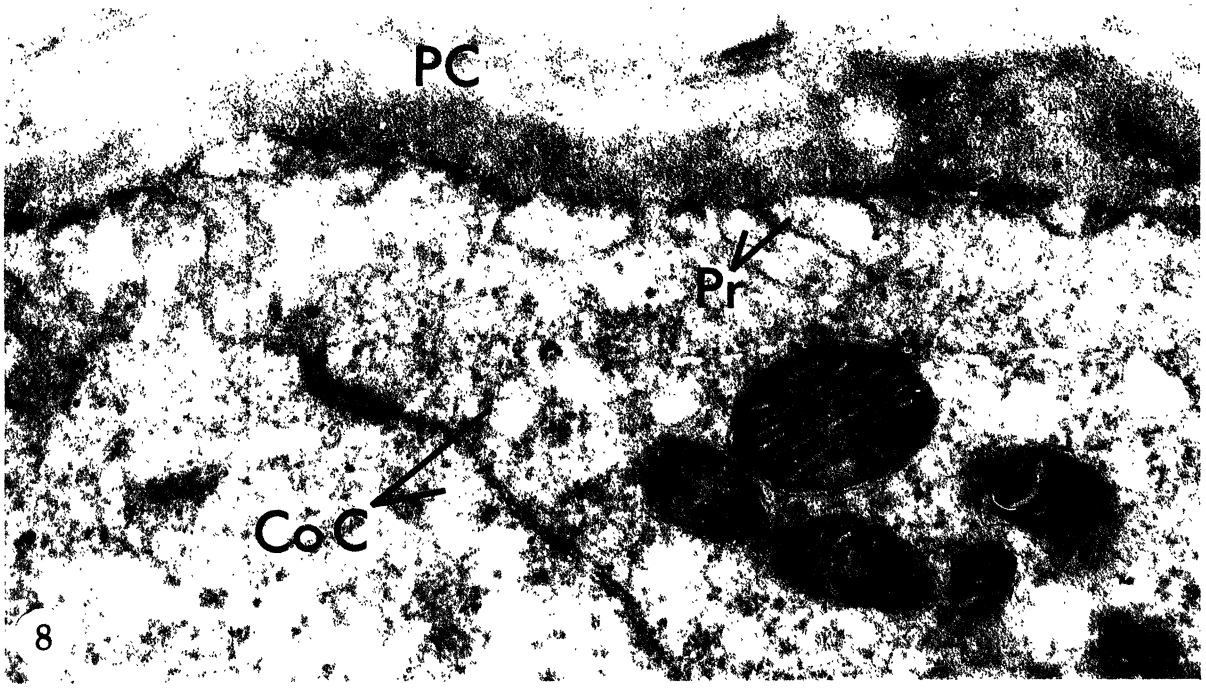

FIGURES 7 and 8. For legends see facing page

(*Facing p.* 348)

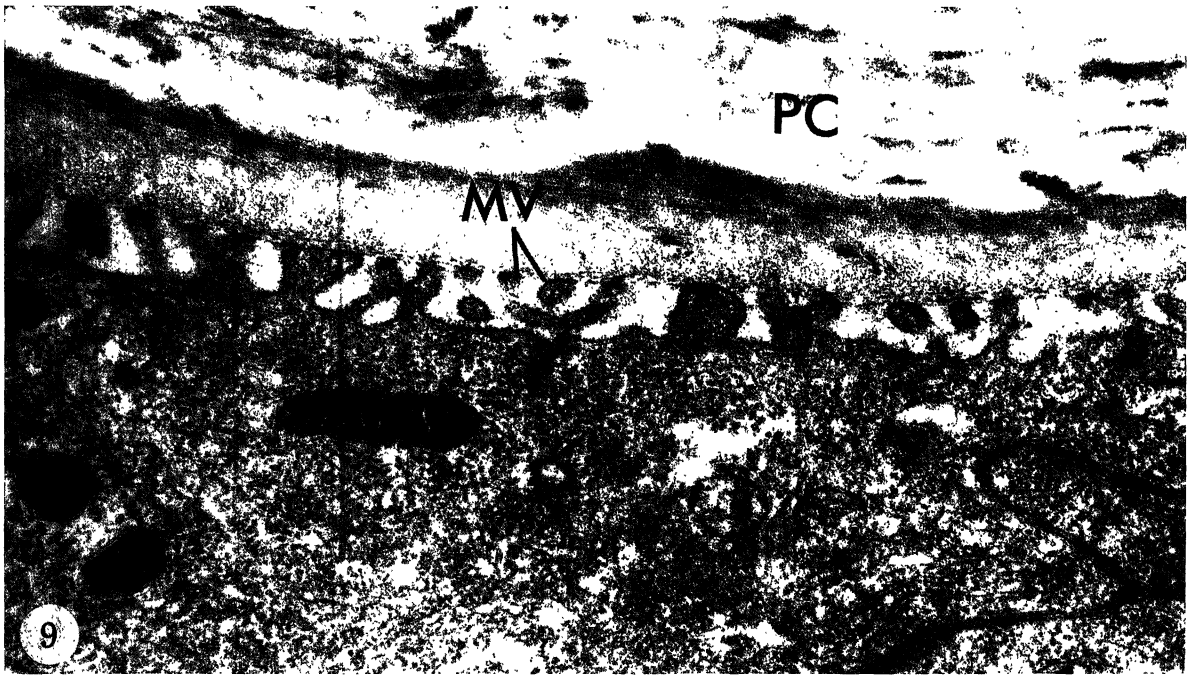

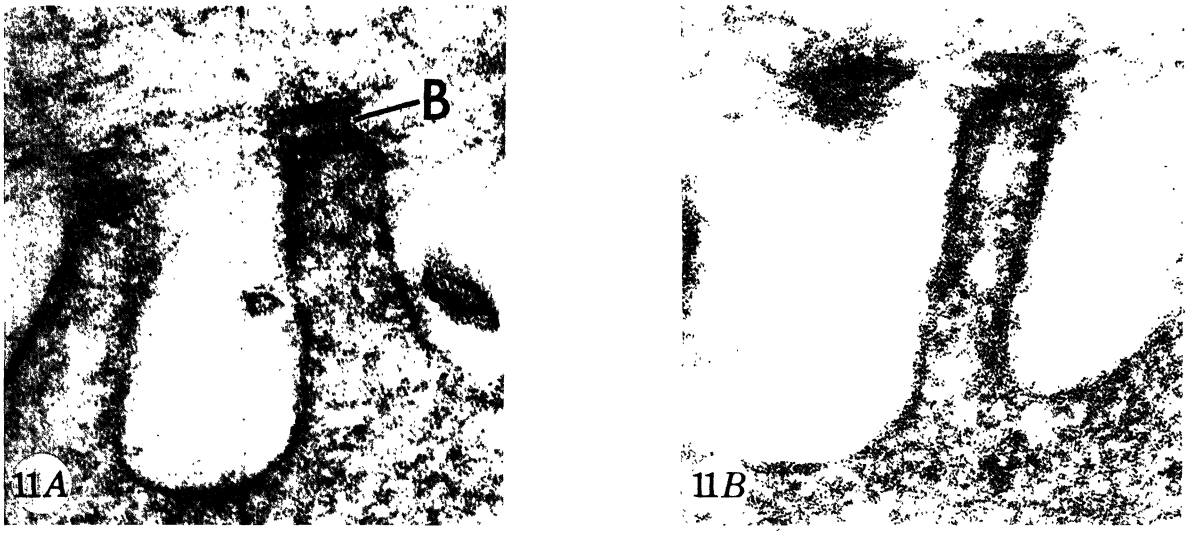

FIGURES 9 to 11. For legends see facing page

TABLE 1A. OSMOLALITY OF HAEMOLYMPH OF NON-DIAPAUSING AND DIAPAUSING PUPAE OF *MANDUCA SEXTA* (MOSMOL)

determination no.	range	mean	comments	method
			non-diapausing pupae	
1	290 to 301	293	haemolymph pooled from 8 pupae, stage PIII, 4 valid values (measurements within same pool)	FII
	270 to 284	278	individual determinations of 11 pupae, stage PIII, 8 valid values	FI
total mean for non-diapausing pupae: 285 mosmol				
			diapausing pupae	
1	298 to 318	305	haemolymph pooled from 8 pupae, 6 valid values (measurements within same pool)	FII
2	350 to 358	354	individual determinations of 5 pupae, 3 valid values	VPI
3	288 to 350	317	individual determinations of 9 pupae, 6 valid values	FI
		(300)	corrected value (osmometer calibrated about 5% too high)	
4	281 to 326	304	individual determinations of 11 pupae, 10 valid values	FIV
5	325 to 365	340	3 samples of pooled haemolymph (5 to 8 specimens for each pool), 3 valid values	FIV
6	347 to 368	354	3 samples of pooled haemolymph (5 to 6 specimens for each pool), 3 valid values	VPI
total mean for diapausing pupae: 326 mosmol				

Abbreviations: F = freezing-point depression; VP = vapour pressure; FIV = Fiske Co. freezing-point depression osmometer (for designations 'I to III', see note to figure 1)

DESCRIPTION OF PLATE 41

FIGURE 9. Electron micrograph of a perpendicular section through the eye anlage of a *Deilephila* pupa shortly after diapause had been broken. The blunt processes of the corneagenous cell have assumed the shape of very short microvilli (MV) with their tips in an approximately regular spacing of about 190 nm. This is the typical electron microscopic picture of the eye epidermis just before the onset of moulting (end of stage P0). × 32400.

FIGURE 10. Electron micrograph of a perpendicular section through the optic imaginal disk of a *Manduca sexta* pupa at stage PI, i.e. at about 5 days after pupation. The microvilli are about 200 nm long and about 90 nm in diameter. Their tips (with a regular centre-to-centre distance of 150 to 160 nm) are interconnected by thin strands (St), which in sections tangential to the epidermis can be seen to form a loose, irregular network of thin filaments. Short 'patches' (P) are present just distal to the microvillar tips. (MF, moulting fluid.) × 51400.

FIGURE 11. Electron micrographs of a perpendicular section through the eye anlage of *Manduca sexta* pupa at stage PI (5 to 5½ days after pupation). The patches forming the initial phase of the epicorneal lamina (see text) are separated from the microvillar tips by a cleft 10 to 15 nm wide. The patches consist of two electron-dense lines, each about 5 nm thick with a clear separating space approximately 2 nm in width. In *A*, a bridge (B) about 6 nm thick, is seen to connect the microvillus with the patch. The triple-layered plasma membrane of the microvillus is approximately 8 nm thick. *A*, × 171000; *B*, × 167000.

fixation in glutaraldehyde in the 'Millonig A' buffer was observed with respect to preservation of ultrastructural details. The description of the results in the present article is based upon fixations using the somewhat hypertonic buffer of about 395 mosmol.

It may be noted from table 1B that the value of 440 mosmol stated by Karlsson & Schultz for the buffer containing 5.0 g of NaCl per 1000 ml of buffer solution—here termed 'Millonig A'—could not be confirmed. The average osmolality for this buffer was found to be 395 mosmol.

TABLE 1B. COMPOSITION OF PHOSPHATE BUFFERS

(Basic composition, 'Millonig C': anhydrous Na_2HPO_4, 12·32 g; anhydrous NaH_2PO_4, 1·57 g; distilled water, 1000 ml.)

	NaCl contents (g/1000 ml buffer)	average osmolality mosmol	no. of determinations	method
Millonig C	0	237	2	VPI
Millonig B	2·04	306	3	FIII
Millonig AB 4	2·42	306	4	FII
Millonig AB 1	3·36	335	2	FII
		340	2	VPI
Millonig AB 3	3·65	352	2	FI
Millonig A	5·0	384	2	FII
		390	3	FIII
		390	2	VPI
		395	2	VPII

RESULTS

Terminology

A definition will be made here of some descriptive terms and of some abbreviations used in the text. The more precise meaning of the terms will be made clear in the Results. The choice of the terms is also commented upon in the Discussion.

The epicorneal lamina (*ECL*). The term being proposed here is an extracellular lamellar system probably deposited by secretion from the microvilli (MV) on the surface of the epidermal cells of the optic imaginal disk immediately underlying the pupal endocuticle. The epicorneal lamina is demonstrable to be a continuation into the ocular region of the outermost layer of the body epicuticle ('cuticulin layer'; Locke 1966). It should be mentioned here that, for purposes of convenience, Locke's term 'cuticulin layer' has been used in the present article, although there

DESCRIPTION OF PLATE 42

FIGURE 12. Electron micrograph of a perpendicular section through the optic imaginal disk of a stage PI (about 5-day-old) *Manduca* pupa. Two microvilli are shown projecting from the surface of the corneagenous cell, the cytoplasm of which contains a 'coated vesicle' (CV). ECL patches (about 100 nm wide) are seen distal to the microvillar tips from which they are separated by a cleft 7 to 9 nm wide. In the lower MV/LE complex, the cleft is traversed by a bridge approximately 7 nm thick. × 130000.

FIGURE 13. Survey electron micrograph of an oblique section through the eye anlage of a *Manduca sexta* pupa approximately 5½ days after pupation (stage PI). The section has passed through the crystalline cone cells, three of which are shown. The developing crystalline cone occurs as small clumps of a very electron-dense substance (Cs). The rim of the corneagenous cell (right) shows an array of cross-sectioned microvilli and associated patches. (Nu, nucleus of crystalline cone cell.) × 8500.

FIGURE 14. Electron micrograph of a section through the eye anlage of a stage PI *Manduca* pupa, similar to the section of figure 13. The ECL patches are seen to be located on top of the microvillar tips. The distance between the centres of the latter is regular, averaging about 150 nm. The origins of the microvilli on the surface of the corneagenous cell (CoC) are considerably less regularly distributed. × 48200.

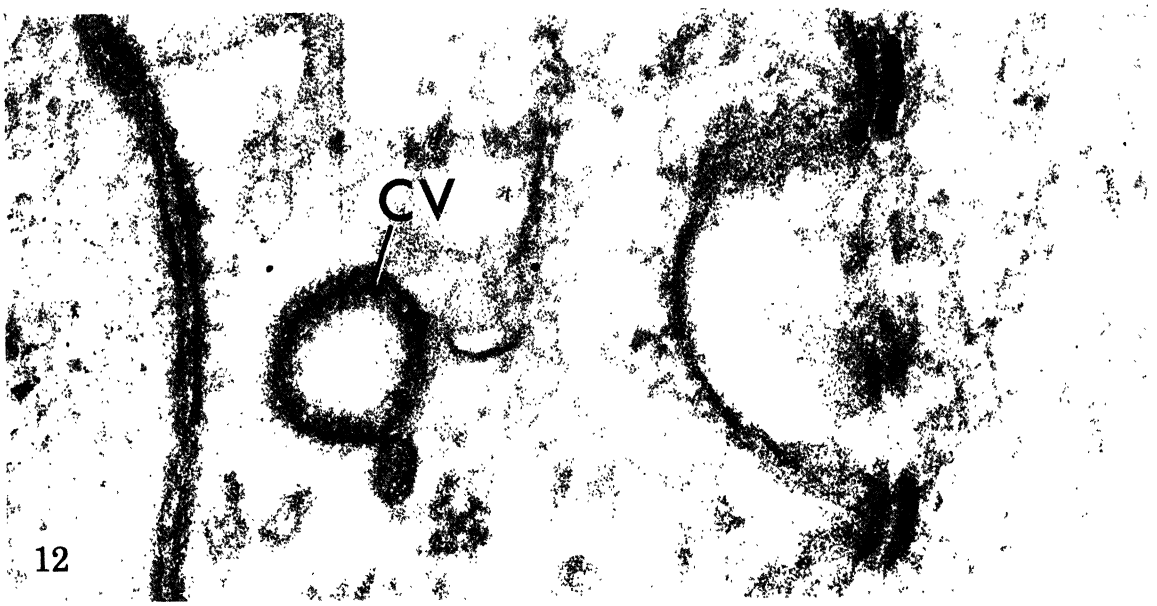

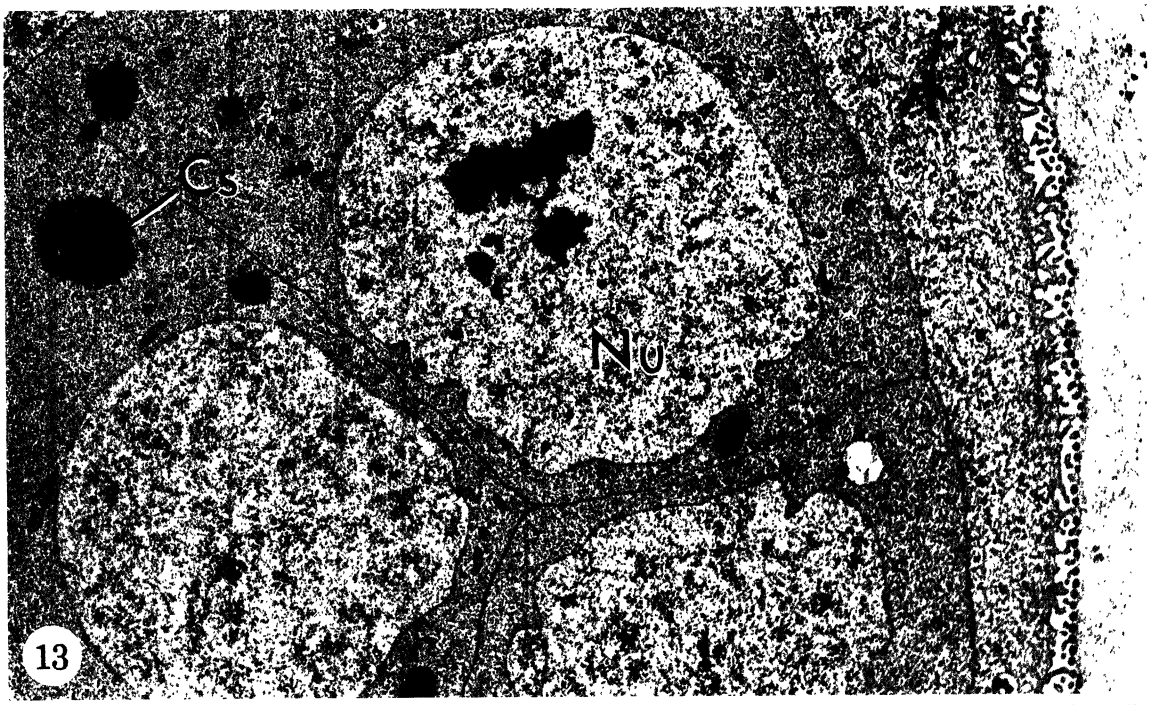

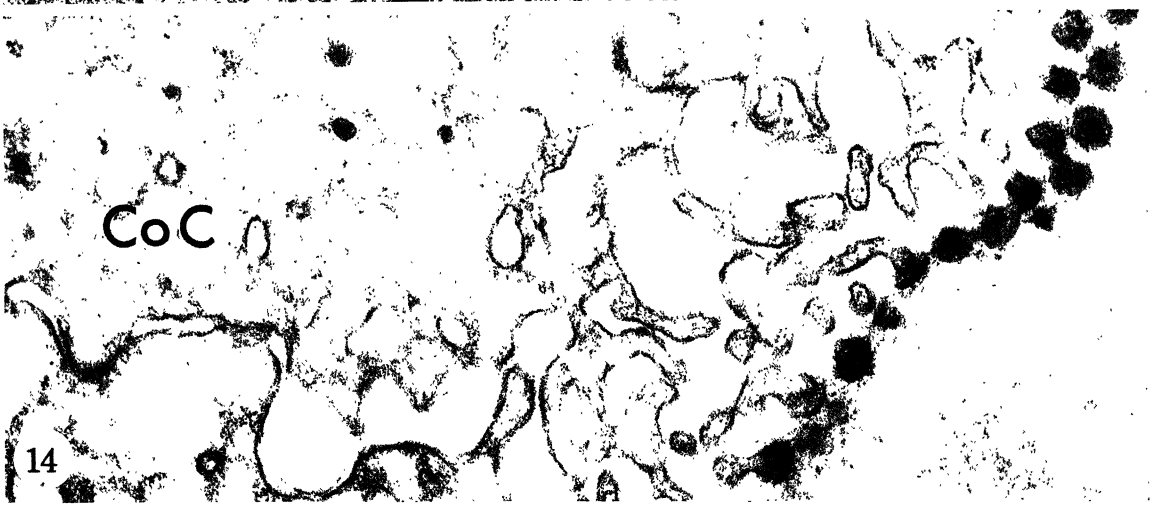

FIGURES 12 to 14. For legends see facing page

(*Facing p.* 350)

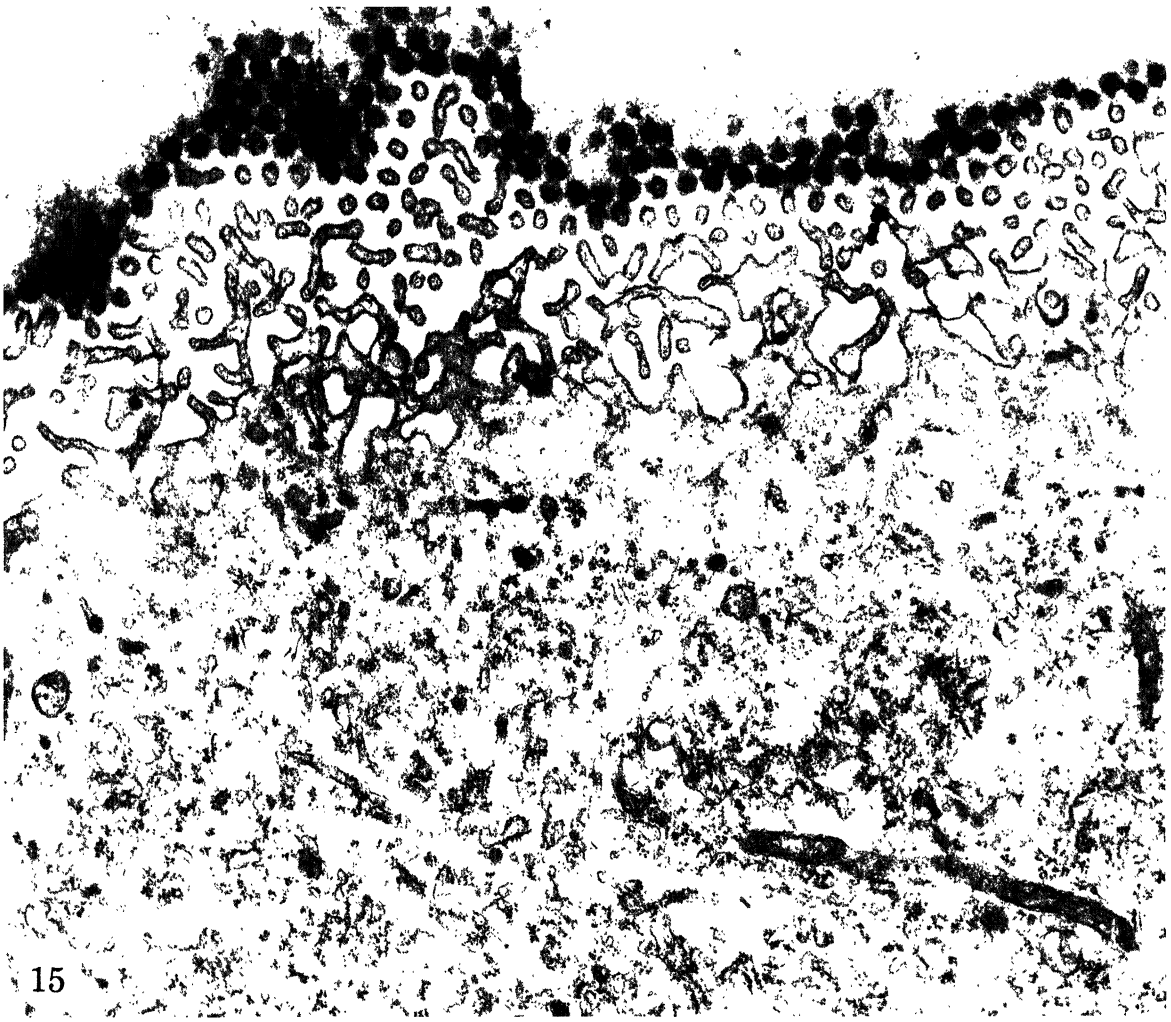

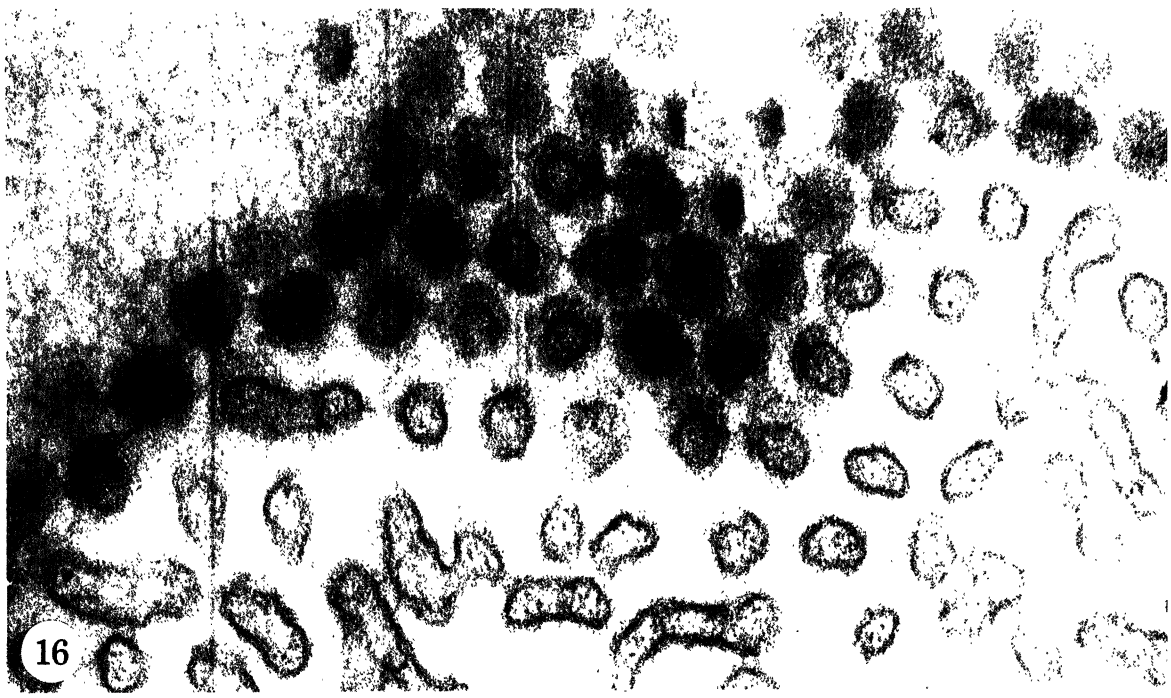

FIGURE 15. Electron micrograph of a section through the eye anlage of a *Manduca sexta* pupa similar to the sections of figures 13, 14, showing the hexagonal array of the epicorneal membrane patches. × 26400.

FIGURE 16. Higher magnification of the top left area of the section in figure 15, showing the relations of the microvillar tips to the ECL patches and the diffuse substance connecting the individual MV/LE complexes. The cross-sectioned microvilli are approximately 30 nm in diameter and contain a number of thin filaments. × 82000.

seems to be some reason for a re-evaluation of its appropriateness, as shown in a recent work by Weis-Fogh (1970).

The corneal nipple anlage is the final form of the epicorneal lamina in the stage terminated by the onset of secretion of the corneal material.

Lamina evaginations (*LE*) arise in those parts of the ECL which are located immediately distal to the tips of the microvilli of the cornea-secreting (corneagenous) cells.

TABLE 2. DESIGNATIONS AND CHARACTERISTICS OF DEVELOPMENTAL STAGES OF THE OPTIC IMAGINAL DISK OF *MANDUCA SEXTA* PUPAE. COMPARISON WITH PHASES IN BODY CUTICLE FORMATION†

approximate age of pupae (days after pupation)	developmental stages: phases in body cuticle formation	optic imaginal disk	epicorneal lamina	figures
0 to about 4	secretion of ecdysial droplets, moulting fluid, and ecdysial membrane	P0	LE0	5*A*, 8, 9, 38*A*, 41, 42
———	beginning of moulting; epidermis separating from pupal endocuticle	———	———	———
5 to 5½	onset of deposition of cuticulin; onset of digestion of pupal endocuticle by enzymes in moulting fluid secreted by epidermal cells; digestion products taken up and lysed in epidermal cells	PI onset of ommatidial differentiation	LEI appearance of MV/LE complex (patches, domes)	5*B*, *C*, 6*A*, 10, 11 to 18, 38*B* to *D*
5½ to 6		PII	LEII low cupoles; continuous epicorneal lamina	19, 20, 23 to 27, 38*E* to *G*
6½ to 7		PIII	LEIII final epicorneal lamina evaginations (nipple anlage), high cupoles	6*B* to *D*, 7, 28, 29, 38*H* to *K*, 39, 40
7½ to about 8	onset of deposition of protein epicuticle (non-lamellate cuticle)	PIV	LEIV unconsolidated nipples (nipple anlage)	7, 30, 34
8	stabilization of non-lamellate cuticle	PV	N final, consolidated nipples	31 to 33, 34, 38*L* to *N*

† Data from Roeder (1953), Wigglesworth (1965), Locke (1966, 1967, 1969, 1970).

MV/LE complex. In the interest of word economy, the term MV/LE complex will be used in the following description to denote the set of structures including the tip of a microvillus, the epicorneal lamina patch, dome or cupole that overlies the MV tip, and the connexions (to be described) that cross the space between the MV and the LE.

Macroscopic and light microscopic observations

A schematic representation of the gross and fine morphological characteristics of the principal developmental stages is given in figure 38, plate 52. The descriptive terms and abbreviations employed in what follows are defined in table 2. In order to facilitate the temporal correlation of the eye developmental stages with those of the rest of the pupa, the main events in *body cuticle* formation occurring during moulting are also listed in table 2.

Gross description of the developmental stages of the optic imaginal disk

Stage P0. The structure of the epidermis of the eye anlage was roughly the same throughout the stage P 0, beginning at pupation. The eye anlage consisted of a very thin epithelial layer which

adhered firmly to the inner layer of the pupal cuticle. Toward the end of the stage the epithelium detached from the cuticle when the eye anlage region was flooded with fixative from a syringe. In those latter cases, the epidermis could be seen as a flimsy, bulging, completely transparent tent without any well-defined surface texture recognizable with the dissection microscope.

Very early in this stage, a grouping of the epidermal cells could be seen in light microscopic sections (figure 5*A*, plate 38). The epithelium was about 40 μm thick nearest to the extraocular region and about 60 μm in the more central parts of the eye anlage. The bulging of the individual facets was barely recognizable.

During the whole of stage P0, the brain was connected to the eye epidermis by a few long strands of tissue. In sections for electron microscopy, the strands were seen to be nerve bundles composed of groups of eight to nine axons which contained microtubules and mitochondria. These groups were surrounded by glial cells. No ultrastructural signs of decomposition were found which would allow an interpretation of the nerve fibres as degenerating axons of the photoreceptor cells of the last larval instar ocelli. Instead, their apparent normality, and the fact that they originate at a site in the eye anlage epidermis where the future retinular cells will be located, make it likely that the nerves have grown out from the optic imaginal disk of the pupa already at this early stage of development. This is in accordance with a statement of Yagi & Koyama (1963) for other Lepidoptera, made on the basis of a light microscopic investigation, and with the observations of Perry (1968) in *Drosophila*. It is also possible, however, that the axons of degenerated larval photoreceptor cells have been maintained intact by a trophic influence from the glial cells in a manner similar to the effect of glia on severed axons in crustaceans (Hoy, Bittner & Kennedy 1967).

Stage PI. In pupae examined 5 to 5½ days after pupation (PI), there was a complete separation of the eye epidermis from the pupa cuticle. Thus, PI is the first of the pharate (Hinton 1946) adult insect. Several small aggregates of material of the future crystalline cones, heavily stainable in toluidine-blue, were seen in the clearly recognizable cell groups of each developing ommatidium. With the dissection microscope, a hexagonal pattern corresponding to the array of facets was seen on the surface of the transparent tent of the eye anlage.

Stage PII. At 5½ to 6 days (PII), the light-yellow, now less transparent tent of the eye anlage had grown in size and facets were conspicuous. The tracheolar tree had the adult appearance.

Description of plate 44

Figure 17. Electron micrographs of perpendicular sections through the eye anlage of *Manduca sexta* pupae at stage PI, showing the epicorneal lamina patches located distal to the tips of the corneagenous cell microvilli. The pictures illustrate the spatial interrelationship of the substructures contained in the MV/LE complex and the appearance and distribution of the bridges between the microvillar tips and the ECL patches.

In *A*, at least three discrete connexions are indicated to bridge the MV/LE cleft. There are two (or three) central bridges, the most conspicuous one being about 6 nm thick. In addition, more diffusely seen peripheral connexions may be present between the MV tip and the edges of the patch. In the uppermost portion of the patch, two electron-dense lines are seen. These two outer lines (OL) of the epicorneal lamina are both approximately 2 nm thick, separated by a 2 nm wide clear space. Another clear space (less distinctly seen and also about 2 nm wide) separates the OL from the rest of the patch. The features of this micrograph, together with those of figures 17*B* to *D*, and the MV/LE connexions seen in other electron micrographs of later stages form the basis of the interpretation of the MV/LE complex structure schematized in figure 37, plate 52. × 672000.

In *B* to *D*, further examples are shown of the MV/LE complex. Note the peripheral connexions in *B* and *C*, and the well-demarcated bridge (B) traversing the MV/LE cleft in *D*. The triple-layered plasma membrane of the microvilli in *D* is uniformly about 7.5 nm thick. *B*, *C*, × 326000; *D*, × 314000.

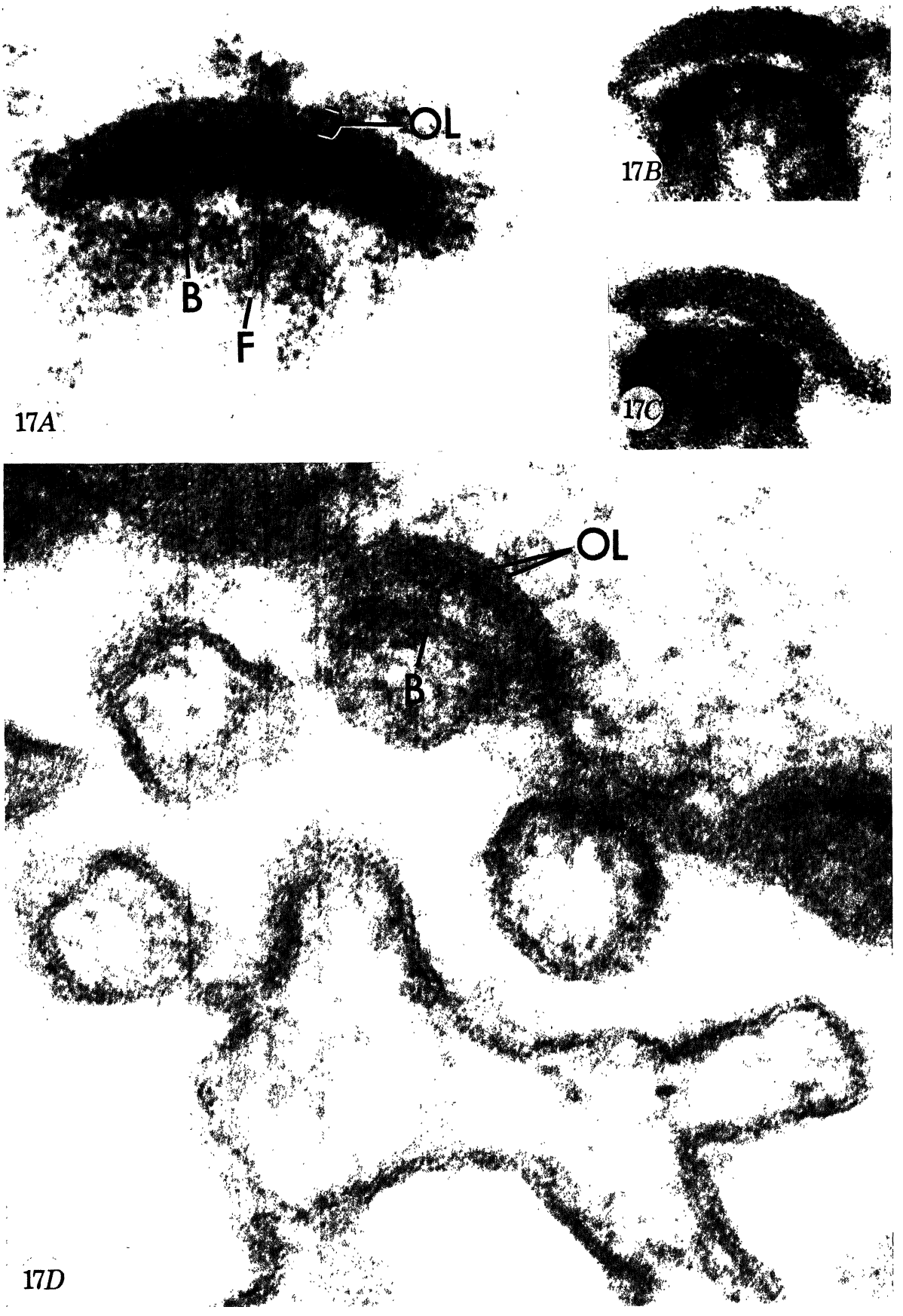

FIGURE 17. For legend see facing page

(*Facing p.* 352)

FIGURE 18. Survey electron micrograph of an oblique section through the eye anlage of a stage P1 to II pupa of *Manduca sexta*. The clumps of crystalline cone substance are in the process of fusing to larger aggregates. The cytoplasm of the corneagenous cells with their fringe of microvilli is approximately 0.5 μm wide. × 5400.

FIGURE 19. Electron micrograph of a perpendicular section through the eye anlage of an approximately 5½-day-old pupa of *Manduca sexta*, showing a continuous epicorneal lamina formed by the coalesced patches of the preceding stage. The lamina evaginations (LE) appear in the section as domes about 65 nm high with an apical centre-to-centre distance of about 190 nm. The MV average 90 nm in diameter and 500 nm in length. × 47500.

In light microscopic sections the crystalline cone material formed a few rounded bodies (figures 5*C*, 6*A*, plates 38, 39). The nuclei of the crystalline cone cells were well seen, being symmetrically located above the cone material (figure 5*C*). At this stage the retinular cell groups could be identified by their nuclei (figure 5*C*) and by their general arrangement in groups that tapered proximally toward the region of the basal lamina. The thickness of the epithelium had increased somewhat, from 50 to 60 μm in the preceding stage to about 75 μm. The width of one ommatidium was the same as in stage PI, i.e. 20 to 30 μm.

Stage PIII. In this stage (6 to about $7\frac{1}{2}$ days after the beginning of pupation, PIII), the eye anlage had assumed a light-brown colour. Light microscopically, the future crystalline cones had become somewhat larger, round or heart-shaped in sections perpendicular to the eye surface (figures 6*B*, *D*, 7, plates 39, 40). The ommatidial cell groups had developed further, and pigment granules were seen in the cells surrounding the retinular cells. The deposition of corneal material (seen as a strongly refractile line on the surface of the eye anlage) marked the beginning of the subsequent stage. The retinular cells were still located in a distinct group closely proximal to the crystalline cone (figure 7).

Stage PIV. The eye of this stage (beginning at about $7\frac{1}{2}$ days from pupation) appeared to an increasing extent macroscopically similar to that of the imago. The colour of the eye was dark-brown from the presence of large amounts of pigment. The distance between the eye and the brain was reduced due to the growth of both these organs. The epidermis very quickly increased in thickness from approximately 60 to 80 μm at the end of stage PIII. The cornea increased in thickness considerably during the following 24 h period (stage PV).

Electron microscopic observations

The description which follows will be restricted to the typical picture of the stages defined above, chosen on the basis of dissection and light microscopy (see Discussion).

Microvilli of the corneagenous cell surface

The surface of the epidermal cells of stage P0 (as seen in *diapausing* pupae) consists of a bilamellar plasmalemma with shallow, irregularly spaced and unequally deep indentations between blunt surface processes (figure 8, plate 40). The processes are in contact with the innermost layer of the pupa endocuticle. From the distal ends of the processes thin filaments seem to emanate in curved groups which are orientated in the same direction and blend with the strands observable in the most proximal endocuticular layer. The cytoplasm of the processes in glutaraldehyde/OsO_4-fixed material contains filaments running parallel to the long axis of the process. Microtubules are present in those parts of the corneagenous cells which lie immediately below the bases of the processes. The general orientation of the microtubules is parallel to the distal surface of the epidermal cells. Early in stage P0, the processes of the corneagenous cell surface have become more slender and are separated from each other (figures 10 ff., plates 41 ff.). With a further increase in length, the processes become true microvilli. At all stages, beginning with PI, they are about 0.4 to 0.5 μm long and 70 to 100 nm wide. The microvillar interdistance averages 170 nm at the level of the tips, increasing to about 200 nm at stages PIII to IV.

In sections made obliquely or parallel to the eye surface, the tips of the cross-sectioned microvilli are seen to be arranged in a roughly hexagonal pattern (figures 13 to 16, plates 42, 43). They are interconnected by a system of filaments which in perpendicular sections appear as

thin strands (figures 10 to 12, plates 41, 42). The spacing of the microvillar bases is considerably less regular than that of the tips of the individual microvilli (see, for instance, figures 14, 15, plates 42, 43). The latter often bifurcate at various distances from the microvillar tips. Vesicles bounded by triple-layered membranes are seen in the spaces between the microvilli.

Morphological changes distal to the corneagenous cell surface

Up to about 4 *days* after pupation, the loosely woven, innermost layer of the pupa endocuticle consists of a fabric of thin filaments, which seem to originate in the immediate vicinity of the tips of the blunt processes of the corneagenous cells.

In the subsequent stage (PI)—pupae *about* 5 *days old*—similar filaments persist, now seen in the form of randomly orientated filamentous material. Immediately distal to the microvillar tips another structure has appeared in the shape of 'patches' of electron-dense, lamellar elements, in sections perpendicular to the eye surface seen as very low domes (figures 10, 11*A*, *B*, 12, 17*A* to *D*, plates 41, 42, 44). There is a strict one-to-one relationship between the patches and the microvillar tips distal to which they appear. The domes are interconnected by thin strands of a filamentous material, which can be only poorly visualized at this stage. In many cases the tips of the microvilli also seem to be loosely connected to each other by a second system of very thin filaments. The most conspicuous feature is the individual domes. There is no evidence of the existence of a continuous lamina connecting the patches or domes at this early stage of development.

At the pupal age of $5\frac{1}{2}$ *to about* 6 *days* from pupation (stage PII), the low domes have assumed the shape of somewhat higher cupoles (figures 23 to 27, plate 47) with amplitude about 150 nm. The individual cupoles are now contiguous with each other (figure 19, plate 45). From this stage on, the term 'epicorneal lamina' is used to denote the set of structures, including the domes and cupoles and the connexions between them. For the sake of consequence, the term is used also for the corresponding set of structures of the preceding stage, although the connexions between the domes are poorly defined. Analogously, the term lamina evaginations (LE) is used also for the domes and patches of stage PI. A striking feature at this stage of development (as well as in stage PI) of the epicorneal lamina is the constant distance between the cupoles, and between the cupoles and the most distal part of the plasmalemma of the microvillar tip. The spatial relationship between the MV and the ECL, as well as other pertinent structural conditions, will be treated more extensively in the latter part of the Results.

In the subsequent stages of development (PIII to IV), *from about* 6 *days* and *up to about* 8 *days*, there is a further increase in height of the lamina evaginations. They ultimately form

Description of plate 46

Figure 20. Survey electron micrograph of an oblique section through the corneal surface of the *Manduca sexta* eye anlage at stage PII ($5\frac{1}{2}$ to 6 days after pupation). The epicorneal lamina (ECL) is seen as a row of low cupoles. The left hand crystalline cone cell (Cy), containing a rounded body of cone substance (Cs), is surrounded by the two corneagenous cells (CoC) of this ommatidium and by pigment cells (Pi). × 7700.

Figure 21. Electron micrograph of a section through the junction between two ommatidia in the optic imaginal disk of a *Manduca* pupa. The corneagenous cells (CoC) and the pigment cells (Pi) of the adjacent ommatidia intercalate extensively. Along most of the junction, the cell contact is specialized in the form of septate desmosomes (figure 22). × 27600.

Figure 22. Electron micrograph of a section through the area of junction between two ommatidia in the eye anlage of a *Manduca* pupa, showing a septate desmosome. The plasma membrane (PM) is seen as two lines about 2.5 nm thick separated by a 2.5 nm wide clear space. Approximately 7 nm thick septa (S), spaced 10 nm apart, bridge the intercellular cleft which has a width of about 10 nm. × 344000.

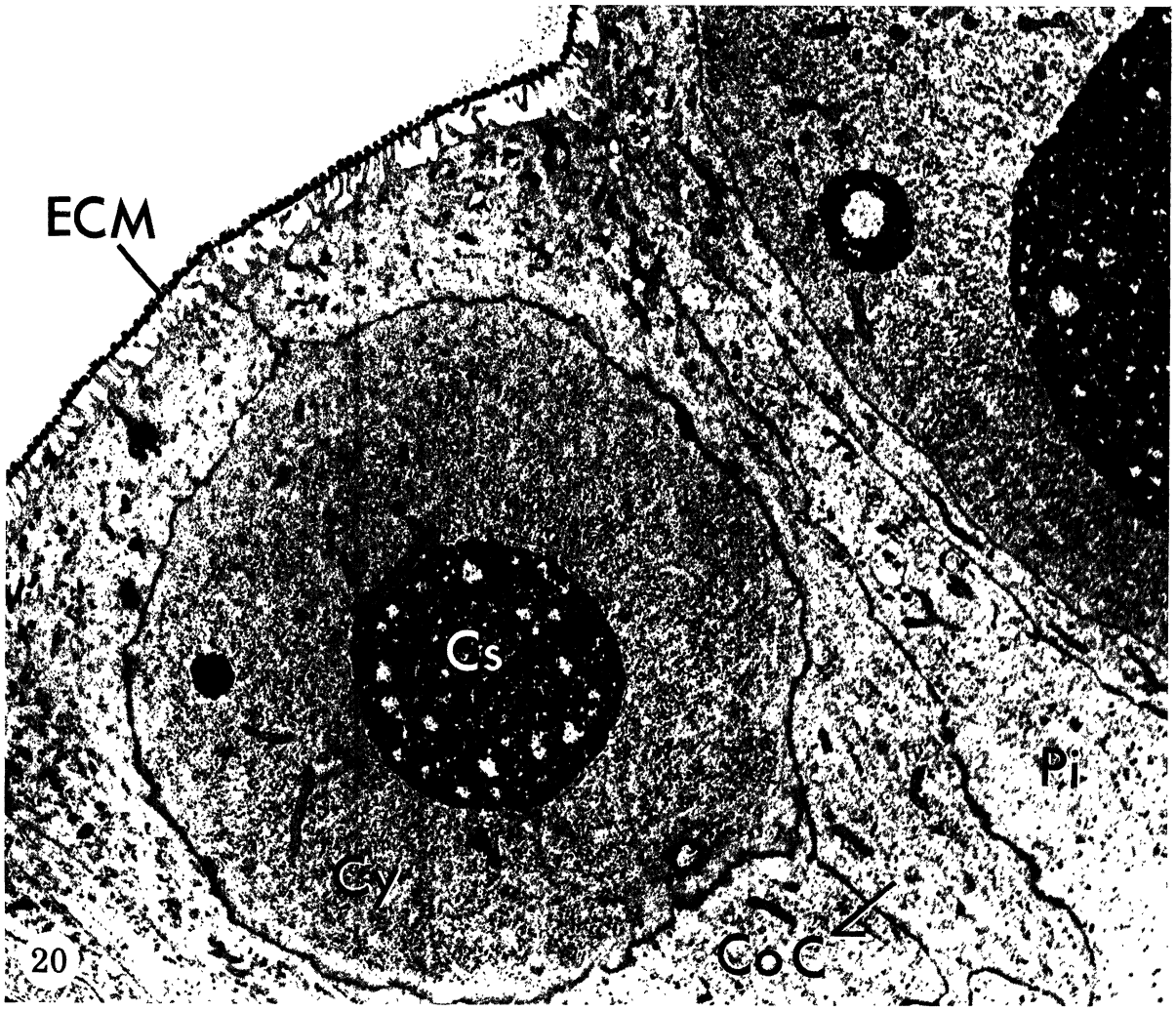

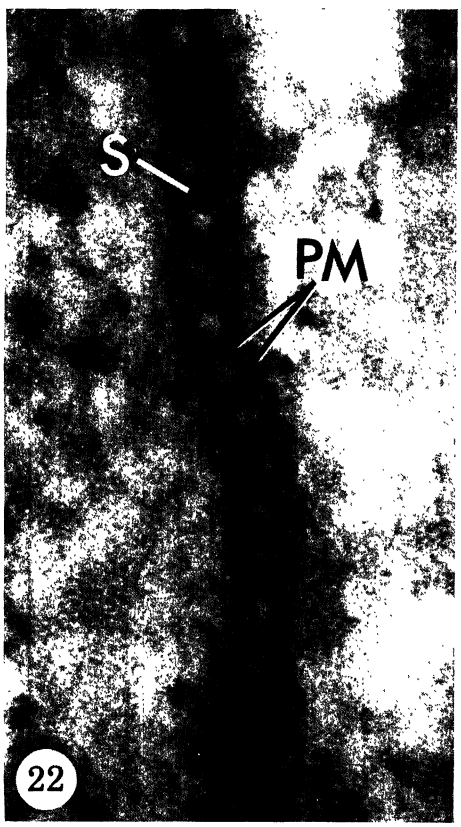

FIGURES 20 to 22. For legends see facing page

(Facing p. 354)

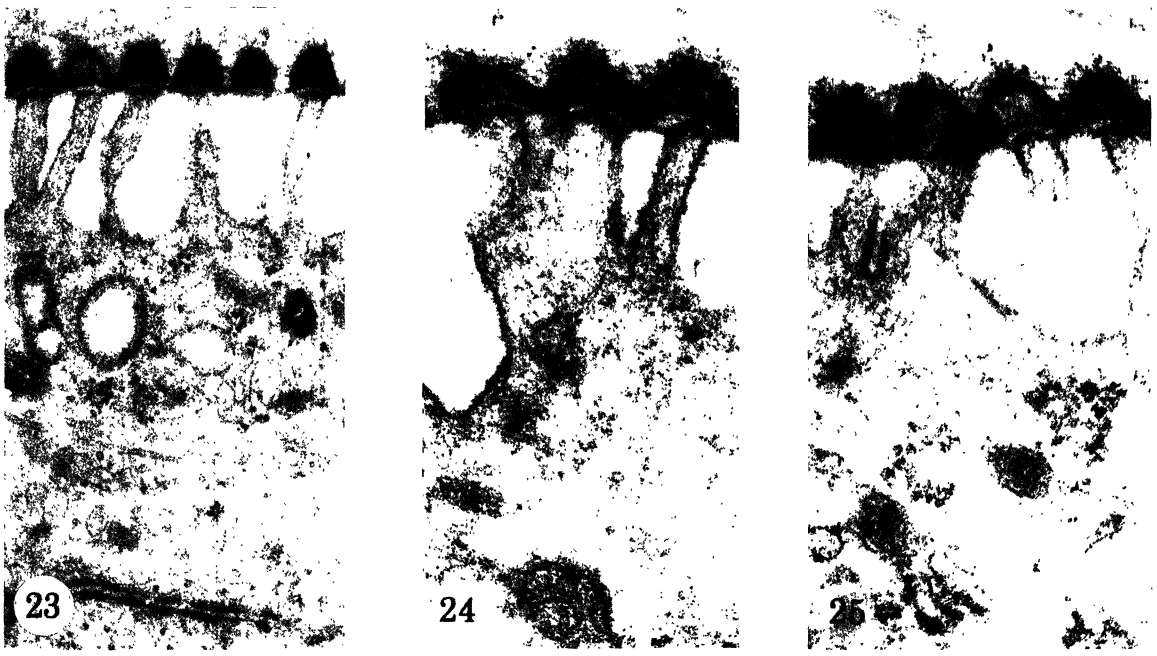

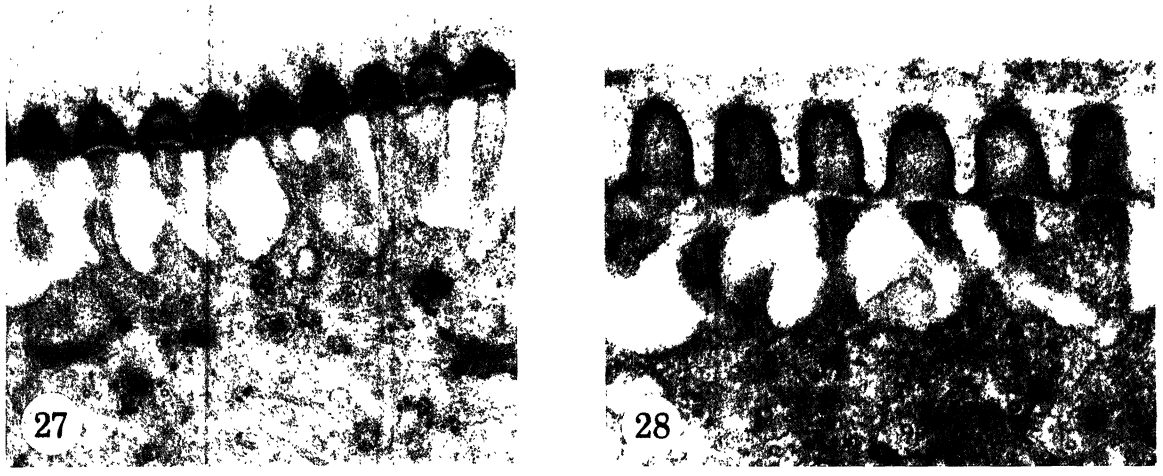

FIGURES 23 to 27. Electron micrographs of perpendicular sections through the eye anlage of *Manduca sexta* pupae, illustrating the typical evaginations of the continuous epicorneal lamina of stage PII ($5\frac{1}{2}$ to 6 days after pupation). The approximately 400 nm long microvilli of the corneagenous cells are 75 to 85 nm thick and their tips spaced 170 to 190 nm apart. The evaginations appear as cupoles, about 150 nm high. Peripheral and central bridges are indicated in the MV/LE cleft. Figures 23 and 27, × 41000; 24, 25, × 68800; 26, × 44700.

FIGURE 28. Electron micrograph of a perpendicular section through the eye anlage of a *Deilephila elpenor* pupa at stage PIII, showing the appearance of the MV/LE complex in its final form before the onset of cornea secretion. The evaginations, whose array forms the completed 'template' of the nipple anlage, are about 200 nm high and their centre-to-centre distance is also about 200 nm. × 57000.

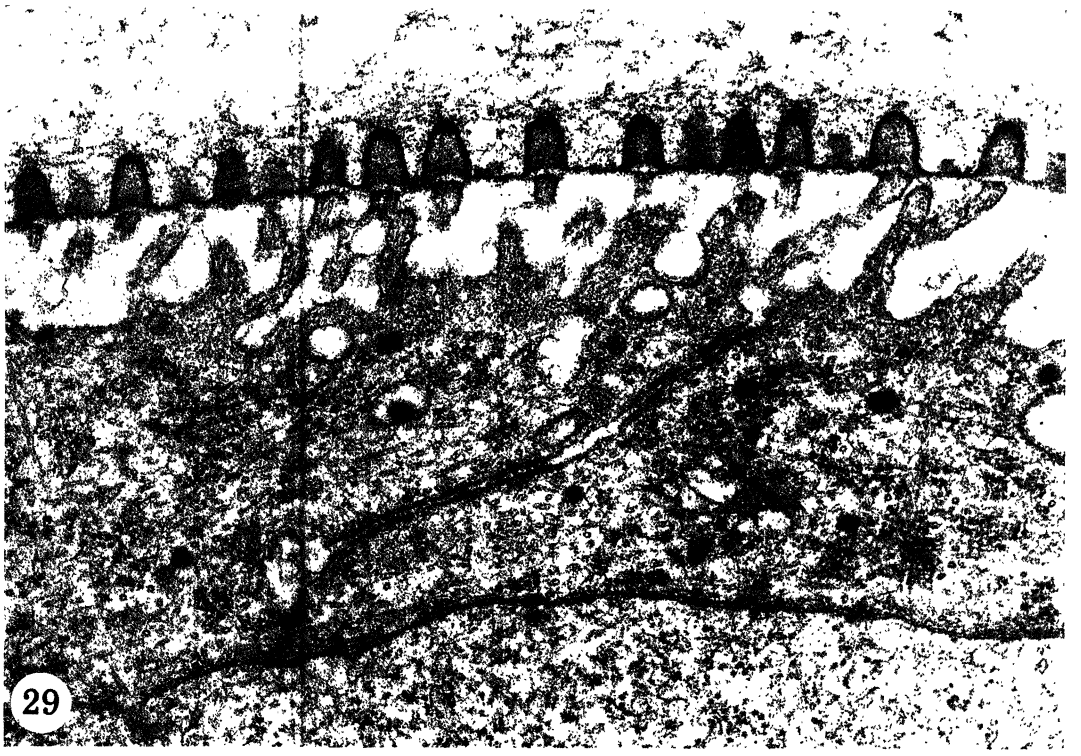

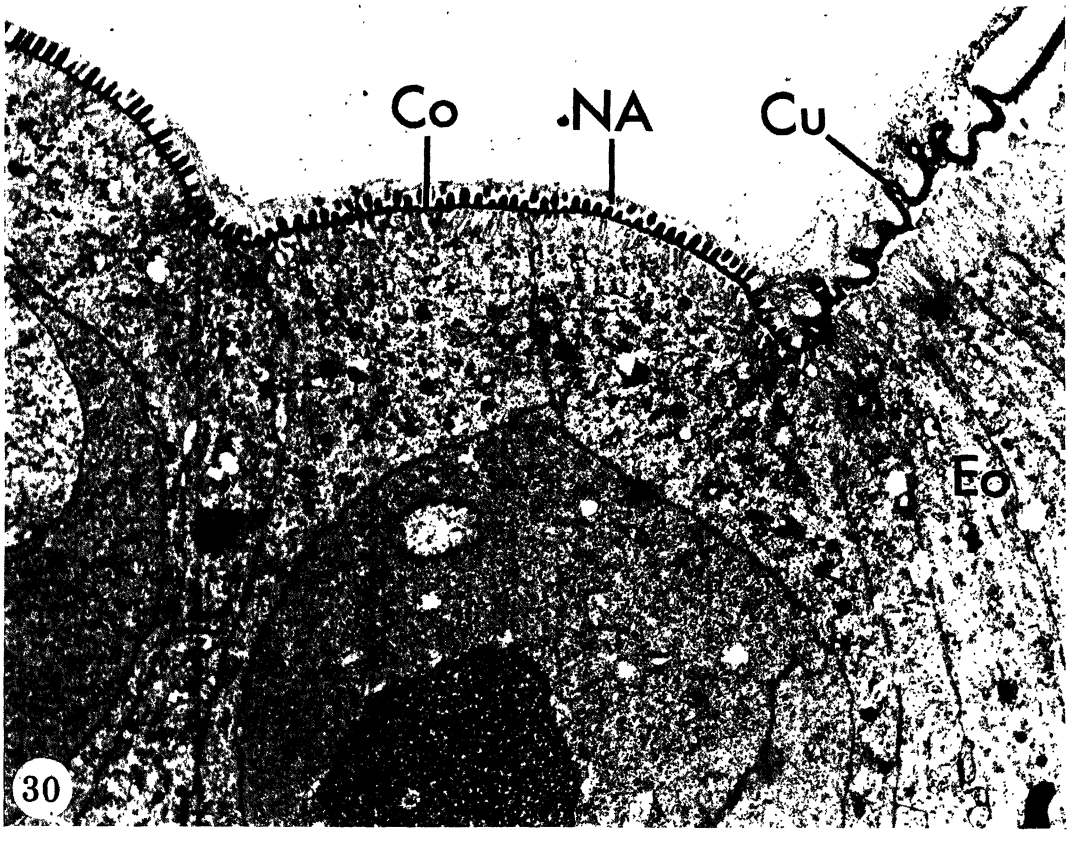

FIGURE 29. Electron micrograph of a perpendicular section through the corneagenous cell surface in the stage PIII eye anlage of a *Manduca* pupa. The epicorneal lamina evaginations of the final nipple anlage are seen as high cupoles with amplitudes and centre-to-centre distances of about 200 nm. 'Coated vesicles' are seen in the corneagenous cell cytoplasm. Both central and peripheral MV/LE bridges are indicated. × 38700.

FIGURE 30. Survey electron micrograph of a section through the zone of transition between the cornea (Co) and the body cuticle (Cu) of the extraocular area (Eo) in the *Manduca sexta* eye anlage at stage PIV. The secretion of the corneal material has started. The final nipple anlage is shown on the distal rim of the corneagenous cells. It is seen to have reached the same stage of development in all facets out to the extraocular area, whereas the degree of differentiation of the ommatidial cell groups is less advanced closest to the transition zone. The picture should be compared with the light micrograph of figure 6*D* at which level the electron microscopic section was made. The outermost layer of the body cuticle (cuticulin and a thin lamina of non-lamellate, 'protein epicuticle') is thrown into folds on top of a fringe of long, regularly spaced microvilli. Although not clearly shown here, such body cuticle folds occurring near the eye anlage generally tend to become progressively more regular in height and width, as well as in interspacing, as the ocular area is approached. This tendency is paralleled by increasing length and regularity of the array of epidermal cell processes (cf. figure 39) until they finally appear as the microvilli shown in this micrograph. × 7900.

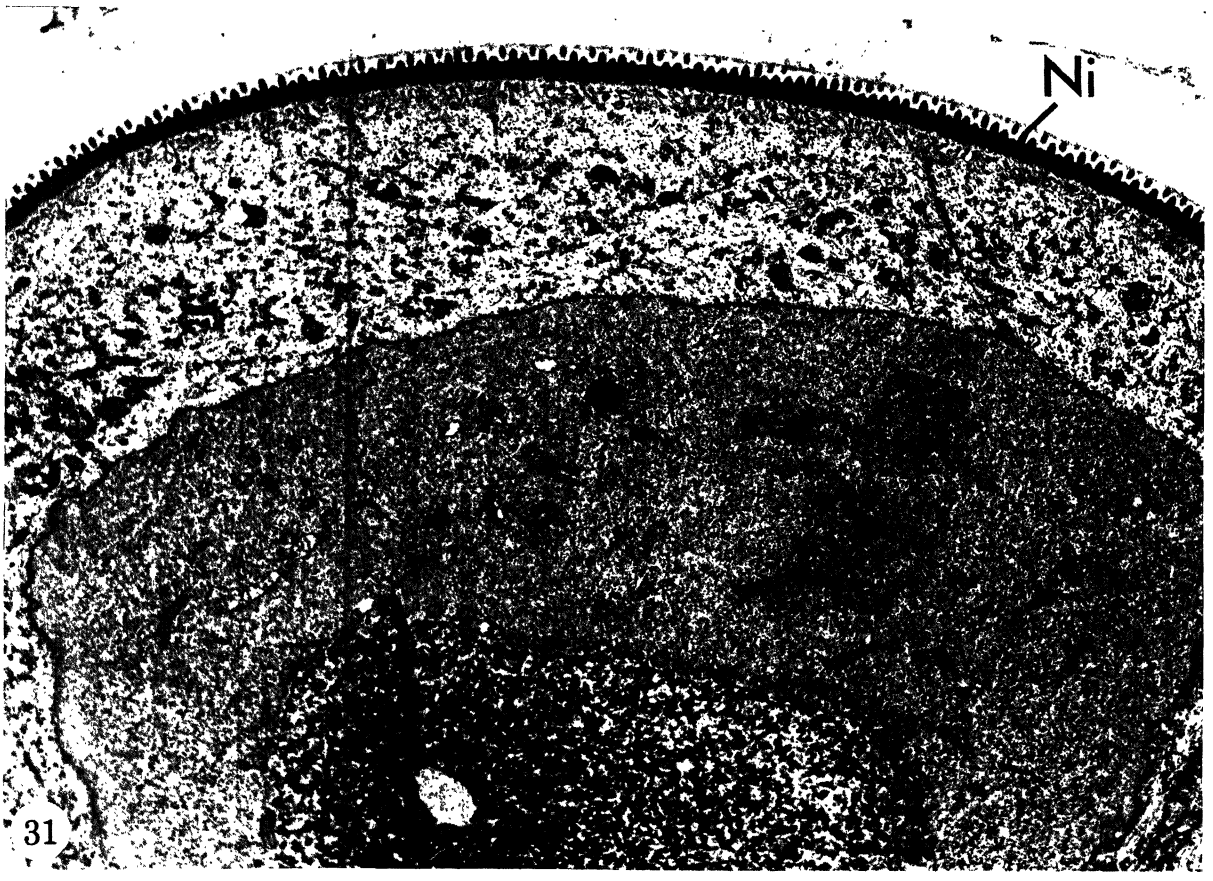

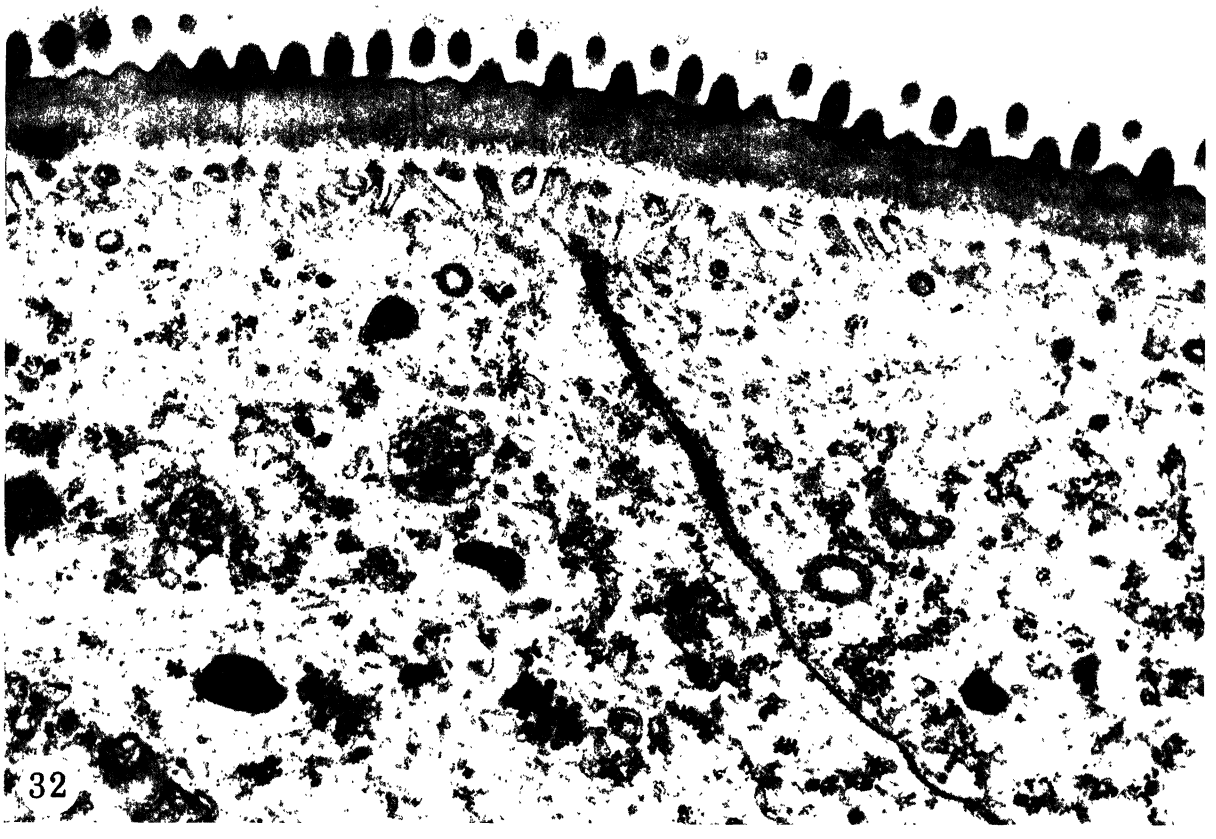

FIGURES 31, 32. Survey electron micrographs of a section through the eye anlage of *Manduca* pupae about 7½ days after pupation. In both pictures, a thin cornea is seen carrying on its surface an array of regularly arranged nipples (Ni) with a tip-to-tip distance of about 200 nm. In figure 32 it can be seen that the regularity in the arrangement of the corneagenous cell microvilli persists also after the completion of the nipple morphogenesis. Figure 31, × 7600; 32, × 28800.

cupoles about 100 nm high, which constitute the LEIII and LEIV stages (figures 28 to 30, plates 47, 48). The final cupole height and base distance are both 200 to 250 nm. Stage LEIV is also the terminal one as far as the growth of the future nipples is concerned. When the eventual dimensions of the LE have been reached, the material of the cornea fills the evaginations and becomes consolidated. The hexagonal LE array at the end of stage PIII constitutes the initial phase of the completed nipple anlage (stage LEIII, table 2, figures 28, 29), which in the form of fully developed nipples (figures 31, 32, 33*A*, *B*, plates 49, 50) will later rest upon the surface of the multilamellar cornea (figure 36, plate 51).

Epicorneal lamina substructure

Substructure of the lamina evaginations

In the LEI stage, the low domes (about 30 nm in amplitude) are composed of two electron-dense lines (figure 11*A*, *B*, plate 41). Later, there are two outer lines (OL) and one thicker, ill-defined inner line (figure 17*A* to *D*, plate 44). The composite thickness of the OL is approximately 6 nm. The outer lines are separated by a clear space, 2 to 3 nm wide, from the inner line, whose thickness can only be estimated (about 10 nm). Its inner margin is poorly demarcated because of the electron-dense material of the lower parts of the convex LE projected on to this region. The total thickness of the ECL from stage LEII can therefore be considered to be approximately 18 nm. In the two stages of ECL development which have been termed LEII and LEIII, there was no observable change in the substructures of the ECL. During the consolidation of the nipple anlage in the PIV stage, there was some indication that part of the ECL becomes detached from the rest of the LE. In figure 33*A*, *B*, plate 50, there is a line, about 5 nm thick, external to the surface of the nipples, separated from the nipple proper by an unevenly wide gap. At close examination in the electron microscope, the remains of the ECL are barely visible in the nipple surface. The separating line may also be interpreted as a condensation from the moulting fluid distal to the nipples.

At all stages, the epicorneal lamina is essentially identical to the cuticulin layer (Locke 1966) of the extraocular body cuticle area except for the dimensions of its substructures, and the shape and regularity of the evaginations. The thickness of the cornea at the beginning of stage PIV (figures 30 to 32) corresponds to that of the so-called protein epicuticle (Locke 1969; for a discussion of the term, see Weis-Fogh 1970) in the extraocular region.

Other observations

The main ultrastructural events in the development of the optic imaginal disk of *Manduca* can be generally said to correspond to those of *Bombyx* as seen in the light microscopic work of Yagi & Koyama (1963). Like in *Bombyx*, the development of the *Manduca* eye consists of a predifferentiation stage (up to 4 or 5 days after pupation), and a subsequent stage of differentiation (which has been followed in the present work from 5 to about 7½ days).

The differentiation of the *ommatidial cells* seems to be slightly but significantly less advanced (figures 5*A*; 6*A*, *B*, *D*, plates 38, 39) nearest the line of transition to the anterior extraocular region (cf. Wolsky 1949) during the whole period up to the time when the nipple anlage is completed (about 7½ days after pupation). The difference can be seen, for instance, in the degree of fusion of the cone material of the individual crystalline cone cells. At least from stage LEII on, the epicorneal lamina shows no such difference in development; the domes and low cupoles are always equally high in all ommatidia. Figure 30 shows this for the very initial part of

stage PIV, where the corneal material forms a layer only about 30 nm thick proximal to the bases of the LE. At about 7½ days after pupation the degree of the differentiation is the same in the whole of the eye anlage—as was reported to be the case also in *Bombyx* (Yagi & Koyama 1963)—except for a group of cells in a very small transition zone at the extraocular border (figures 6*D*, 30, plates 39, 48).

The microvilli of the rhabdomeres first begin to appear in stage PII, when they can be seen as slender, widely spaced and tortuous processes from the inner margins of the developing retinular cells. This corresponds roughly to the stage of development when the rhabdoms of the *Drosophila* eye begin to form (Perry 1968).

Connexions between microvilli and lamina evaginations

Strands of unstructured material bridge the peripheral parts of the narrow space between the flattened distal rim of the microvillus and the ECL patch (see, for instance, figure 17*B*, *C*, plate 44, and the schematic drawings C, F, J in figure 38, plate 52). The connexions reach the most proximal part on the base of the nearest dome or cupole. The ends at the ECL of two adjacent peripheral connexions seem to meet and merge at a point about half-way between two cupoles. Bridges with regular spacing are often seen to extend across the middle parts of the MV/LE gap at discrete points. The thickness of one bridge is approximately 6 nm and the spacing between the bridges about 20 nm. Three to four bridges may be seen in a MV/LE complex, including the peripheral connexions which may be superimposed images of individual bridges. It has not been possible to distinguish clearly any demarcation between the bridging substance and the MV or LE. The bridges sometimes appear contiguous with the filaments of the interior of the microvillus. The number of intramicrovillar filaments in cross-sectioned microvilli is difficult to estimate, but seems to be 5 to 7. The discreteness of the bridges and the way they are distributed in the MV/LE space support the interpretation that the bridges may be extracellular continuations of the filaments. It is suggested that they radiate more or less symmetrically out from the microvillus and insert at discrete points on the (fictive) annular base of the domes and cupoles (see schematic drawing in figure 37, plate 52). The possible implications of the presence of the bridges will be treated in the Discussion.

There are several large and small vesicles bounded by triple-layered membranes in the most distal strands of cytoplasm of the corneagenous cells (see, for instance, figures 12, 29, plates 42, 48). Interior to the membrane they contain a material which is mostly amorphous but sometimes seems to be at least pseudo-organized. These vesicles—which resemble 'coated vesicles' (Roth & Porter 1962, 1964)—reside in the plasma membrane of the distal surface of the corneagenous cells, or appear to be in various stages of detachment from the membrane. Similar vesicles with some electron-dense contents and bounded by a triple-layered membrane are also seen between the microvilli. These vesicles are less numerous in the more proximal parts of the corneagenous cells and are not found in the crystalline cone cells.

Discussion

Comparison with body cuticle morphogenesis

The morphogenesis of the larval body cuticle of the Brazilian skipper, *Calpodes ethlius* Stoll (Lepidoptera: Hesperiidae), has been described by Locke (1966). Essentially identical results were obtained by Filshie & Waterhouse (1969) for the development of body surface pattern in

Nezara viridula, the green vegetable bug. The body cuticle formation seems to have some features in common with the events taking place in the morphogenesis of the epicorneal surface in *Manduca* and in the formation of the cornea of *Drosophila* (Perry 1968). Such common features are to be expected, since the epicorneal structures constitute a direct continuation of the outermost layer of the body cuticle ('cuticulin layer', Locke 1966). In both cases, an essential feature is the initial deposition of extracellular material just distal to the epidermal cells in the form of patches of lamellar elements.

In *Manduca*, the present results show that the first elements of the future nipple anlage are the patches of membranous material that arise distal to the microvillar tips. At a somewhat later stage, the future nipple anlage is made up of a continuous epicorneal lamina, and the substructure of the material between the microvillar tips is now seen to be that of the domes and cupoles.

Some of Locke's findings will be summarized and discussed here. In the 5th instar of the *Calpodes* larva, the cuticulin layer is the outer 'membrane' of the epicuticle that arises *de novo* as a triple layer growing by accretion of material secreted from the epidermal cells. It is first seen as convex patches covering the tips of individual and, later, *groups* of epidermal cell microvilli. The growth of the cuticulin was suggested to take place at the edges of the patches. At all sites, the cuticulin could be resolved into three lamellae. At the stage when the cuticulin completely covers the epidermal surface, the outer lamella becomes detached, to form what Locke interpreted as a lipid monolayer, possibly being a surface layer of wax. (This interpretation has been questioned by Filshie (1970) on the grounds that these epicuticular structures are resistant to lipid solvents and to acids.)

The mechanism of growth which (in Locke's words) 'most easily fits the observations' was 'the side-to-side accretion of membrane units'. As evidence for this, Locke stressed the presence of gaps in the cuticulin layer and of strands of dense material which connected the plasma membrane of the microvilli only with the *edges* of the cuticulin patches. The alternative hypothesis of growth by intussusception over the whole cuticulin surface was dismissed by Locke on the somewhat vague grounds that, with such a mode of growth, one should expect the gaps to become closed. This is stated not to happen. Instead, gaps are said to remain until the final (folded) area of the epicuticular surface is completed, 'as though these gaps are necessary for the increase in area'.

At least from stage PII on, no sites could be found in the present work where the cuticulin layer in the extraocular region of the *Manduca* eye could be unequivocally demonstrated to show true gaps. Instead, it was considered more likely that the diffuse substance seen to connect better defined stretches of cuticulin might represent projections in the EM image of tangentially sectioned portions of a continuous layer.

Figure 39, plate 53, demonstrates the appearance of the cuticulin of the *body cuticle* in the extraocular area of the anterior rim of the *Manduca* eye immediately adjacent to the eye anlage. The surface of the epidermal cells are seen to bear blunt processes. As little as about 25 μm closer to the eye anlage, however, the processes are true microvilli (cf. figure 30, plate 48), and there is often an increasing tendency for the small cuticulin evaginations to appear in shapes simulating that of the ECL evaginations. The regularity of the interspacing of these evaginations, too, increases and tends towards the LE interdistance of about 170 to 200 nm.

A correlation between the epicorneal lamina and the cuticulin of the *Calpodes* larva proves difficult when the substructure dimensions are compared. Whereas the cuticulin of earlier larval

developmental stages in *Calpodes* was reported to be composed of three lines 4 to 5 nm thick, separated by clear spaces 2 nm wide, the *Manduca* epicorneal lamina lines have the following approximate dimensions throughout the stages observed here: outermost line, 2 nm; middle line about 2 nm; the clear space separating them, also about 2 nm; inner line about 10 nm; the clear space between the two outer lines and the inner line, about 2 nm. Thus, the total thickness of the ECL is about 18 nm. In the extraocular region of the insects of the present study, the cuticulin before onset of protein epicuticle secretion shows lines with the same dimensions as those of the ECL (figure 40, plate 53).

At the stage of deposition of the protein body epicuticle in the 5th instar *Calpodes* larva, the cuticulin substructures have other dimensions, as stated by Locke, viz. three lines each 5 nm thick and two separating clear spaces both 2 nm wide. The total thickness therefore amounts to about 23 nm, which should be compared with the figure for the markedly thinner epicorneal lamina (about 18 nm) at the end of stage PIII and the initial part of stage PIV (as long as the individual LE lines can still be distinguished clearly enough to be measured). After the onset of secretion of corneal material proper, the ECL lines become rapidly less discernible; the extraocular cuticulin dense lines, however, remain visible somewhat longer. They constitute a layer about 16 nm thick at this stage (figure 34, plate 50).

The presence of MV/LE bridges

The electron microscopic image of the MV/LE complex depends on many factors, e.g. the orientation of the plane of section through the complex, section thickness, and staining properties. Although uncertain as to dimensions and exact spatial relationships, the representation of the MV/LE complex in figures 37, 38, plate 52, seems validated by the observations in the present material. The limited number and the discreteness of the bridging structures, as well as their interspacing, support such an interpretation. In all the electron microscopic sections which show proper preservation and triple-layered membranes, the bridges are seen in random MV/LE complexes. The appearance of the bridges is not affected by variations in the preparatory procedures, e.g. changes in fixation, embedding, and staining. Geometrical considerations, the constancy of the bridges in various respects, their discreteness and their dimensions (which

---

Description of plate 50

Figure 33. Electron micrograph of a perpendicular section through the cornea of a *Manduca* pupa eye anlage showing the shape, size and distribution of the fully developed, consolidated corneal nipples. Their amplitude averages about 275 nm and their centre-to-centre tip distance is about 220 nm. The thickness of the cornea of this stage (PV, about 8 days after pupation) is about 800 nm in the centre of the facet and about 600 nm in the peripheral parts. A thin, electron-dense line (marked SL in *B*) is seen to follow the nipple surface. It has the thickness of the two outer lines of the epicorneal membrane of previous developmental stages and gives the impression of having separated from the nipples. It may, however, represent a condensation product of the proximal layers of the fibrous substance (moulting fluid?) overlying the cornea. Pore canals (PoC), 30 to 50 nm wide, traverse the cornea and open into the area between the nipple bases. *A*, × 33600; *B*, × 87000.

Figure 34. Electron micrograph of a perpendicular section through the optic imaginal disk of a *Manduca* pupa at stage PIV showing a portion of the outermost layers of the extraocular body cuticle about 50 μm from the anterior rim of the eye. A thin layer of the non-lamellate, 'protein epicuticle' (PE) has formed proximal to the cuticulin. The latter is composed of three dense lines (CL) with a thickness of about 2 nm (outer line), 3 nm, 7 nm respectively. The clear spaces separating the lines are about 2 nm and 3 nm wide. Thus, the total thickness of the cuticulin at this stage is about 17 nm. For a discussion on the dimensions of the cuticulin of the *Manduca* extraocular body cuticle in comparison with that of the 5th instar larva of *Calpodes* (Locke 1966), see text. × 314000.

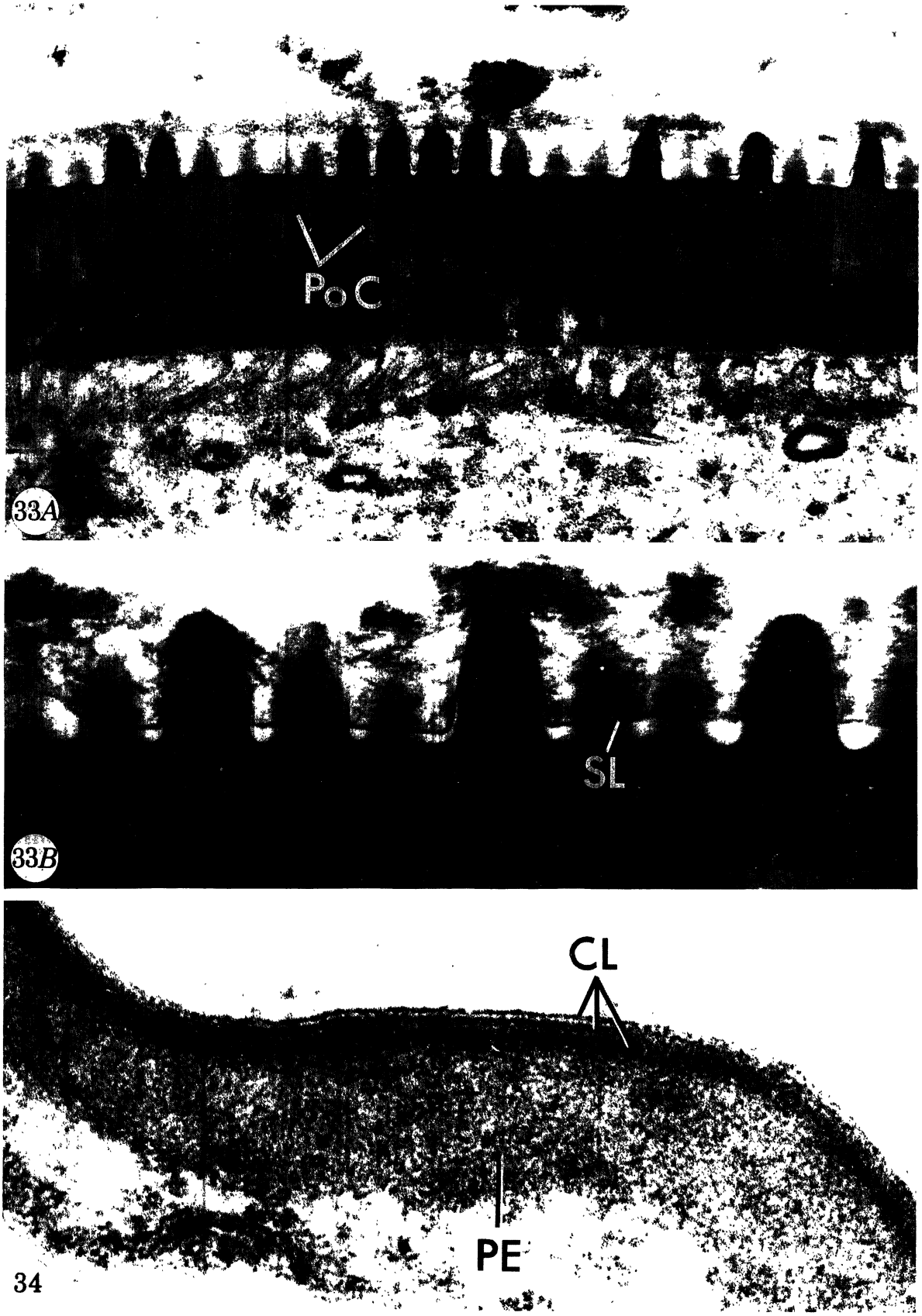

FIGURES 33 and 34. For legends see facing page

(*Facing p.* 358)

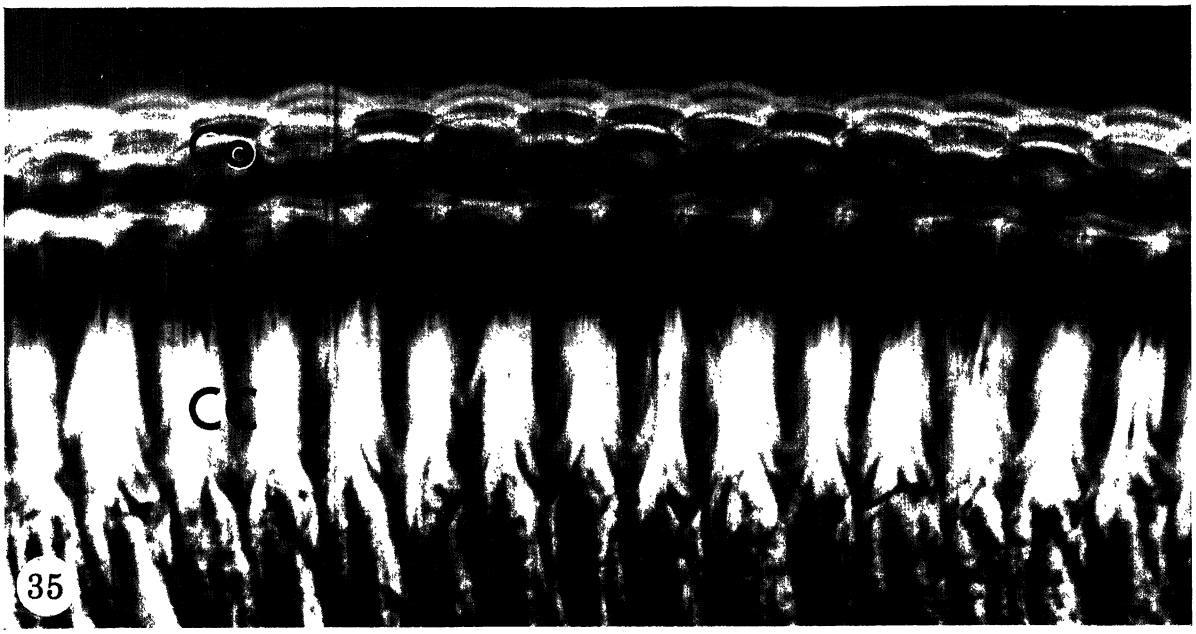

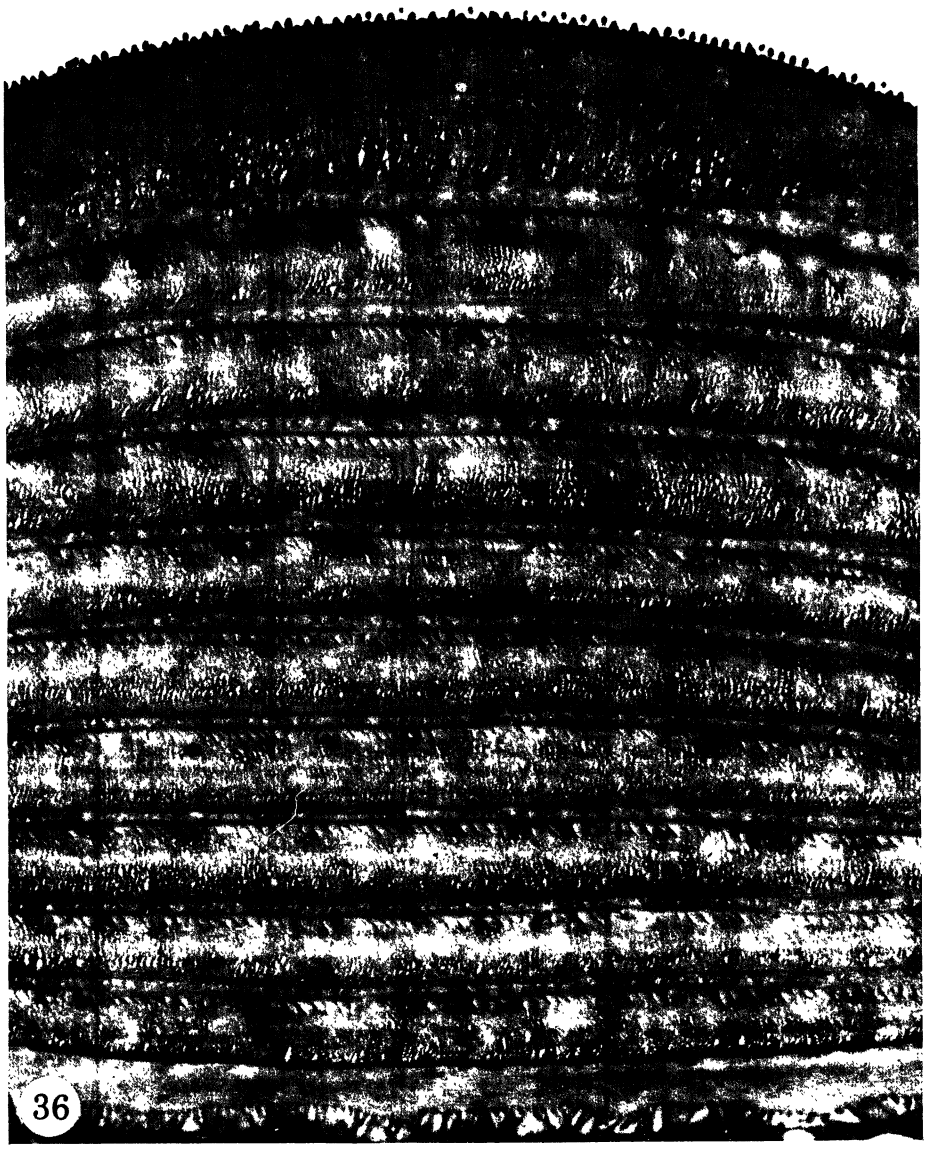

FIGURES 35 and 36. For legends see facing page

are well above the working resolution of the microscope) make it unlikely that they should be artefacts. It can therefore be concluded that the observations indicate the presence in the space between the microvilli and the epicorneal lamina elements of well-demarcated physico-chemical differences imaged as the MV/LE bridges.

Growth of the epicorneal lamina

If secretion of substances from the epidermal cells to build the epicorneal lamina goes on from the entire microvillar surface—which is likely, since there is no morphological evidence for secretion at discrete points in the region of the MV/LE complex—the secreted material is most plausibly added by intussusception over the whole surface of the LE. This would result in the buckling of the entire epicorneal lamina by a combination of mechanical stress—like the cylindrical buckling of the tracheolar lining (Locke 1966)—and surface tension forces (see, for example, Snell, Shulman, Spencer & Moos 1965) rather than by evagination above each microvillus. If, however, there are areas of 'constraint' at some places along the annular base of the first formed ECL patches, the addition of new material would cause the LE lamellae to bulge symmetrically in the region between those areas of constraint. The presence and radial arrangement of the MV/LE bridges observed in the present work make their LE ends suitable as such areas of constraint. Addition by intussusception of new material to the LE then results in a series of stages like the ones described in *Manduca*, i.e. a continuous development of the LE from the originally low domes to the high cupoles of the final nipple anlage.

On the basis of the sequence of events described here, the proposed morphogenetic mechanism seems to provide a plausible explanation of the mode of growth of the membrane evaginations. It cannot be ruled out that such a mechanism also applies for the growth of the *Calpodes* cuticulin, perhaps in addition to the mechanism suggested by Locke.

The role of microvilli and MV/LE bridges in corneal topography formation

The tips of the corneagenous cells very early assume a regular spacing and a roughly hexagonal distribution over the surface of the eye epidermis. Such a distribution and very similar spacing is found in a wide variety of microvillate surfaces, and seems to be a common feature in the epidermal cells of invertebrates. The pattern and spacing assumed may be the result of packing of the microvillar tips as closely as possible. In the case of the optic imaginal disk, the corneagenous cell microvilli seem to determine the hexagonality of the nipple array (by way of the MV/LE complex). The width, at the level of their bases, of the individual nipples and their centre-to-centre distance are therefore also dependent on the corresponding data for the MV tips. The patterned array of low protuberances covering the corneas of many insects (Bernhard,

---

Description of plate 51

Figure 35. Light micrograph of a thick perpendicular section through the compound eye of an adult *Manduca sexta*, showing a number of ommatidia with their corneas (Co), crystalline cones (CC), and a distal portion of the layer of crystalline tracts and pigment cells. The facet is about 30 μm in diameter and about 25 μm thick. × 380.

Figure 36. Electron micrograph of a slightly oblique section through the cornea of a *Deilephila elpenor* pupa shortly before the expected emergence of the imago. About 80 % of the lamellate cornea has formed, being approximately 20 μm thick. Nipples are seen on the corneal surface. Microvilli persist on the corneagenous cell surface with their tips regularly spaced. × 7400.

Gemne & Sällström 1970), may also be dependent on epidermal cell microvilli and arise like the full-sized nipples of *Manduca*. The lower height of some corneal surface protuberances could be produced by the process of growth going on at a lower rate or being stopped at an earlier point of time during the secretion of epicorneal lamina material. The absence of regularity in the arrays of corneal protuberances exhibited by certain insect species (Bernhard, Gemne & Sällström 1970) may be caused by 'defects' in the constraint effected by MV/LE bridges on the ECL. It is obvious that the morphogenesis of epicorneal ultrastructure in insects with smooth corneas and with various types of regularly or irregularly arranged surface protuberances should be investigated.

Waddington & Perry (1960), who studied the development of the (normal, wild-type) *Drosophila* eye, make a comment which is relevant to the role of microvilli in the formation and maintenance of the regularity of epicorneal structures. Concerning what they call 'the superficial plasma membrane processes of the primary pigment cells' (i.e. the corneagenous cell microvilli), they remark that since the cornea 'has a smooth surface...it seems likely

Description of plate 52

Figure 37. Schematic drawing of the continuous epicorneal lamina (ECL) at stage PII of the pupa of nocturnal Lepidoptera (about 6 days after pupation). One lamina evagination (LE) is located distal to the tip of each corneagenous cell microvillus (MV). Extracellular continuations of the intramicrovillar filaments cross the MV/LE cleft as bridges (B) which insert on the (fictive) annular base of the LE. Growth of the epicorneal lamina evaginations to form successively higher cupoles is suggested to take place by addition of new material to the ECM at all points of the LE surface within the palisade of bridges. The latter are proposed to act as structures of constraint which prevent the ECL from buckling randomly and cause the evaginations to grow in a regular, symmetrical fashion in accordance with the morphogenetic events described for the nipple formation in the present work (see figure 38).

Figure 38. Schematic drawings, illustrating the main characteristics of some stages of development of the most distal portions of the optic imaginal disk in the pupa of nocturnal Lepidoptera. *B*, *E*, *H* and *L*, based upon light microscopic observations; all other drawings based upon observations with the electron microscope. For explanation, see text.

Symbols

B	bridge connecting the tip of the microvillus with the base of the patches and cupoles of the epicorneal lamina
CC	crystalline cone
Cn	nucleus of crystalline cone cell
Co	cornea
CoC	corneagenous cell
Cs	crystalline cone substance
CV	'coated vesicle'
ECL	epicorneal lamina
HC	high cupoles of the epicorneal lamina, fully formed 'template' of the nipple anlage (stage LEIII)
LC	low cupoles of the epicorneal lamina (stage LEII)
LE	epicorneal lamina evagination
MF	moulting fluid
Mt	microtubules
MV	microvilli
N	bundles of retinular cell axons
NA	nipple anlage (LE not yet filled by corneal substance)
OL	outer two electron-dense lines of the epicorneal lamina
P	initial patch of the epicorneal lamina, stage LEI
PC	pupal endocuticle
Pr	processes of the corneagenous cell
R	retinular cells
SL	separating line
UN	lamina evaginations filled by corneal substance not yet consolidated (stage LEIV)
V	vacuole bounded by triple-layered membrane.

Phil. Trans. Roy. Soc. Lond. B, volume 262, *plate* 52

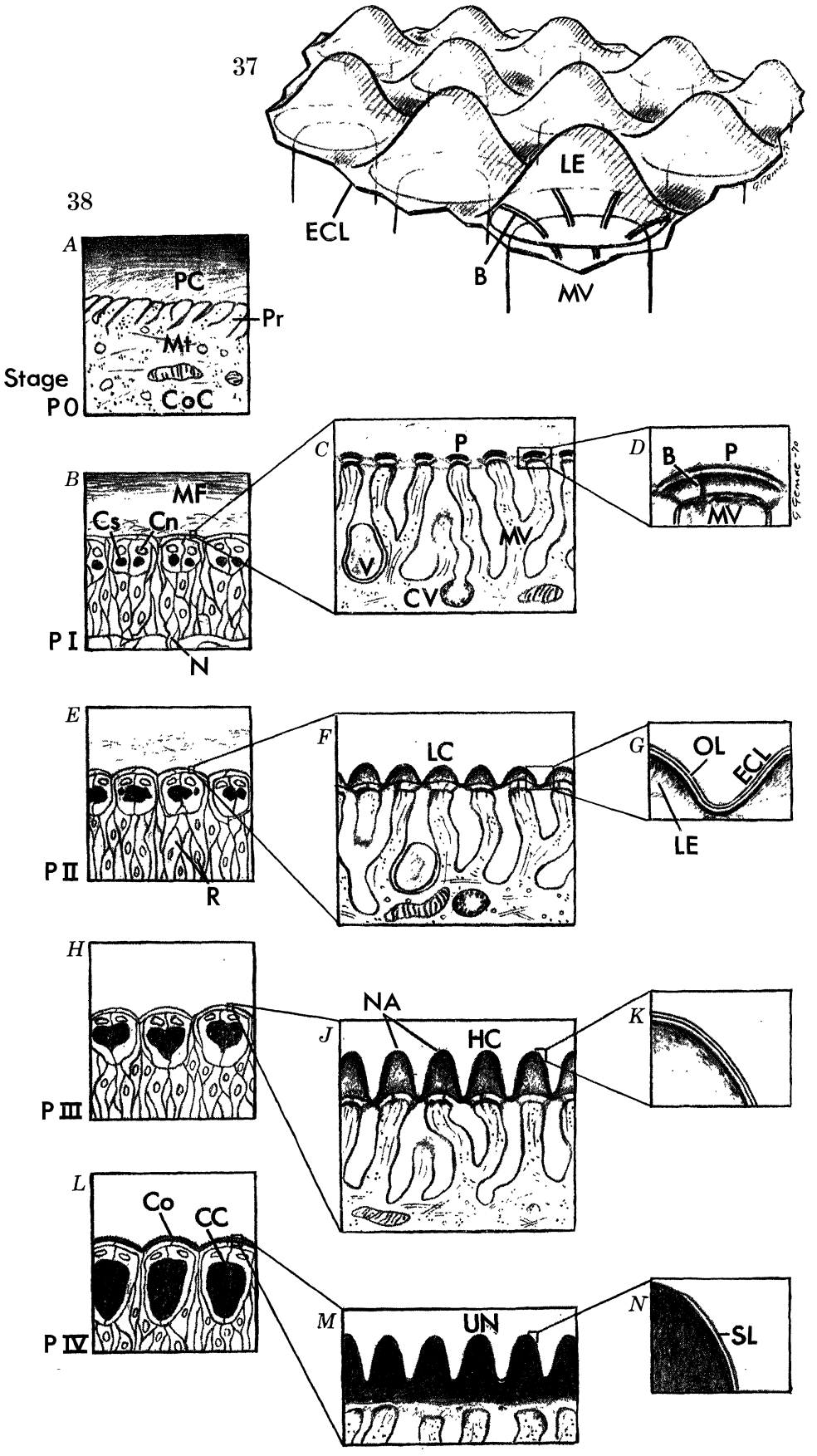

FIGURES 37 and 38. For legends see facing page

(*Facing p.* 360)

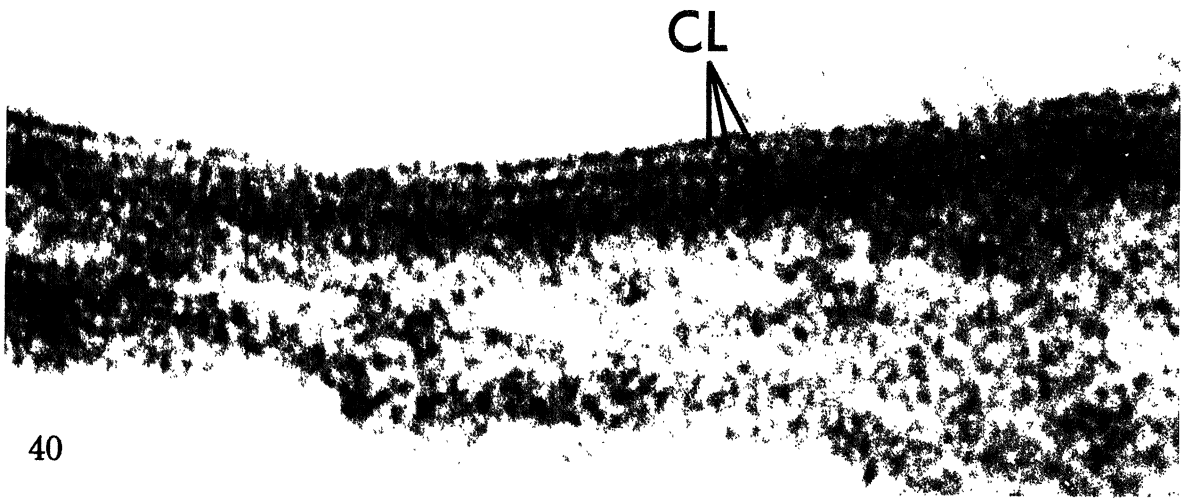

FIGURE 39. Electron micrograph of a perpendicular section through the developing body cuticle about 50 μm from the anterior rim of the eye anlage of a *Manduca sexta* pupa at stage PIII (about 7 days after pupation). The epidermal cells bear short, blunt, irregularly spaced processes. The cuticulin, extending over the tips of the processes, appears continuous in this picture. × 46500.

FIGURE 40. Electron micrograph of a perpendicular section through the cuticulin layer of the body cuticle close to the anterior rim of the eye anlage of the *Manduca* pupa at stage PIII, showing two, possibly three, dense lines, the outer two of which are about 2 nm thick. The two clear spaces are likewise about 2 nm wide. The inner line is ill-defined; its thickness can be estimated to about 10 nm. The total thickness of the extraocular cuticulin at this stage is therefore about 18 nm. × 670000.

that the superficial processes must move about and not remain stationary in one place for very long; there is, however, no direct evidence for this in the sections'. Indeed, the microvilli should remain stationary *if* the corneal surface topography of *Drosophila* arises in the way shown for the Lepidoptera in the present work, *and if* the stationariness of the microvillar tips is a prerequisite for the formation and maintenance of the position of the epicorneal membrane evaginations upon which the surface topography is based. In the electron micrographs of the quoted paper, the microvillar tips are hexagonally distributed, and their centre-to-centre distance very closely corresponds to that of the low corneal surface oscillations (not observed by Waddington & Perry). It is noteworthy that the authors arrived at the same idea as the one suggested in the present work about the importance of microvillar distribution for the formation of a regular corneal surface pattern although they did not base their considerations upon any particular case where they knew that such a pattern existed.

Whatever evolutionary pathways have been followed in the development of the nipples (for discussion see Gemne 1970), a host of evidence for the universality of certain components in insect cuticle morphogenesis seems to be accumulating. Microvilli have been shown to be present where and when cuticle formation is going on (see the previously cited papers by Locke; Rinterknecht & Levi; Filshie & Waterhouse; Noirot & Noirot-Timothée; Delachambre). At least the initial phases in the cuticle morphogenesis and in that of epicorneal structures (Gemne 1966*a*, *b*; Perry 1968) appear to be the same in all insects studied so far. It therefore seems as though the basic requirements for a common mode of formation of various types of epicorneal (or epicuticular) topography exist in the insect class. The production of the different *end* results (corneal nipples, low corneal surface protrusions in regular or irregular arrangement, body cuticle tubercles of various kinds) would depend on genetic factors.

Some further comments seem appropriate concerning the comparison between epicorneal morphogenetic events and the formation of the body cuticle outermost layers (cf. Gemne 1970). With the mechanism of growth of the cuticulin patches and of the sculpturing of the epicuticle proposed by Locke (1966), no bridges like the ones described here seem to be needed. Instead, the sculpturing of the cuticle surface arises as a result of an interplay between, on the one hand, cytoarchitectonic structures (bundles of cytoplasmic filaments, microtubules) causing the whole epidermal cell to grow in a certain way (see Locke 1967) and, on the other, the rate and mode of growth of the cuticulin patches. It seems difficult, in the case of the epicorneal lamina, to conceive of cytoarchitectonic factors, operating wholly *within* the corneagenous cell, that could maintain throughout the ontogenesis the relationship between the lamina evaginations and the microvillar tips. Instead, it seems almost necessary that some *extracellular* constraints act upon the MV/LE complex in order to produce the 'desired' effect on the ECL.

This work has been sponsored in part by the Air Force Office for Scientific Research through the European Office of Aerospace Research, OAR, United States Air Force, under grants Nos. AF EOAR 66-34 and EOOAR-68-0036, and supported by grants from the Swedish Medical Research Council, Stiftelsen Gustaf och Tyra Svenssons Minne, Wallenbergs-Stiftelsen, Svenska Sällskapet för Medicinsk Forskning, and Reservationsanslaget, Karolinska Institutet.

I am deeply indebted to Mr A. H. Baumhover, Investigations Leader, United States Department of Agriculture, ARS, ERD, Oxford Tobacco Research Station, Oxford, North Carolina, for his truly generous and considerate aid in making his laboratory and rearing facilities available to me, and for supplying the bulk of the insect material.

I also thank Drs W. E. Robbins and J. N. Kaplanis, US Department of Agriculture, ARS, ERD, Insect Physiology Laboratory, Beltsville, Md., and Drs D. L. Dahlman and R. Thurston, Department of Entomology, University of Kentucky, Lexington, Kentucky, for their help in providing part of the insect material.

For the very kind permission to use his electron microscopy facilities, I am grateful to Professor D. R. Misch, Department of Zoology, University of North Carolina, Chapel Hill, North Carolina.

The skilful technical assistance of Miss Maj-Britt Jansson, Miss Marianne Liljeros, and Mrs Gunilla Linder is most gratefully acknowledged.

Special tanks are due to Dr M. Fischler, Astra Co., Södertälje, Sweden, for the supply of Tifosyl®.

References

Baumhover, A. H. 1968 Mass rearing of tobacco hornworms. *Oxford Tobacco Research Station, Techn. Bull.* 9/9/68.

Bernhard, C. G., Gemne, G. & Møller, A. R. 1968 Modification of specular reflexion and light transmission by biological surface structures. *Quart. Rev. Biophys.* **1**, 89–105.

Bernhard, C. G., Gemne, G. & Sällström, J. 1970 Comparative ultrastructure of corneal surface topography in insects with aspects on phylogenesis and function. *Z. vergl. Physiol.* **67**, 1–25.

Bernhard, C. G. & Miller, W. H. 1962 A corneal nipple pattern in insect compound eyes. *Acta physiol. scand.* **56**, 385–386.

Bernhard, C. G., Miller, W. H. & Møller, A. R. 1963 Function of the corneal nipples in the compound eyes of insects. *Acta physiol. scand.* **58**, 381–382.

Bernhard, C. G., Miller, W. H. & Møller, A. R. 1965 The insect corneal nipple array. A biological, broad-band impedance transformer that acts as an antireflection coating. *Acta physiol. scand.* **63** (Suppl. 243), 1–79.

Delachambre, J. 1970 Étude sur l'épicuticule des insectes. I. Le développement de l'épicuticule chez l'adulte de *Tenebrio molitor* L. *Z. Zellforsch.* **108**, 380–396.

Estes, L. W. & Apicella, J. V. 1969 A rapid embedding technique for electron microscopy. *Lab. Invest.* **20** (2), 159–163.

Filshie, B. K. 1970 The resistance of epicuticular components of an insect to extraction with lipid solvents. *Tissue & Cell* **2** (1), 181–190.

Filshie, B. K. & Waterhouse, D. F. 1969 The structure and development of a surface pattern on the cuticle of the green vegetable bug *Nezara viridula*. *Tissue & Cell* **1** (2), 367–385.

Fyhn, H. J. & Saether, T. 1970 Regulation of the haemolymph osmolality during metamorphosis in the oak silk moth, *Antherea pernyi*. *J. Insect Physiol.* **16**, 263–269.

Gemne, G. 1966*a* Ultrastructural ontogenesis of cornea and corneal nipples in the compound eye of insects. *Acta physiol. scand.* **66**, 511–512.

Gemne, G. 1966*b* Fine structure of the insect cornea and corneal nipples during ontogenesis. In *Electron microscopy* 1966, *Proc. 6th Int. Congr. El. Micr., Kyoto* vol. II, pp. 511–512. Tokyo: Maruzen Co.

Gemne, G. 1970 Ultrastructure of epicorneal topography and morphogenesis in insects with aspects on phylogenesis and function. Thesis, Karolinska Institutet, Stockholm, Sweden.

Haydon, G. B. 1968 On the interpretation of high resolution micrographs of macromolecules. *J. Ultrastruct. Res.* **25**, 349–361.

Hinton, H. E. 1946 Concealed phases in the metamorphosis of insects. *Nature, Lond.* **157**, 552–553.

Hoffman, J. D., Lawson, F. R. & Yamamoto, R. 1966 Tobacco Hornworms. In *Insect colonization and mass production* (ed. C. N. Smith), pp. 479–486. New York: Academic Press.

Hoy, R. R., Bittner, G. D. & Kennedy, D. 1967 Regeneration in crustacean motoneurons: evidence for axonal fusion. *Science, N.Y.* **156**, 251–252.

Karlsson, U. & Schultz, R. S. 1965 Fixation of the central nervous system for electron microscopy by aldehyde perfusion. I. Preservation with aldehyde perfusates versus direct perfusion with osmium tetroxide with special reference to membranes and the extracellular space. *J. Ultrastruct. Res.* **12** (1/2), 160–186.

Locke, M. 1966 The structure and formation of the cuticulin layer in the epicuticle of an insect, *Calpodes ethlius* (Lepidoptera, Hesperiidae). *J. Morph.* **118** (4), 461–494.

Locke, M. 1967 What every epidermal cell knows. In *Insects and physiology* (eds. J. W. L. Beament and J. E. Treherne), vol. 7, pp. 69–82. Edinburgh and London: Oliver and Boyd.

Locke, M. 1969 The structure of an epidermal cell during the development of the protein cuticle and the uptake of molting fluid in an insect (*Calpodes ethlius*). *J. Morph.* **127** (1), 7–40.

Locke, M. 1970 The molt/intermolt cycle in the epidermis and other tissues of an insect *Calpodes ethlius* (Lepidoptera, Hesperiidae). *Tissue & Cell* **2** (2), 197–223.

Miller, W. H., Møller, A. R. & Bernhard, C. G. 1966 The corneal nipple array. In *The functional organization of the compound eye* (ed. C. G. Bernhard), pp. 21–33. London: Pergamon Press.

Moor, H. & Mühlethaler, K. 1963 Fine structure in frozen-etched yeast cells. *J. Cell Biol.* **17** (3), 609–628.
Noirot, Ch. & Noirot-Timothée, C. 1969 La cuticule proctodéale des Insectes. I. Ultrastructure comparée. *Z. Zellforsch.* **101**, 477–509.
Palade, G. E. & Bruns, R. R. 1968 Structural modulations of plasmalemmal vesicles. *J. Cell Biol.* **37** (3), 633–649.
Peachey, L. D. 1958 Thin sections. I. A study of section thickness and physical distortion produced during microtomy. *J. biophys. biochem. Cytol.* **4**, 233–242.
Perry, M. M. 1968 Further studies on the development of the eye of *Drosophila melanogaster*. I. The ommatidia. *J. Morph.* **124**, 227–248.
Reynolds, E. S. 1963 The use of lead citrate of high pH as an electron-opaque stain in electron microscopy. *J. Cell Biol.* **17**, 208–213.
Rinterknecht, E. & Levi, P. 1966 Étude au microscope électronique du cycle cuticulaire au cours du 4ème stade larvaire chez *Locusta migratoria*. *Z. Zellforsch.* **72**, 390–407.
Roeder, K. D. (ed.) 1953 *Insect physiology*. New York: Wiley and Sons, Inc.
Roth, T. F. & Porter, K. R. 1962 Specialized sites on the cell surface for protein uptake. In *Proc. 5th Int. Conf. El. Micr.* (ed. S. S. Breese, Jr.), vol. 2, LL-4. New York and London: Academic Press.
Roth, T. F. & Porter, K. R. 1964 Yolk protein uptake in the oocyte of the mosquito, *Aedes aegypti* L. *J. Cell Biol.* **20**, 313–332.
Ryter, A. & Kellenberger, E. 1958 L'inclusion au polyester pour l'ultramicrotomie. *J. Ultrastruct. Res.* **2**, 200–214.
Snell, F. M., Shulman, S., Spencer, R. P. & Moos, C. 1965 *Biophysical principles of structure and function*. Reading, Mass.: Addison-Wesley Publ. Co.
Stempak, J. G. & Ward, R. T. 1964 An improved staining method for electron microscopy. *J. Cell Biol.* **22** (3), 697–701.
Waddington, C. H. & Perry, M. M. 1960 The ultra-structure of the developing eye of *Drosophila*. *Proc. Roy. Soc. Lond.* B. **153**, 155–178.
Weis-Fogh, T. 1970 Structure and formation of insect cuticle. In *Insect ultrastructure* (ed. A. C. Neville), *Symp. Roy. Entom. Soc. London* **5**, 165–185. Oxford and Edinburgh: Blackwell Scientific Publications.
Wigglesworth, V. B. 1965 *The principles of insect physiology*. London: Methuen Co.
Williams, N. E. & Luft, J. H. 1968 Use of a nitrogen mustard derivative in fixation for electron microscopy and observations on the ultrastructure of *Tetrahymena*. *J. Ultrastruct. Res.* **25**, 271–292.
Wolsky, A. 1949 The growth and differentiation of the retinular cells in the compound eye of the silkworm (*Bombyx mori* L.). In *Proc. 6th Int. Congr. Expl. Cytol.*, Stockholm 1947 (Casparsson, T. and Monné, L. eds.), *Expl Cell Res.*, Suppl. 1, 549–554.
Yagi, N. & Koyama, N. 1963 *The compound eye of Lepidoptera*. Tokyo: Maruzen Co.

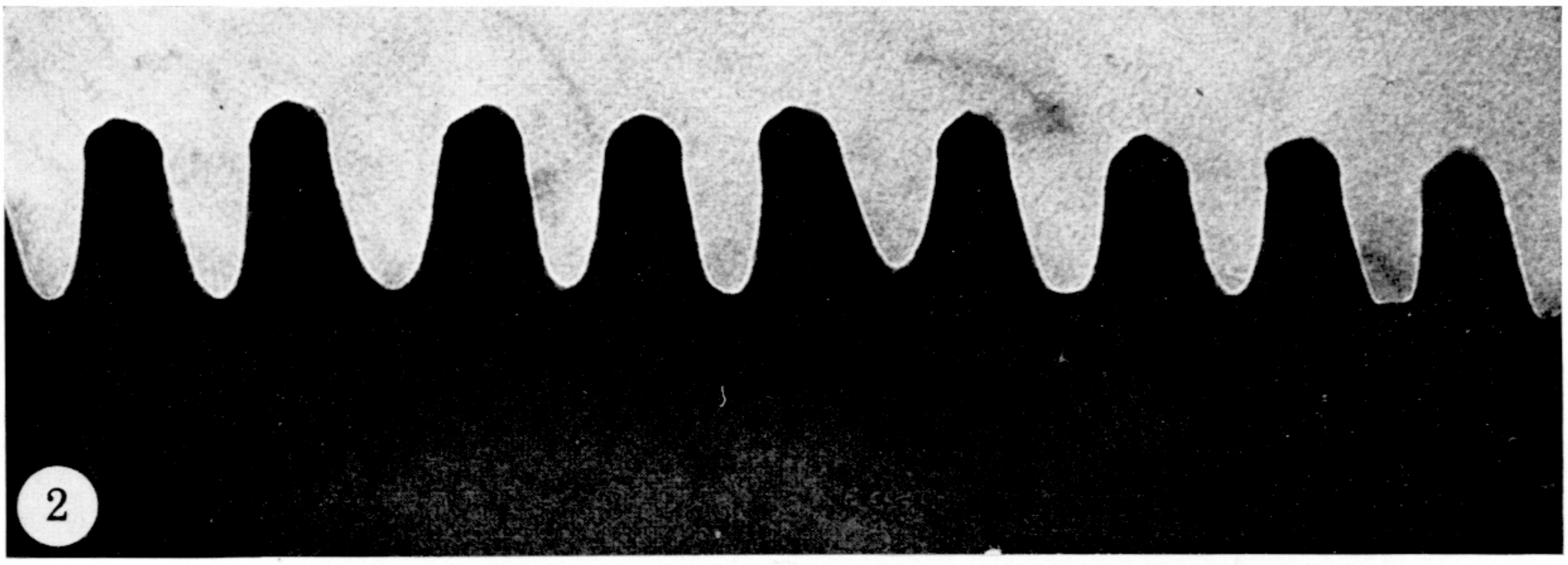

FIGURES 2 and 3. For legends see facing page

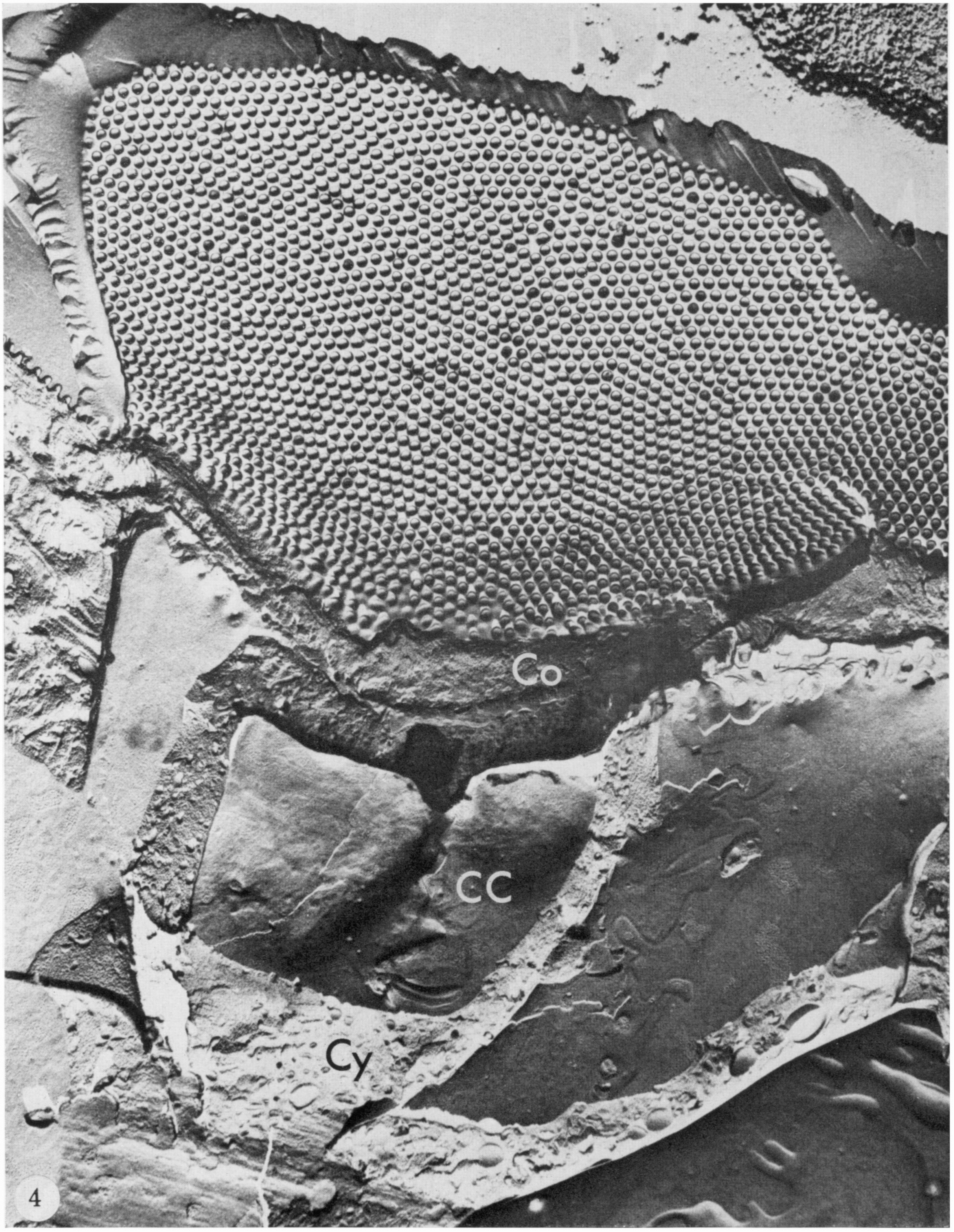

FIGURE 4. Electron micrograph of the same freeze-etching replica as in figure 3. The fracture has passed tangential to part of the corneal surface. The nipple array has been exposed and is seen in a bird's-eye view. The distance between the nipple tips averages about 195 nm. There are about 40 nipples per μm^2, giving a total of about 30000 on one facet, the diameter of which is about 30 μm. The arrangement of the nipples is only roughly hexagonal, the imperfections being due to the fact that the cornea is convex. (CC, crystalline cone; Co, cornea; Cy, cytoplasm of crystalline cone cell.) The direction of platinum evaporation is from 5 to 11 o'clock. × 13400.

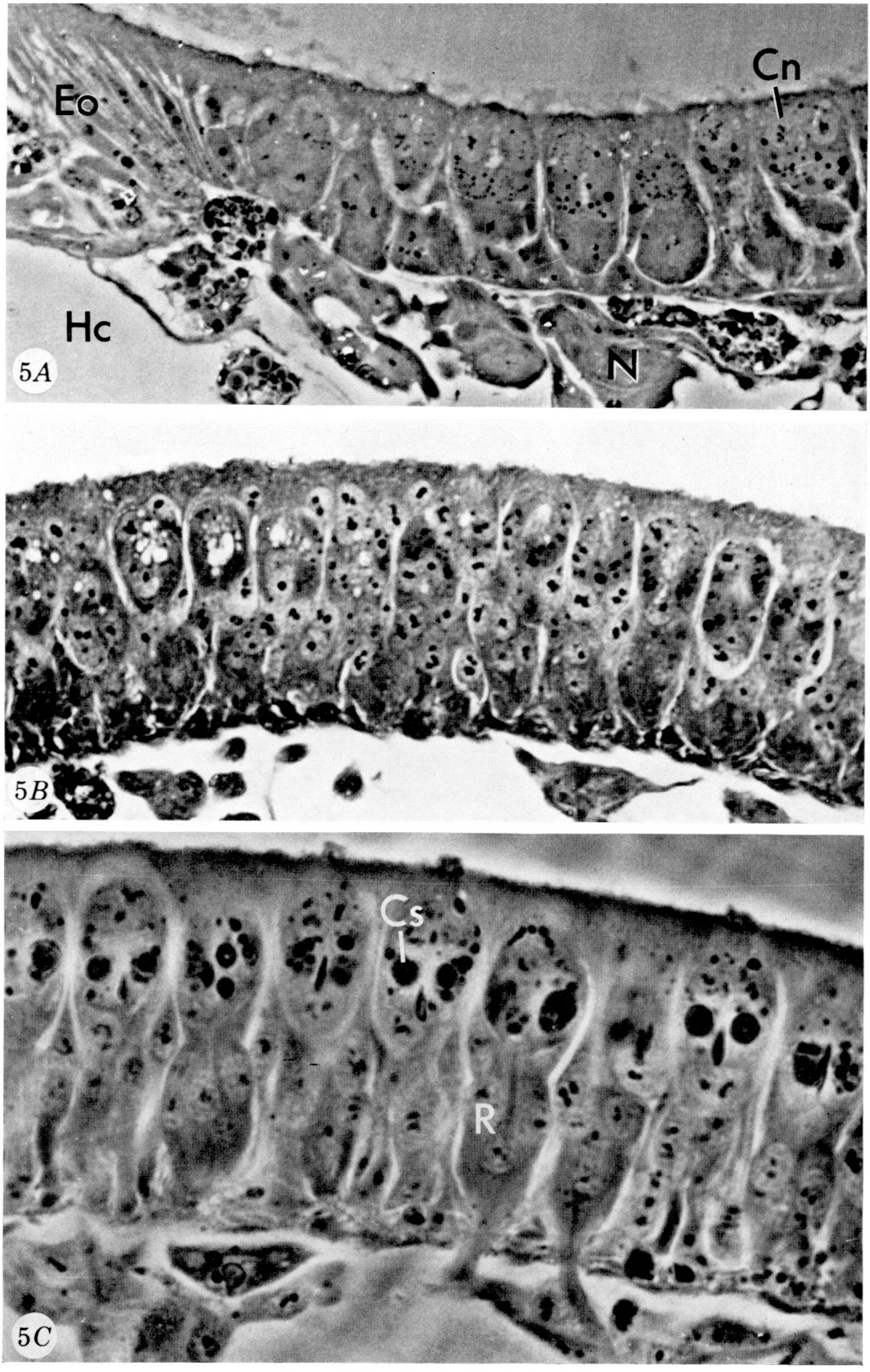

FIGURE 5. For legend see facing page

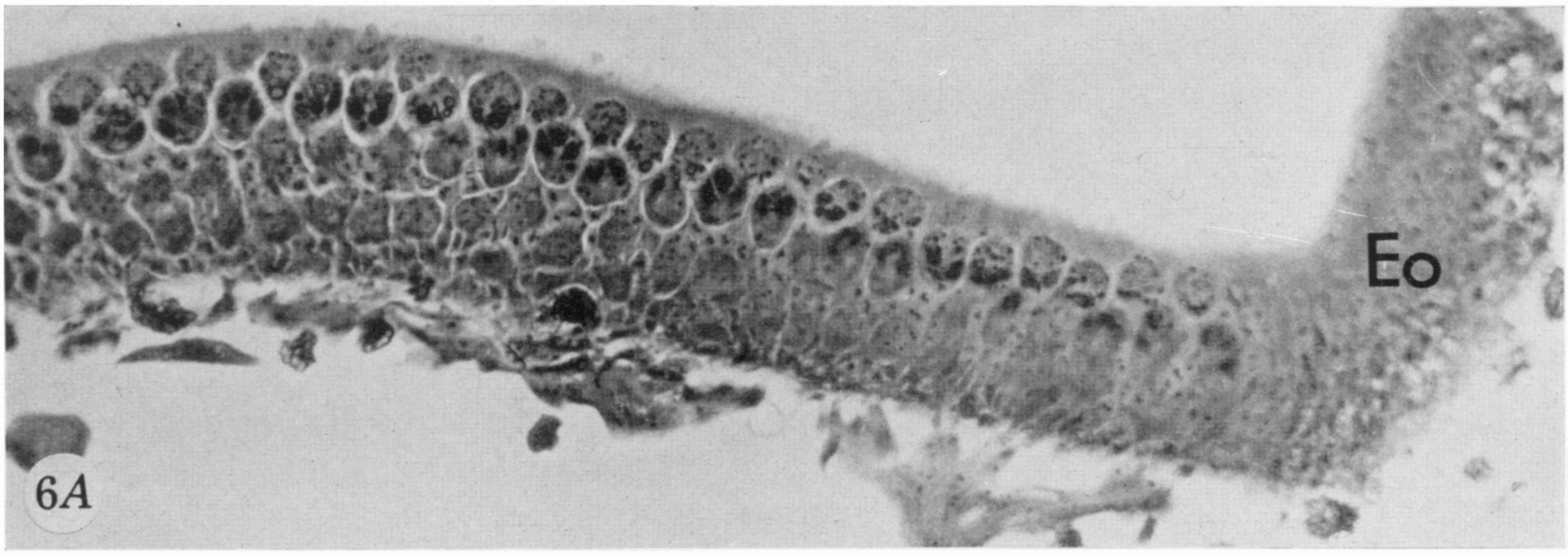

6A

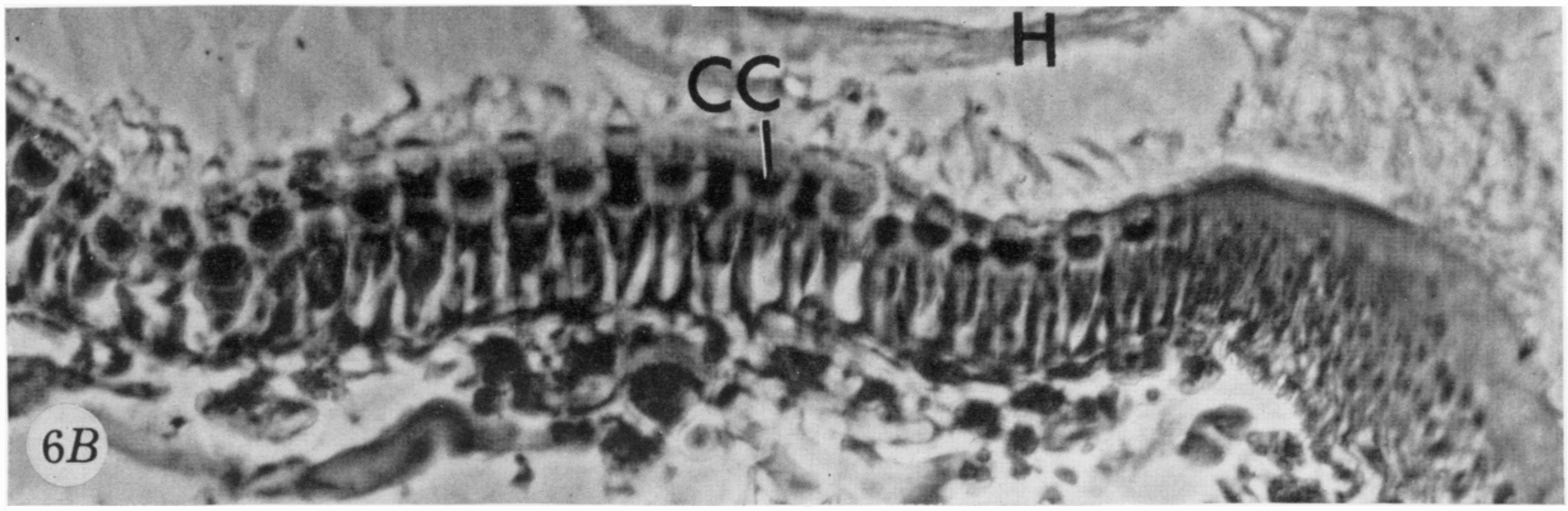

6B

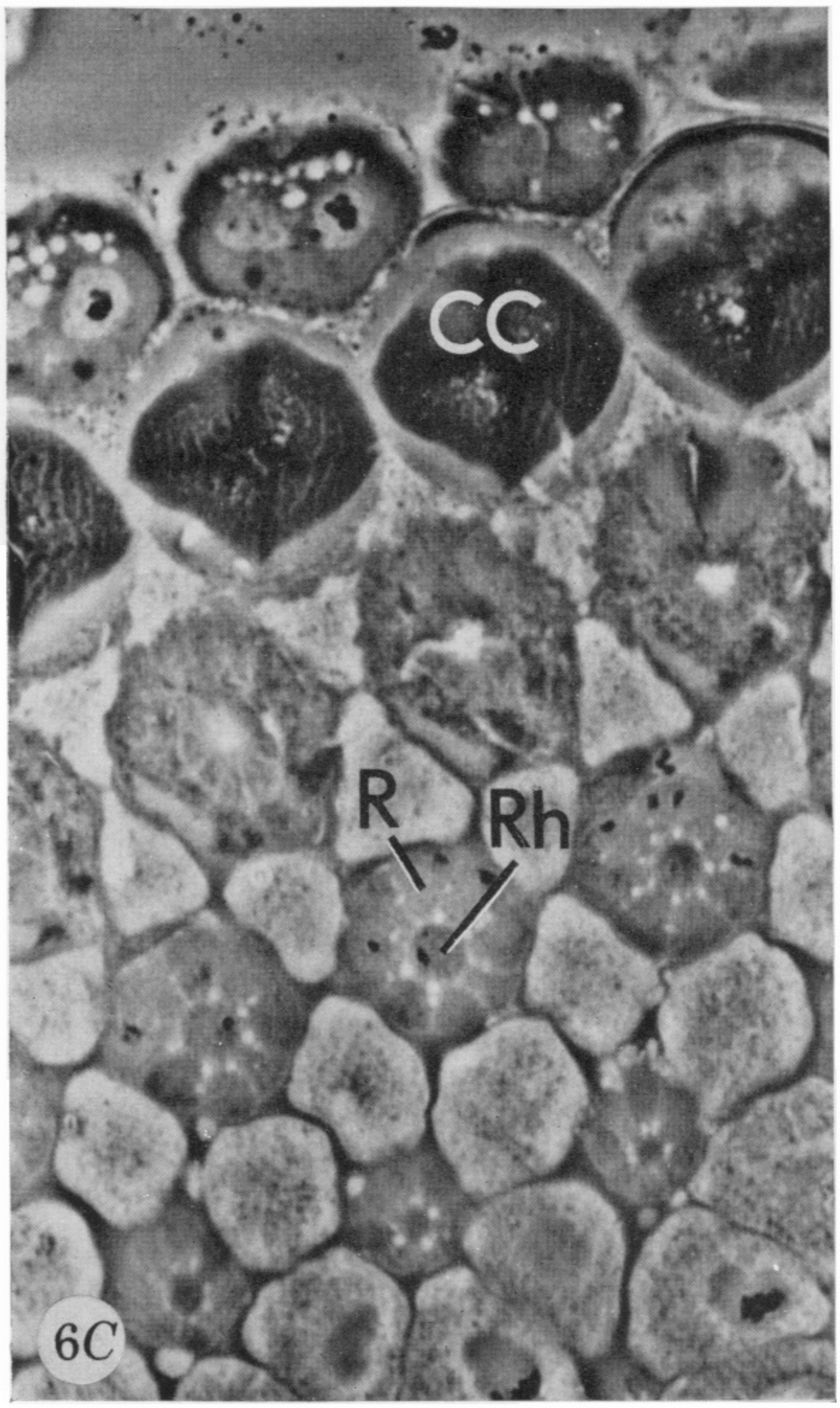

6C

6D

FIGURE 6. For legend see facing page

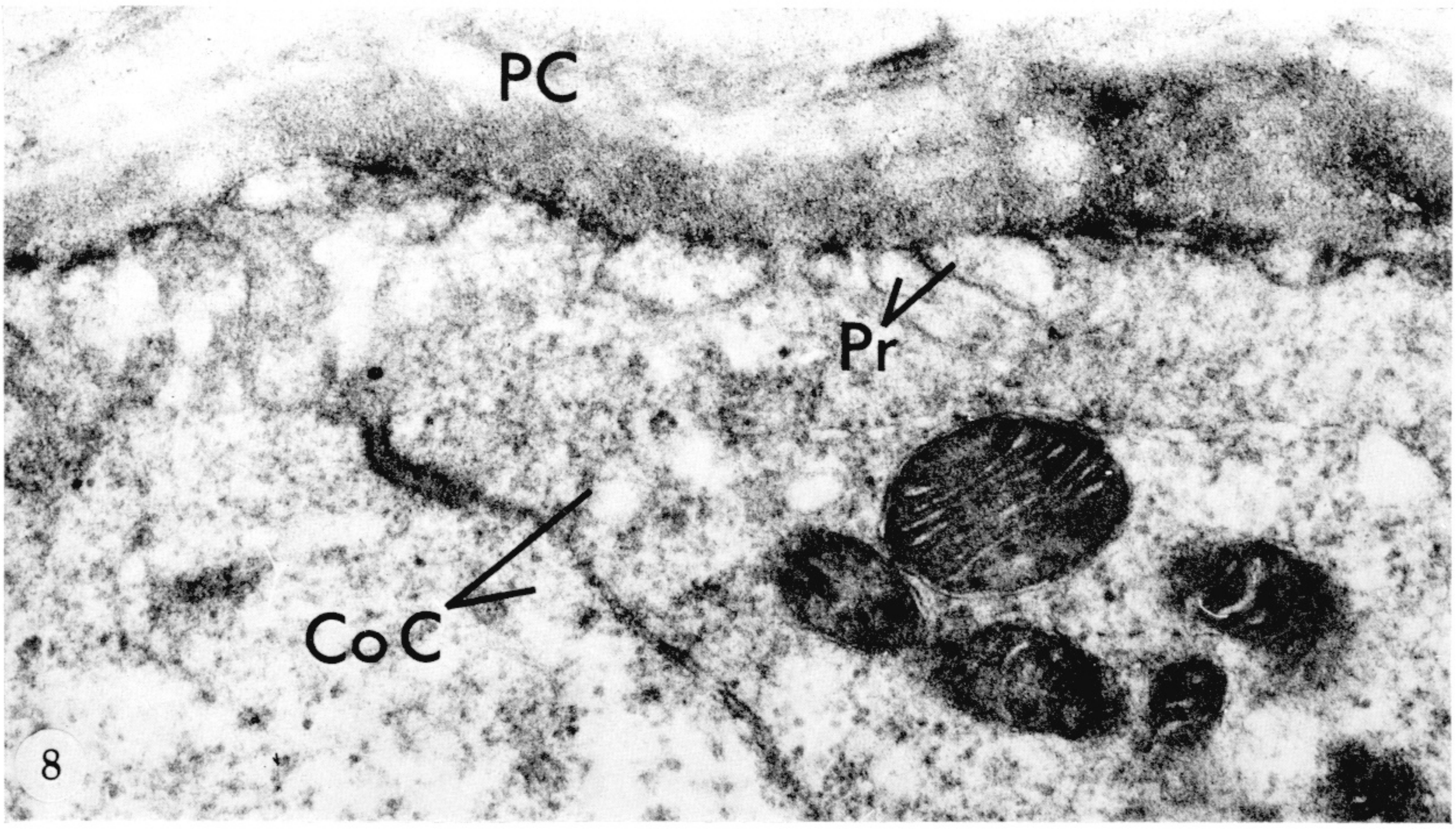

FIGURES 7 and 8. For legends see facing page

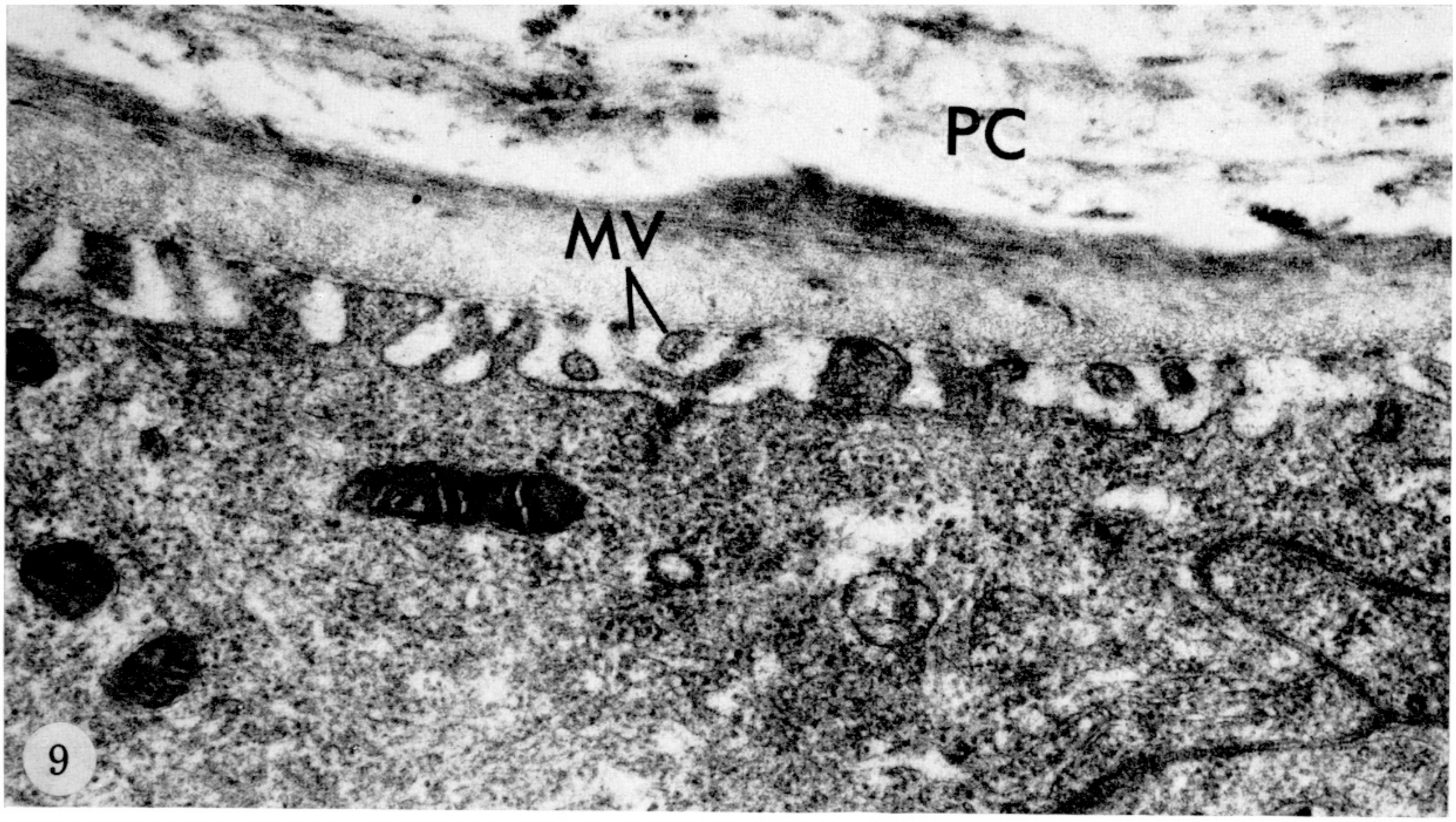

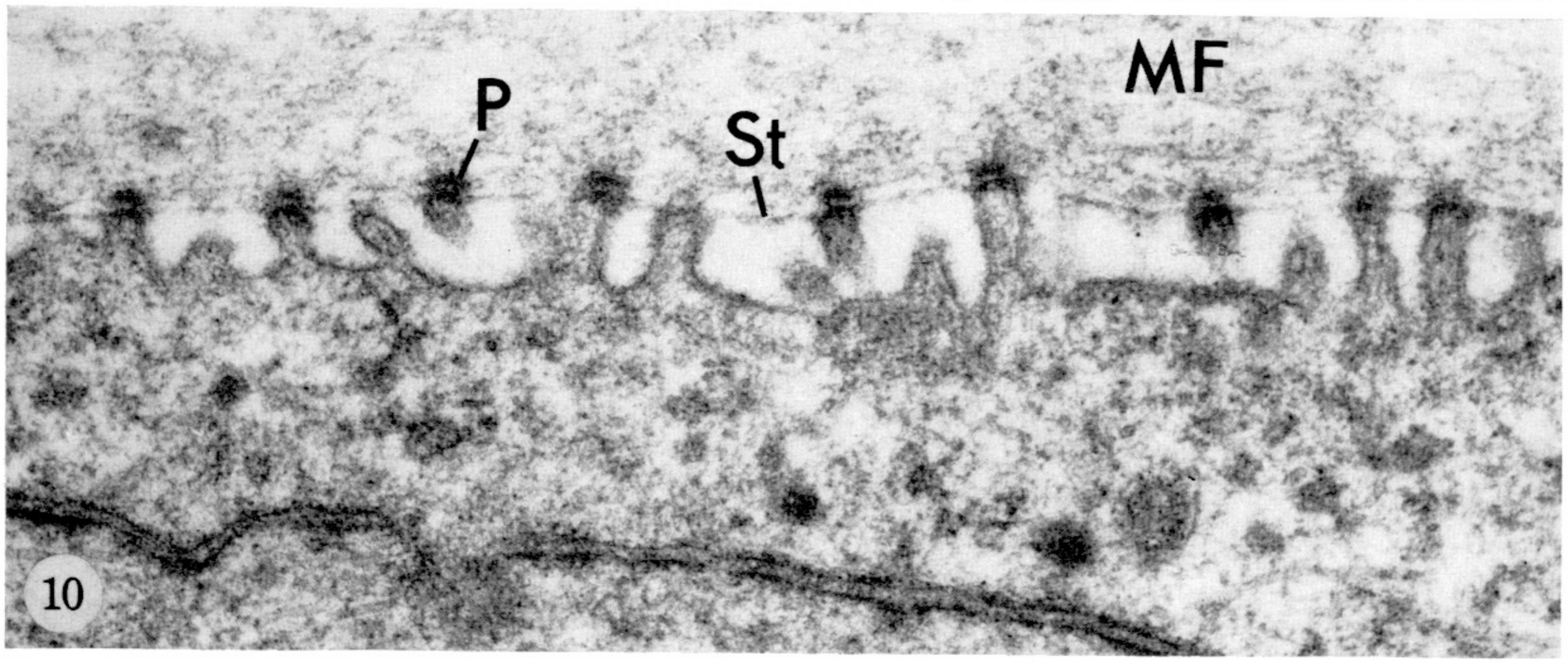

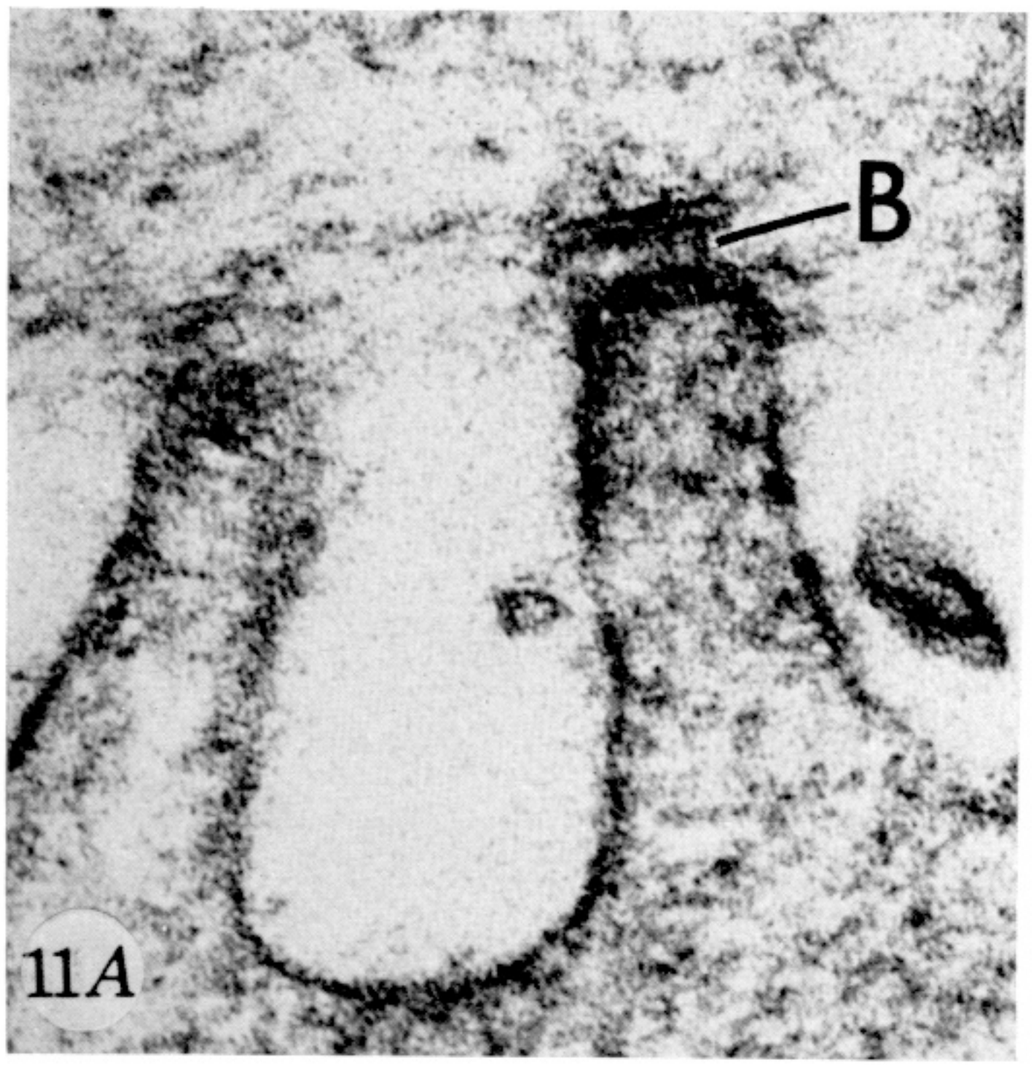

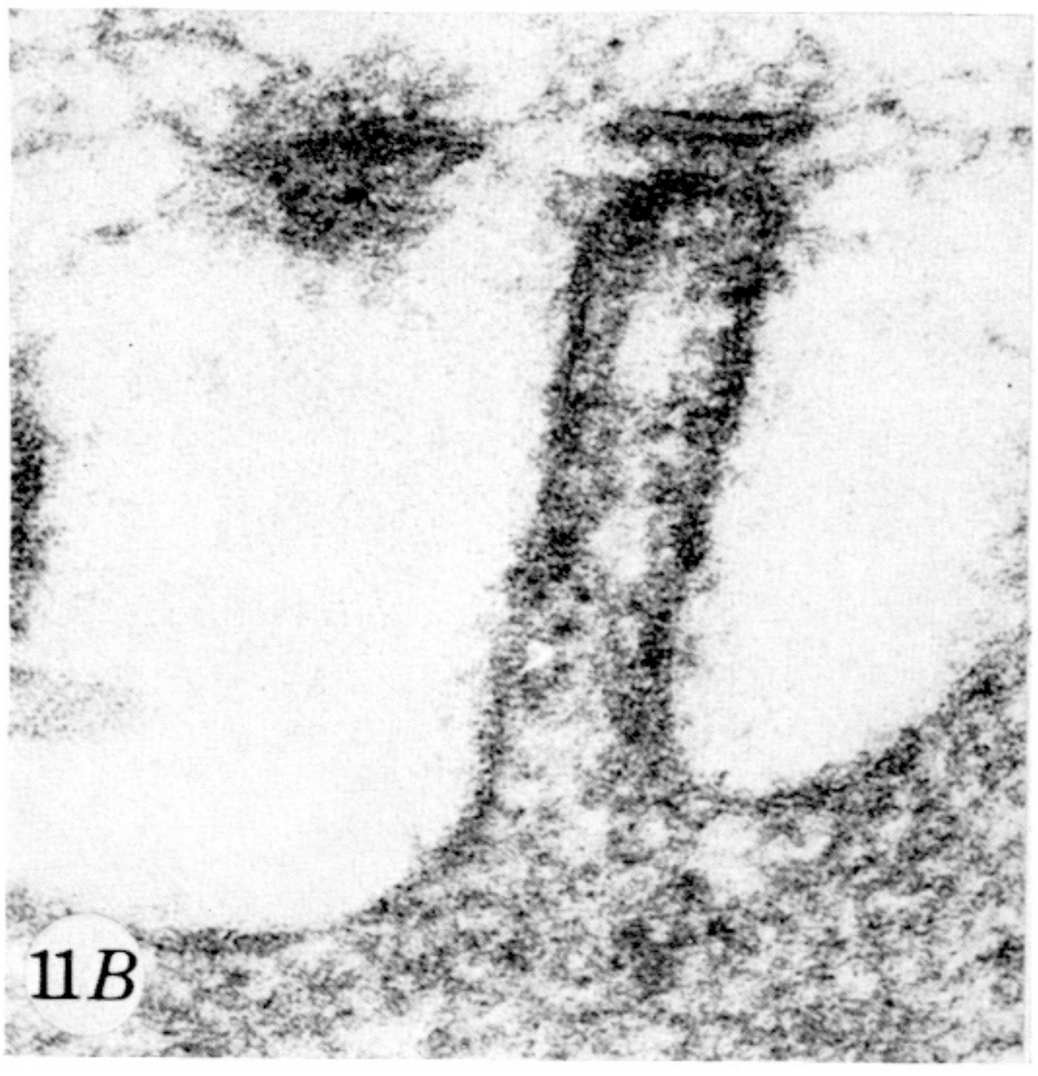

FIGURES 9 to 11. For legends see facing page

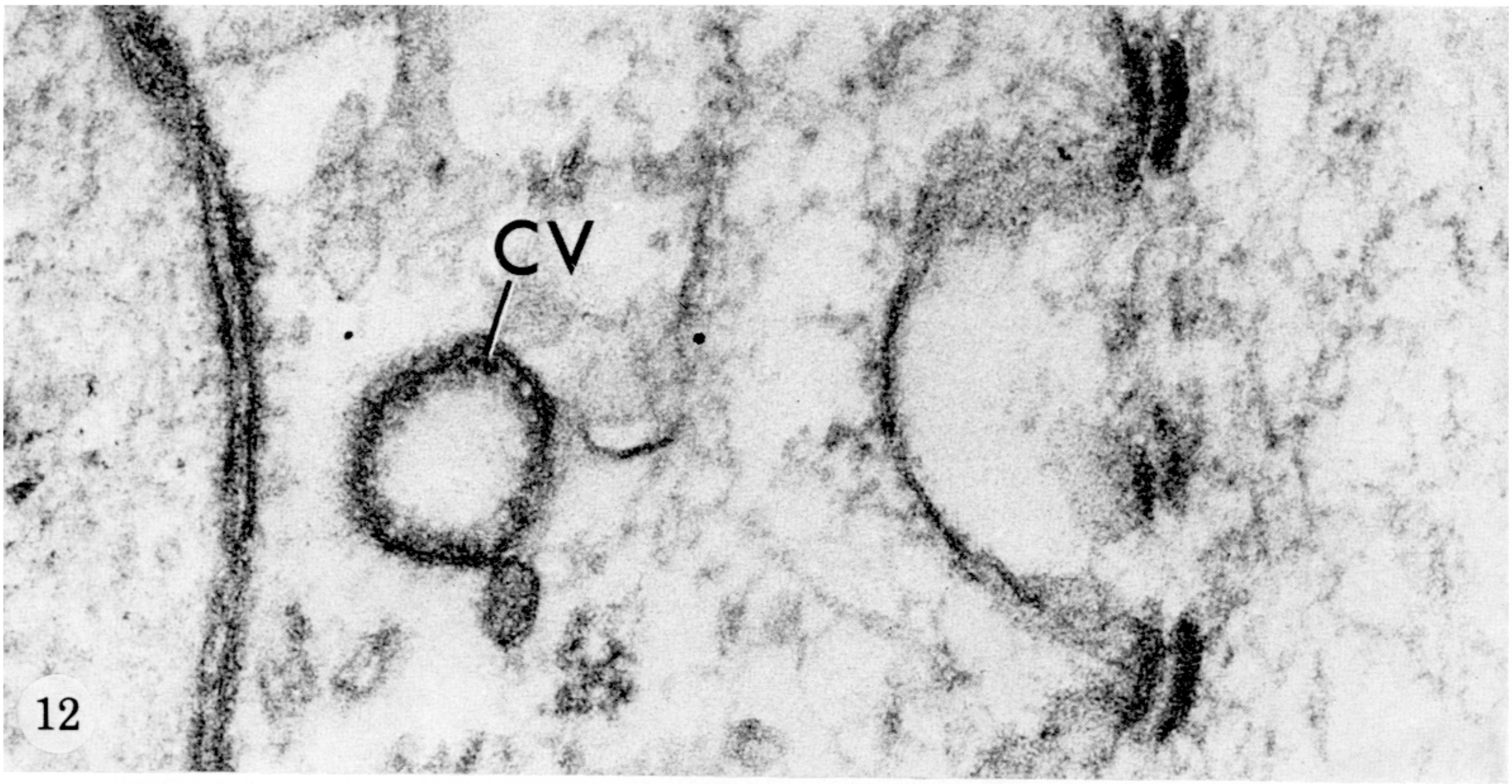

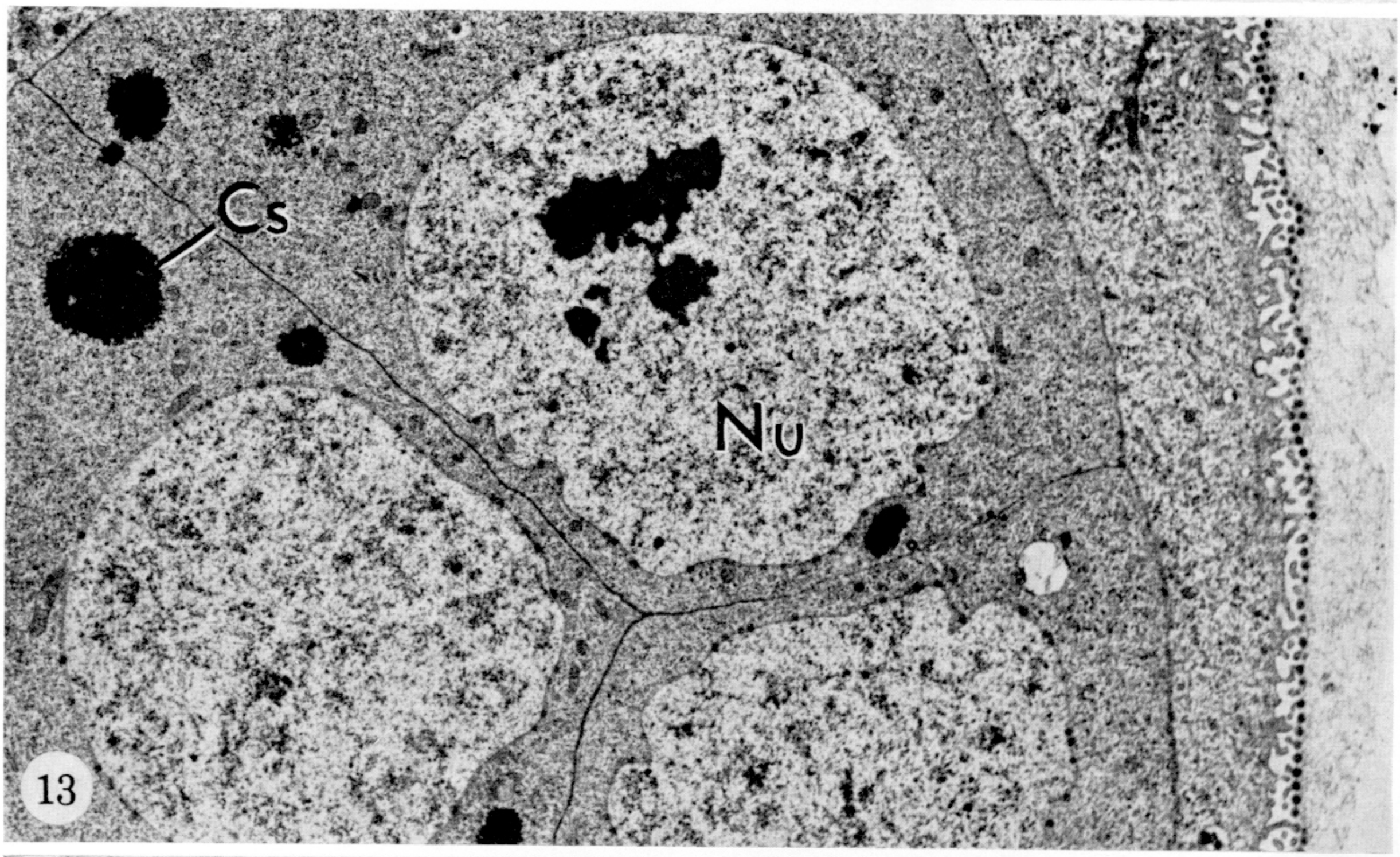

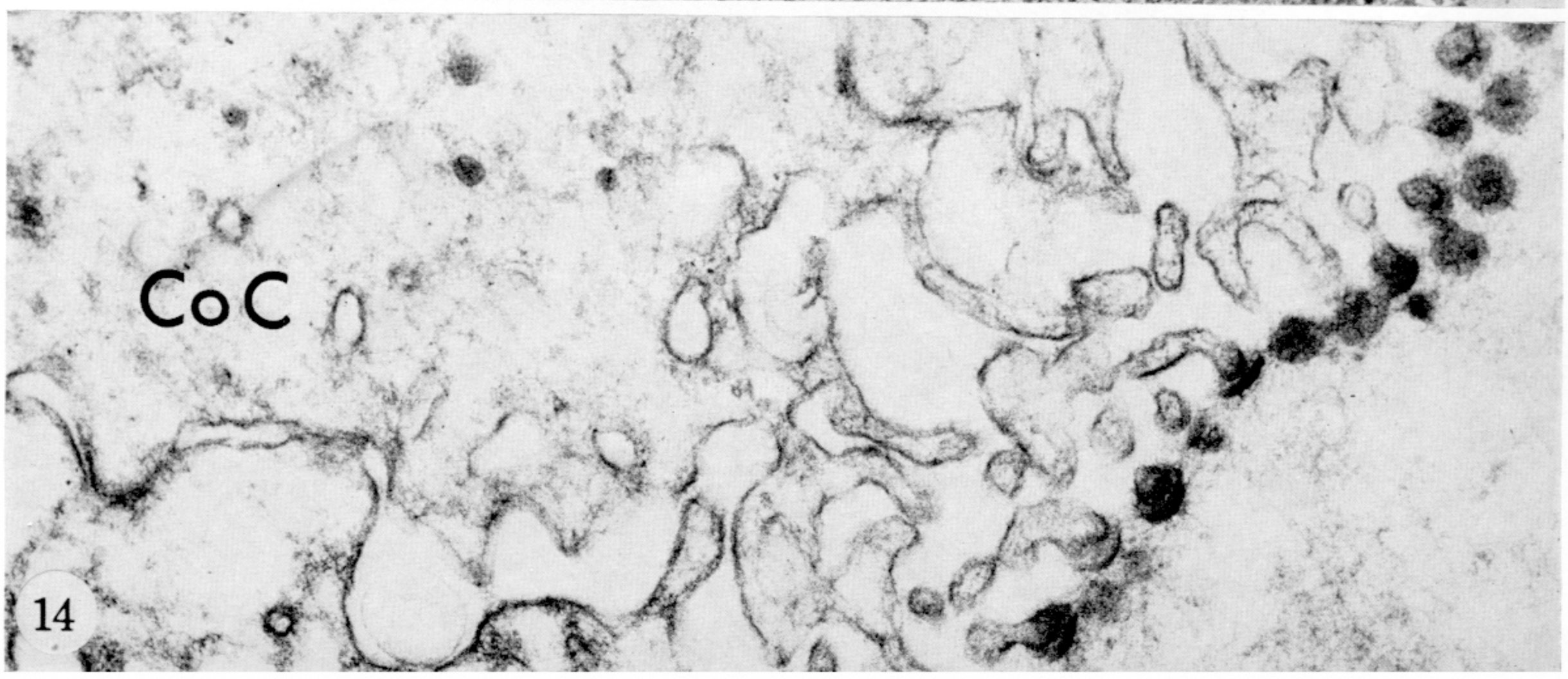

FIGURES 12 to 14. For legends see facing page

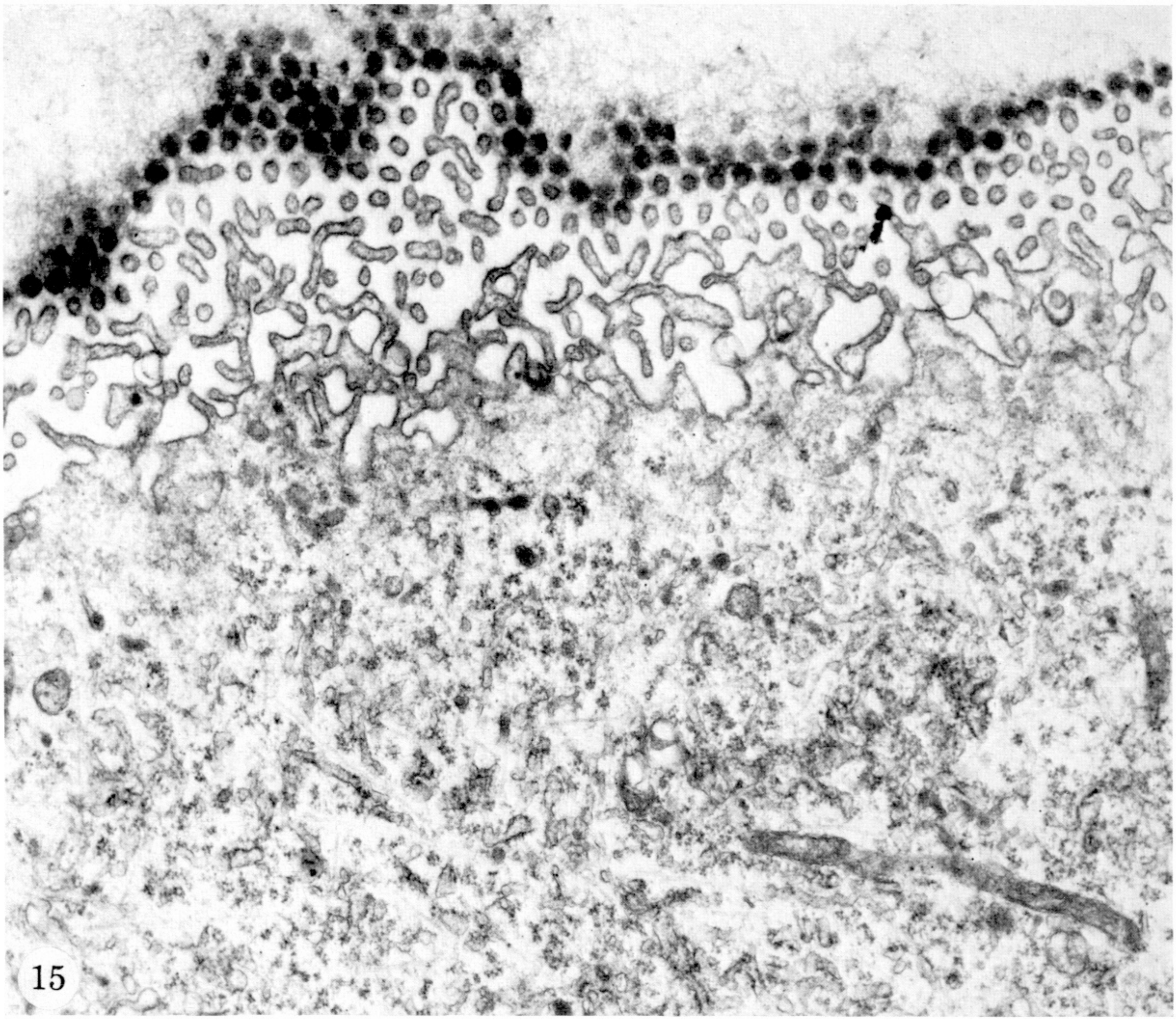

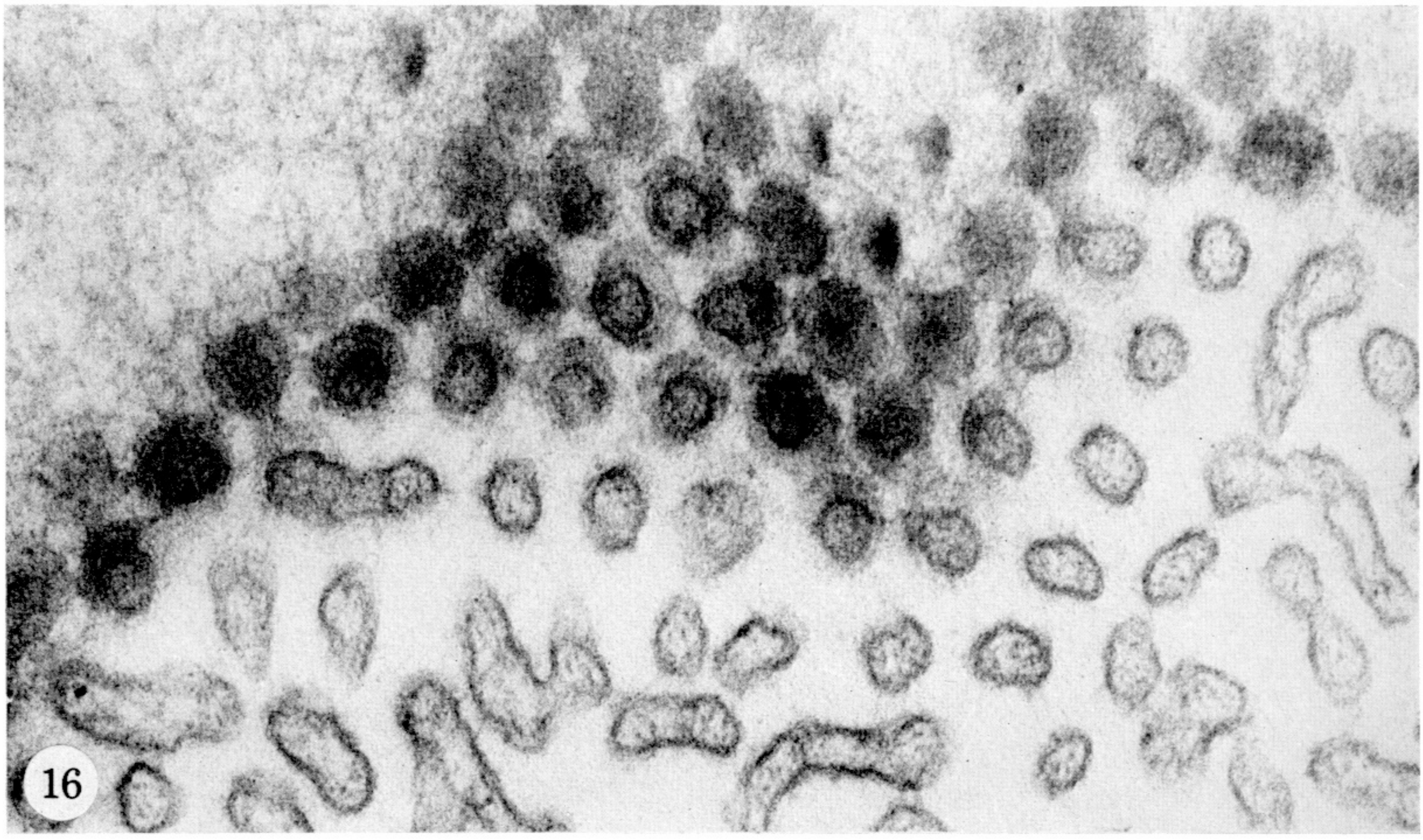

FIGURE 15. Electron micrograph of a section through the eye anlage of a *Manduca sexta* pupa similar to the sections of figures 13, 14, showing the hexagonal array of the epicorneal membrane patches. × 26400.

FIGURE 16. Higher magnification of the top left area of the section in figure 15, showing the relations of the microvillar tips to the ECL patches and the diffuse substance connecting the individual MV/LE complexes. The cross-sectioned microvilli are approximately 30 nm in diameter and contain a number of thin filaments. × 82000.

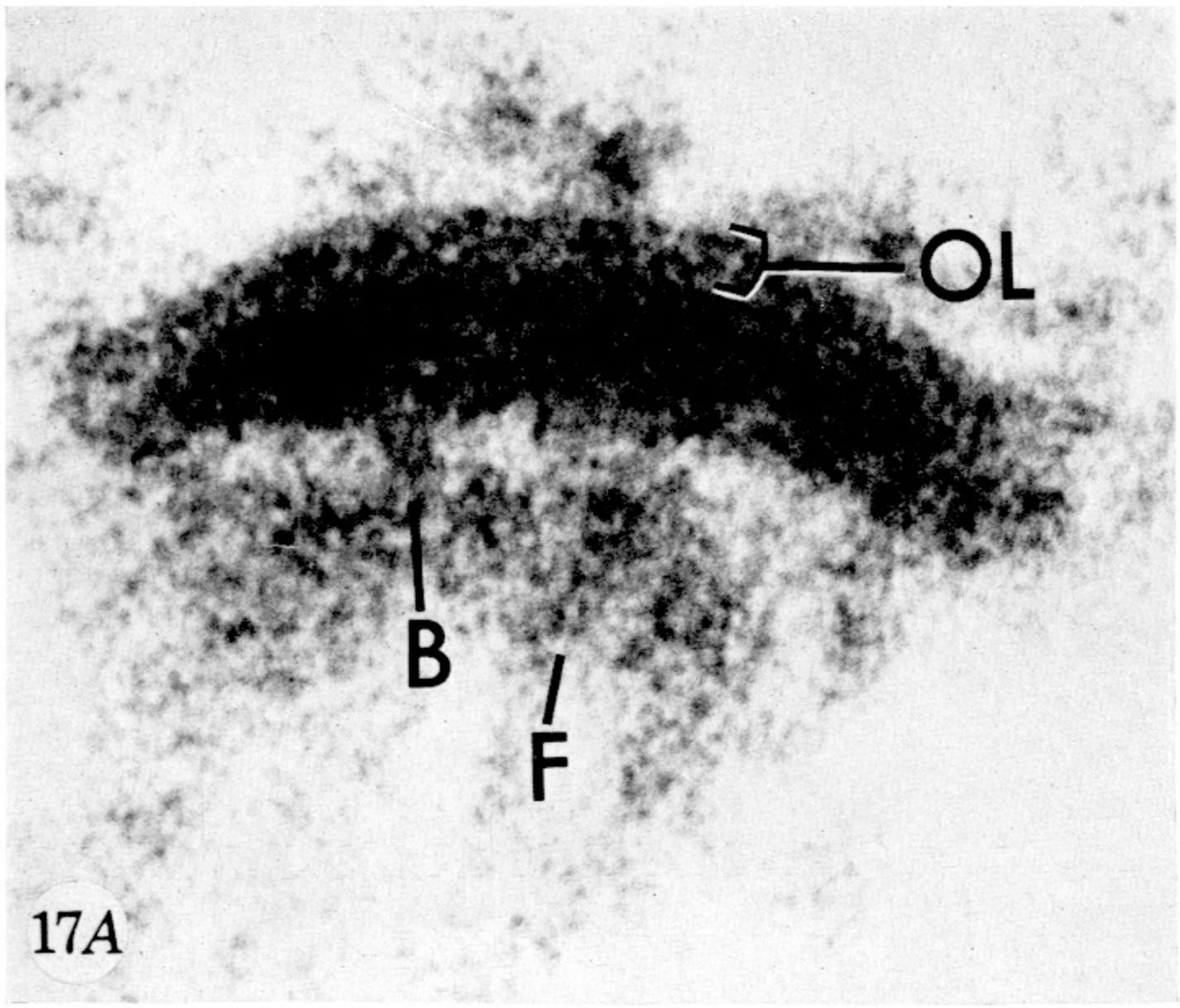

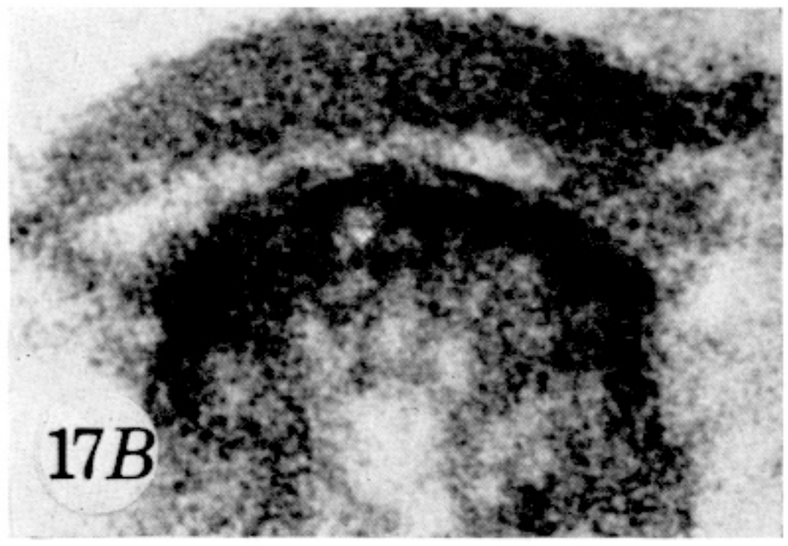

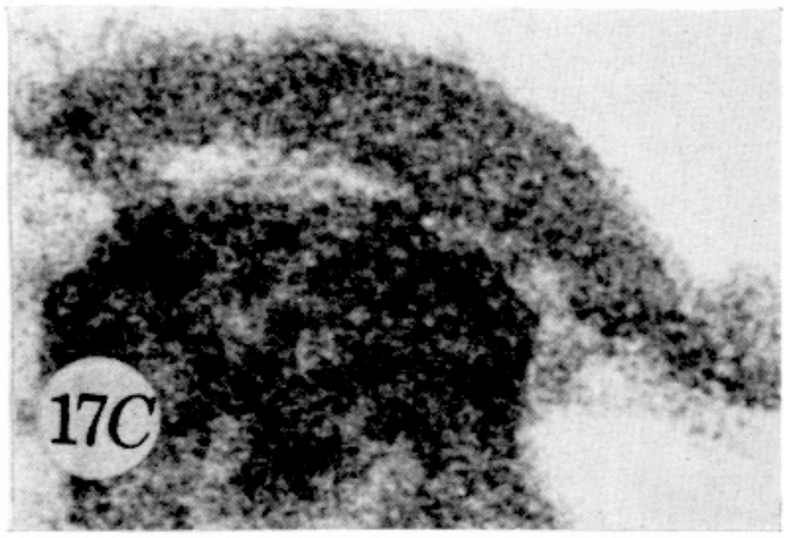

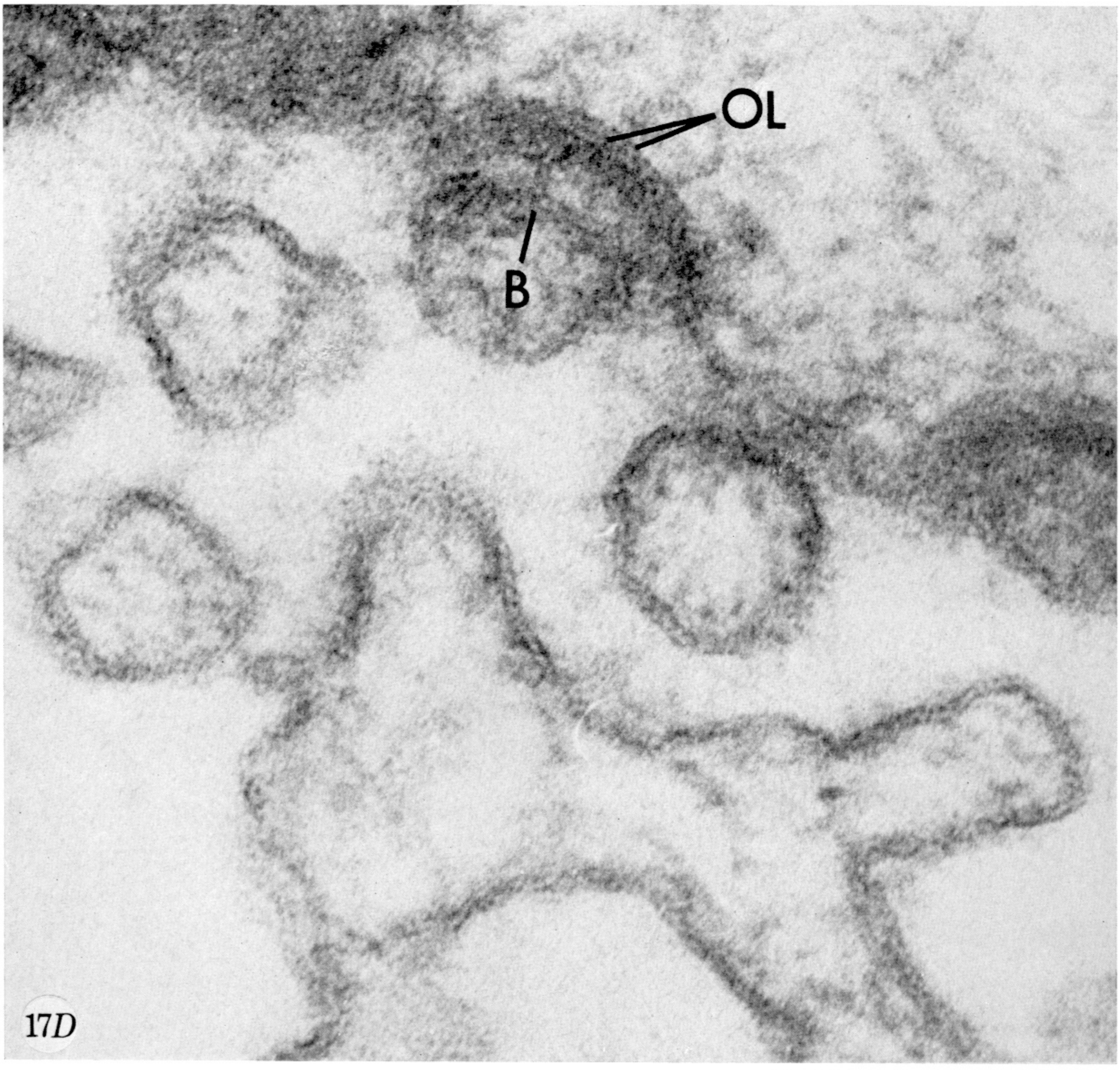

FIGURE 17. For legend see facing page

FIGURE 18. Survey electron micrograph of an oblique section through the eye anlage of a stage PI to II pupa of *Manduca sexta*. The clumps of crystalline cone substance are in the process of fusing to larger aggregates. The cytoplasm of the corneagenous cells with their fringe of microvilli is approximately 0.5 μm wide. × 5400.

FIGURE 19. Electron micrograph of a perpendicular section through the eye anlage of an approximately 5½-day-old pupa of *Manduca sexta*, showing a continuous epicorneal lamina formed by the coalesced patches of the preceding stage. The lamina evaginations (LE) appear in the section as domes about 65 nm high with an apical centre-to-centre distance of about 190 nm. The MV average 90 nm in diameter and 500 nm in length. × 47500.

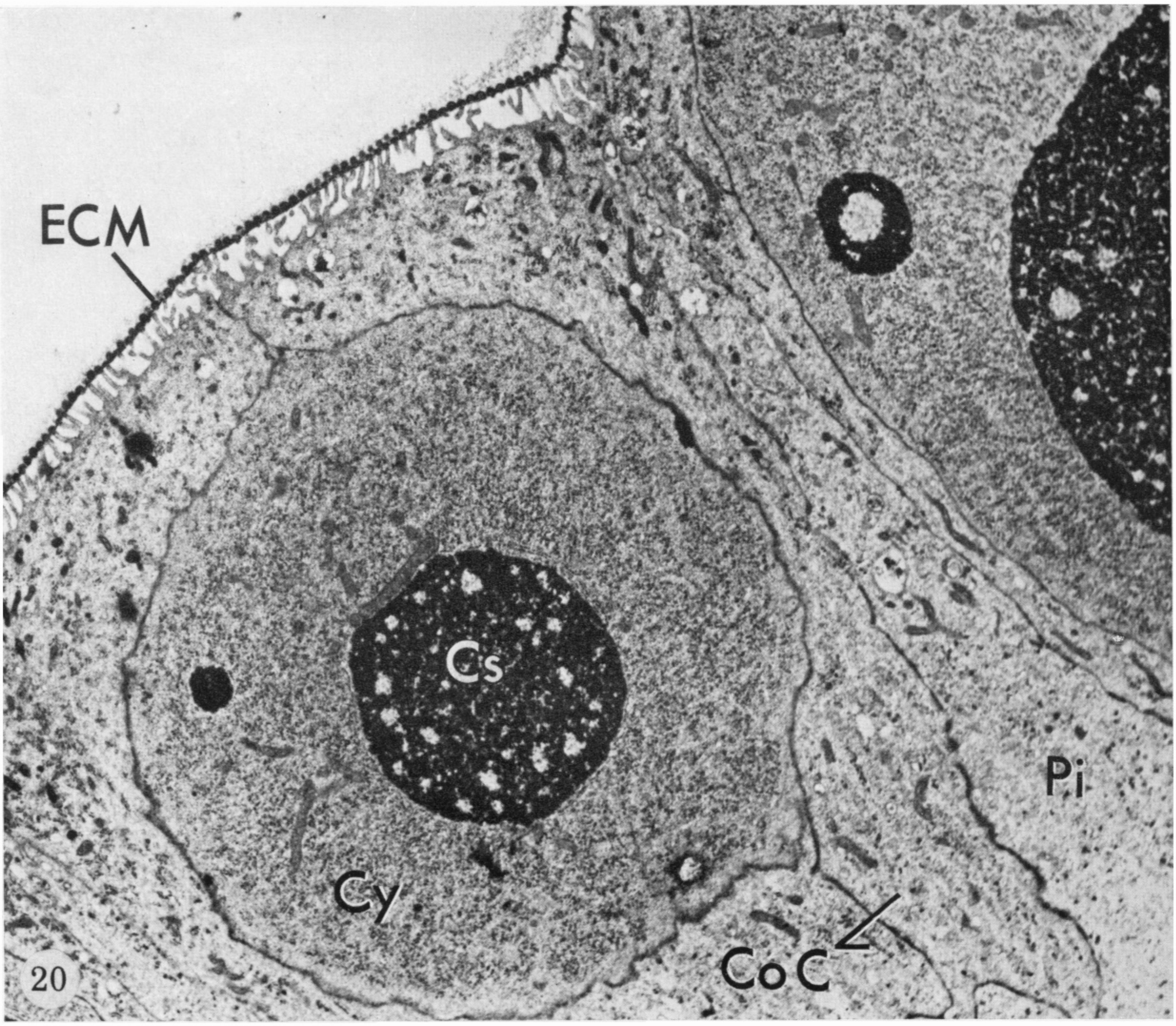

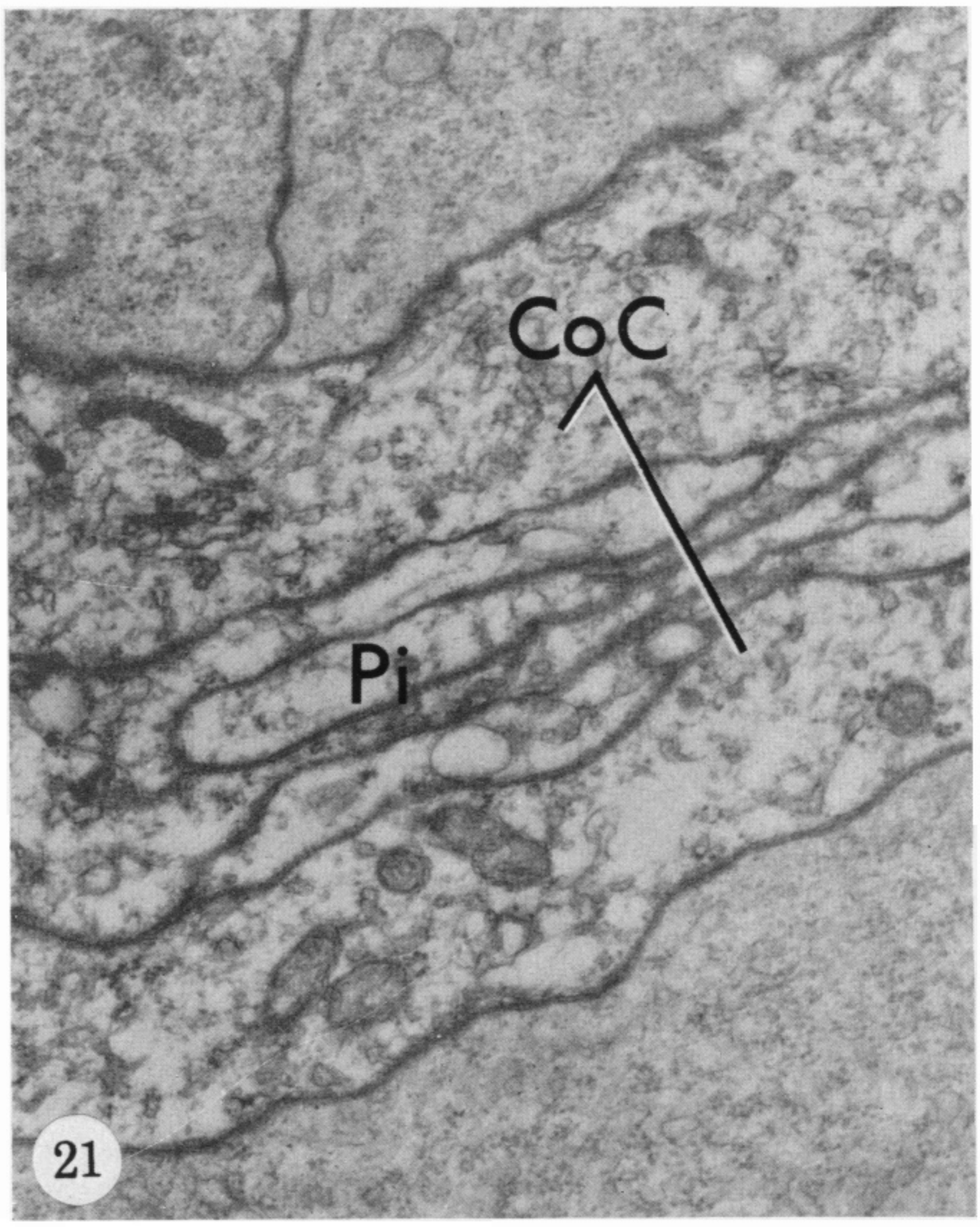

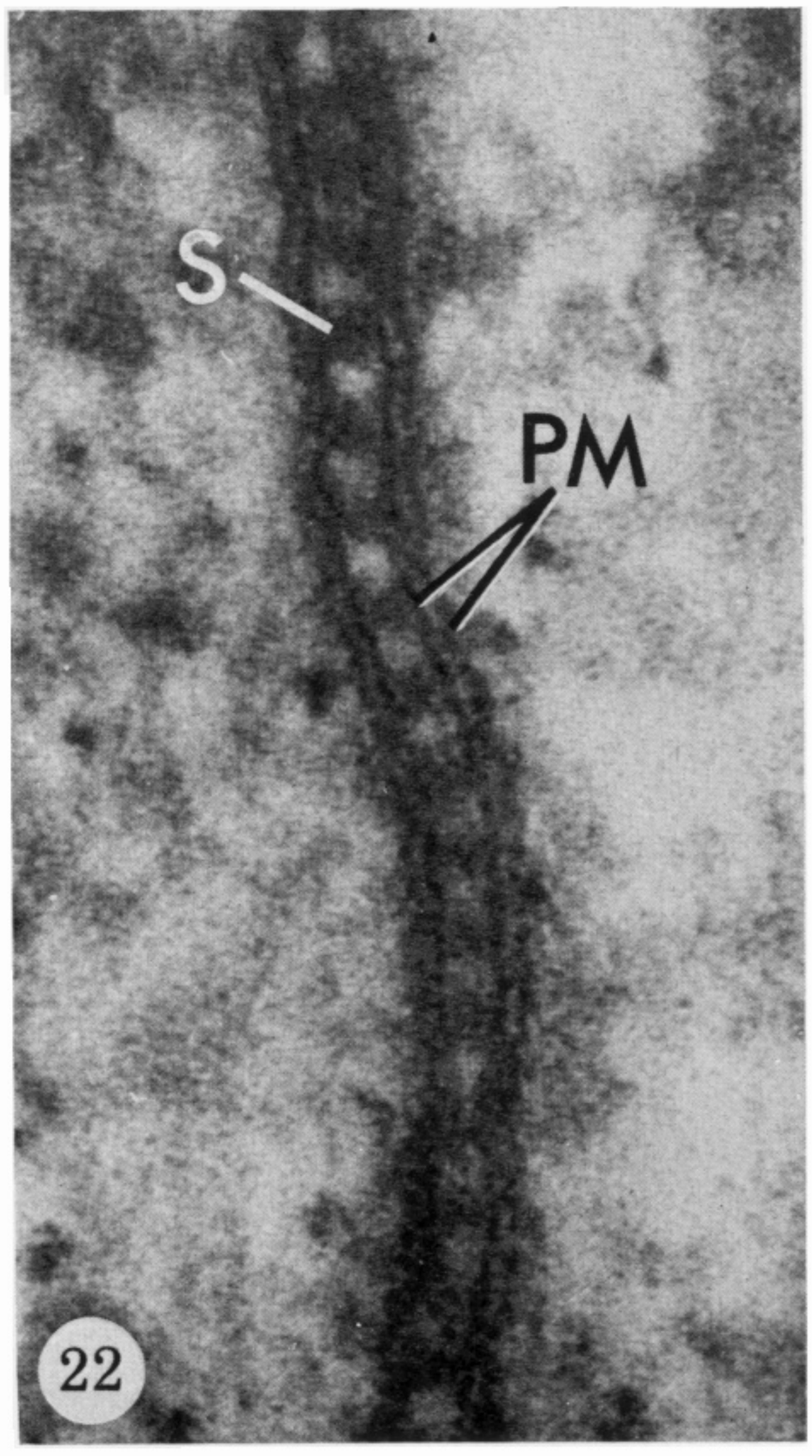

FIGURES 20 to 22. For legends see facing page

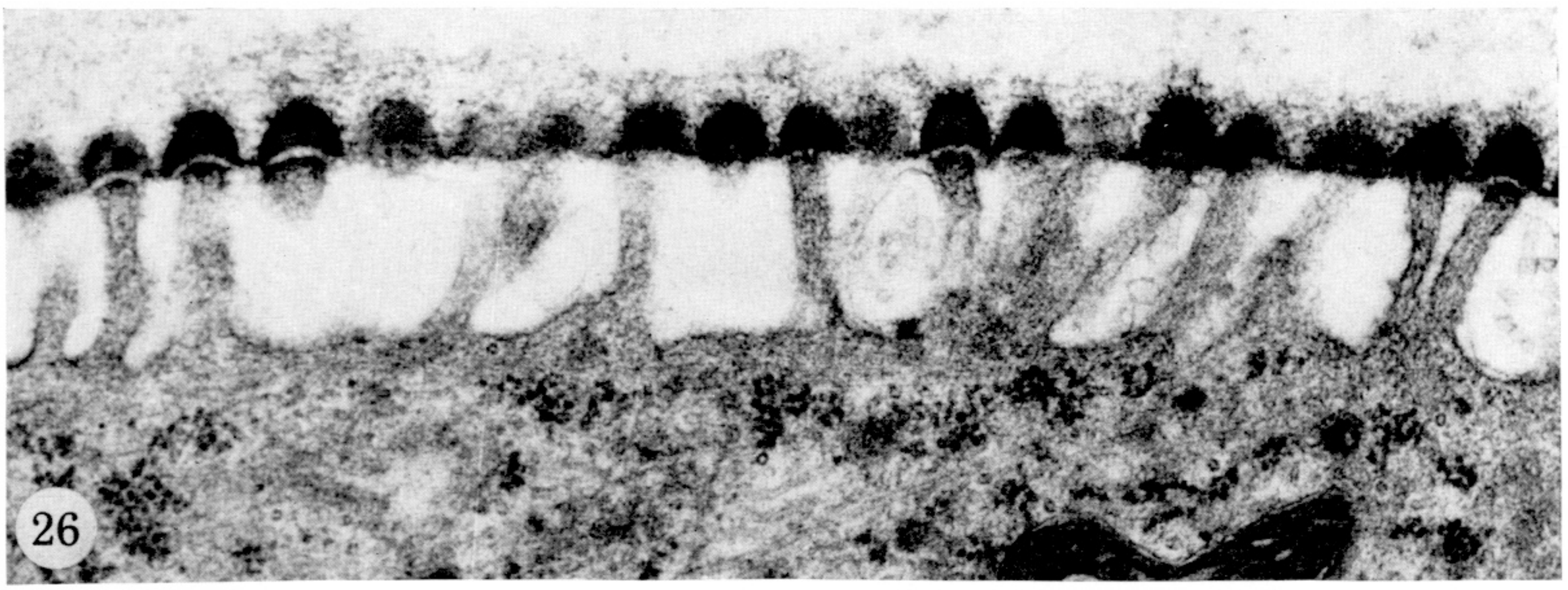

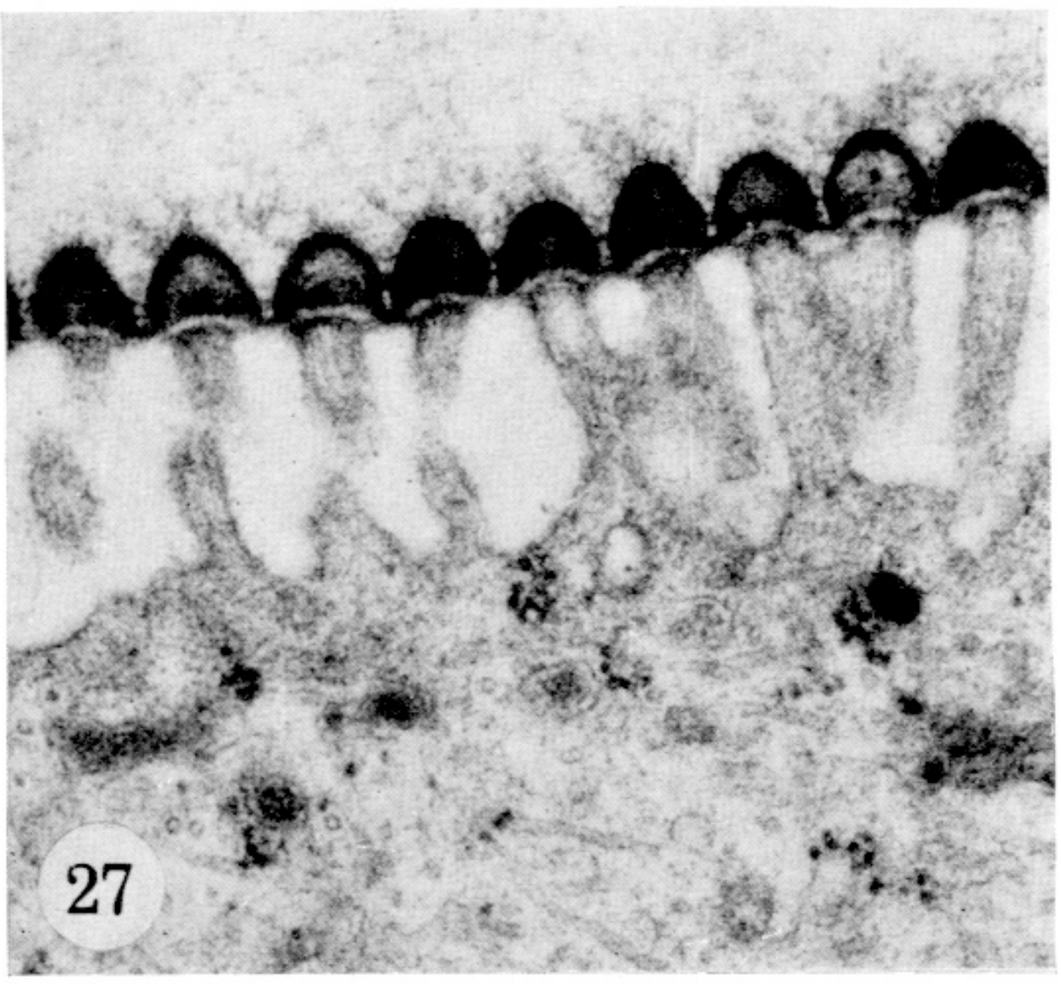

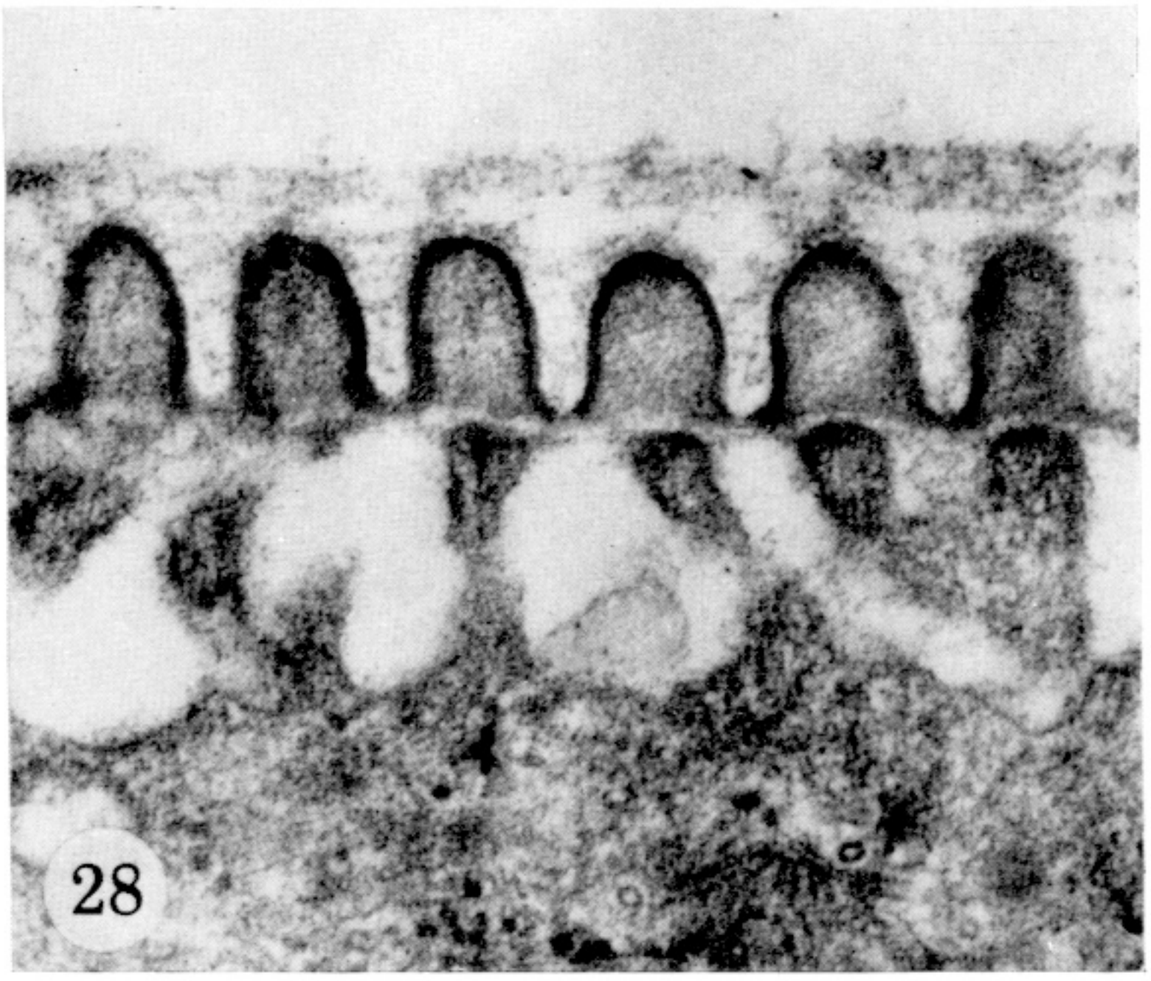

FIGURES 23 to 27. Electron micrographs of perpendicular sections through the eye anlage of *Manduca sexta* pupae, illustrating the typical evaginations of the continuous epicorneal lamina of stage PII ($5\frac{1}{2}$ to 6 days after pupation). The approximately 400 nm long microvilli of the corneagenous cells are 75 to 85 nm thick and their tips spaced 170 to 190 nm apart. The evaginations appear as cupoles, about 150 nm high. Peripheral and central bridges are indicated in the MV/LE cleft. Figures 23 and 27, × 41000; 24, 25, × 68800; 26, × 44700.

FIGURE 28. Electron micrograph of a perpendicular section through the eye anlage of a *Deilephila elpenor* pupa at stage PIII, showing the appearance of the MV/LE complex in its final form before the onset of cornea secretion. The evaginations, whose array forms the completed 'template' of the nipple anlage, are about 200 nm high and their centre-to-centre distance is also about 200 nm. × 57000.

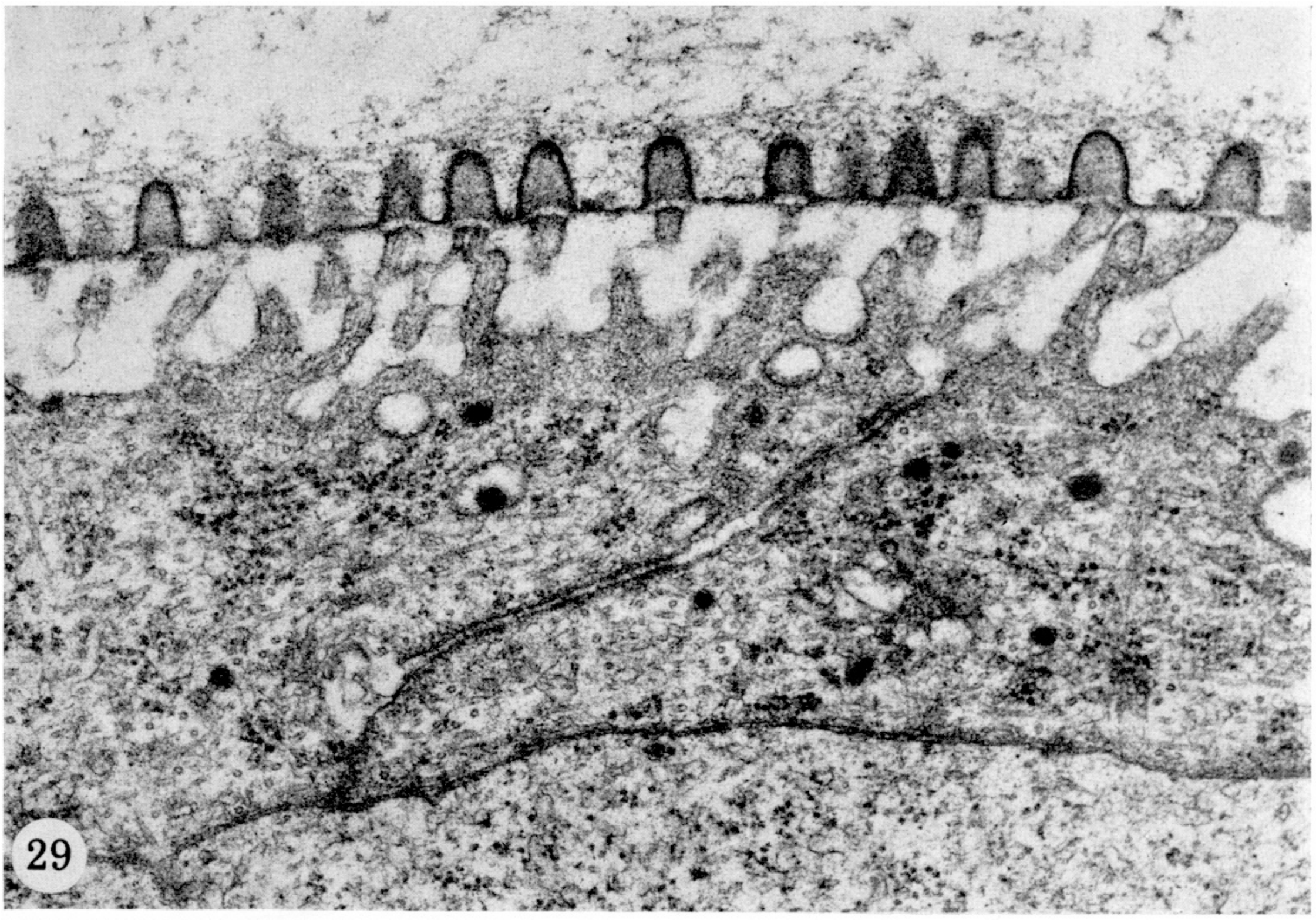

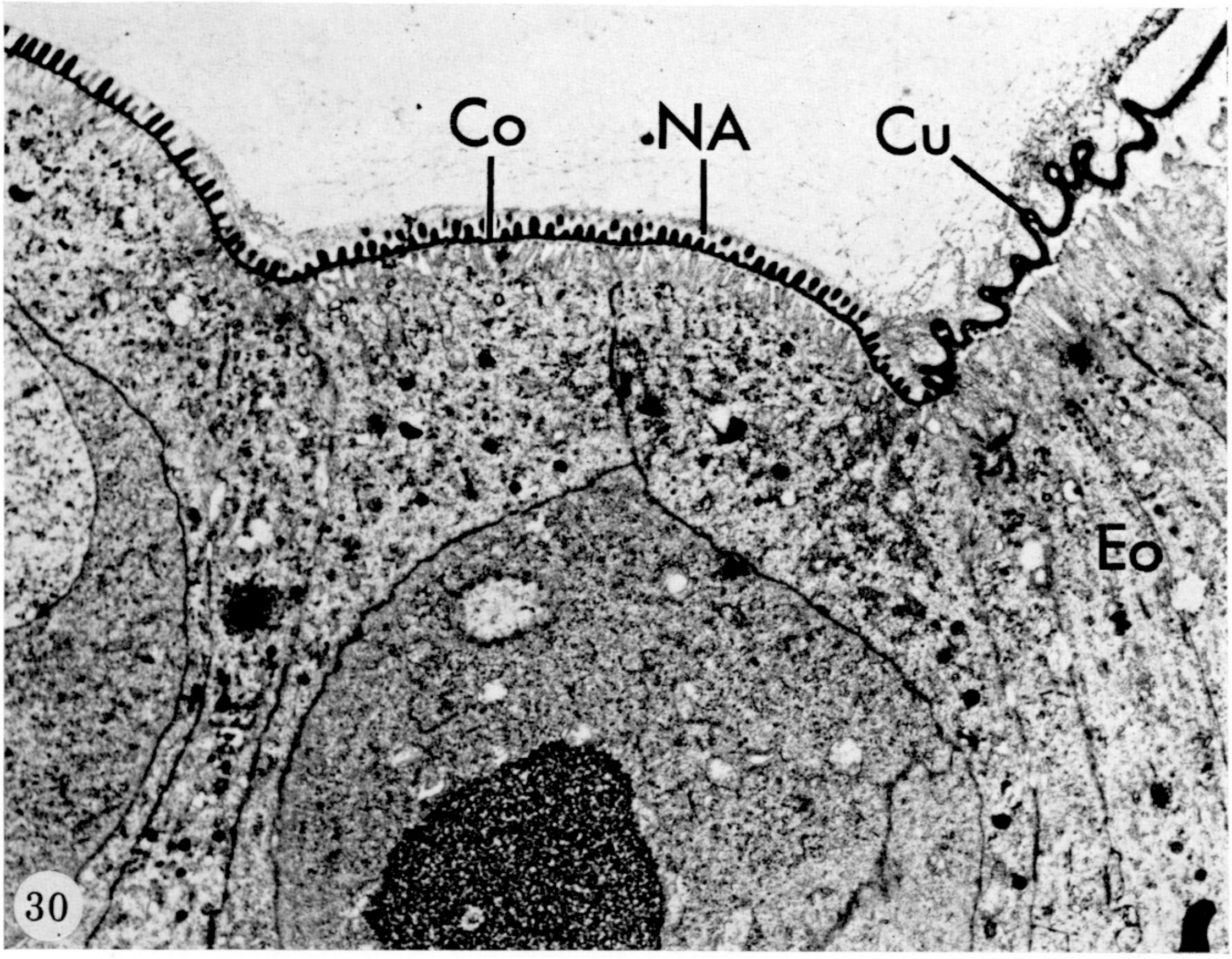

FIGURE 29. Electron micrograph of a perpendicular section through the corneagenous cell surface in the stage PIII eye anlage of a *Manduca* pupa. The epicorneal lamina evaginations of the final nipple anlage are seen as high cupoles with amplitudes and centre-to-centre distances of about 200 nm. 'Coated vesicles' are seen in the corneagenous cell cytoplasm. Both central and peripheral MV/LE bridges are indicated. × 38700.

FIGURE 30. Survey electron micrograph of a section through the zone of transition between the cornea (Co) and the body cuticle (Cu) of the extraocular area (Eo) in the *Manduca sexta* eye anlage at stage PIV. The secretion of the corneal material has started. The final nipple anlage is shown on the distal rim of the corneagenous cells. It is seen to have reached the same stage of development in all facets out to the extraocular area, whereas the degree of differentiation of the ommatidial cell groups is less advanced closest to the transition zone. The picture should be compared with the light micrograph of figure 6*D* at which level the electron microscopic section was made. The outermost layer of the body cuticle (cuticulin and a thin lamina of non-lamellate, 'protein epicuticle') is thrown into folds on top of a fringe of long, regularly spaced microvilli. Although not clearly shown here, such body cuticle folds occurring near the eye anlage generally tend to become progressively more regular in height and width, as well as in interspacing, as the ocular area is approached. This tendency is paralleled by increasing length and regularity of the array of epidermal cell processes (cf. figure 39) until they finally appear as the microvilli shown in this micrograph. × 7900.

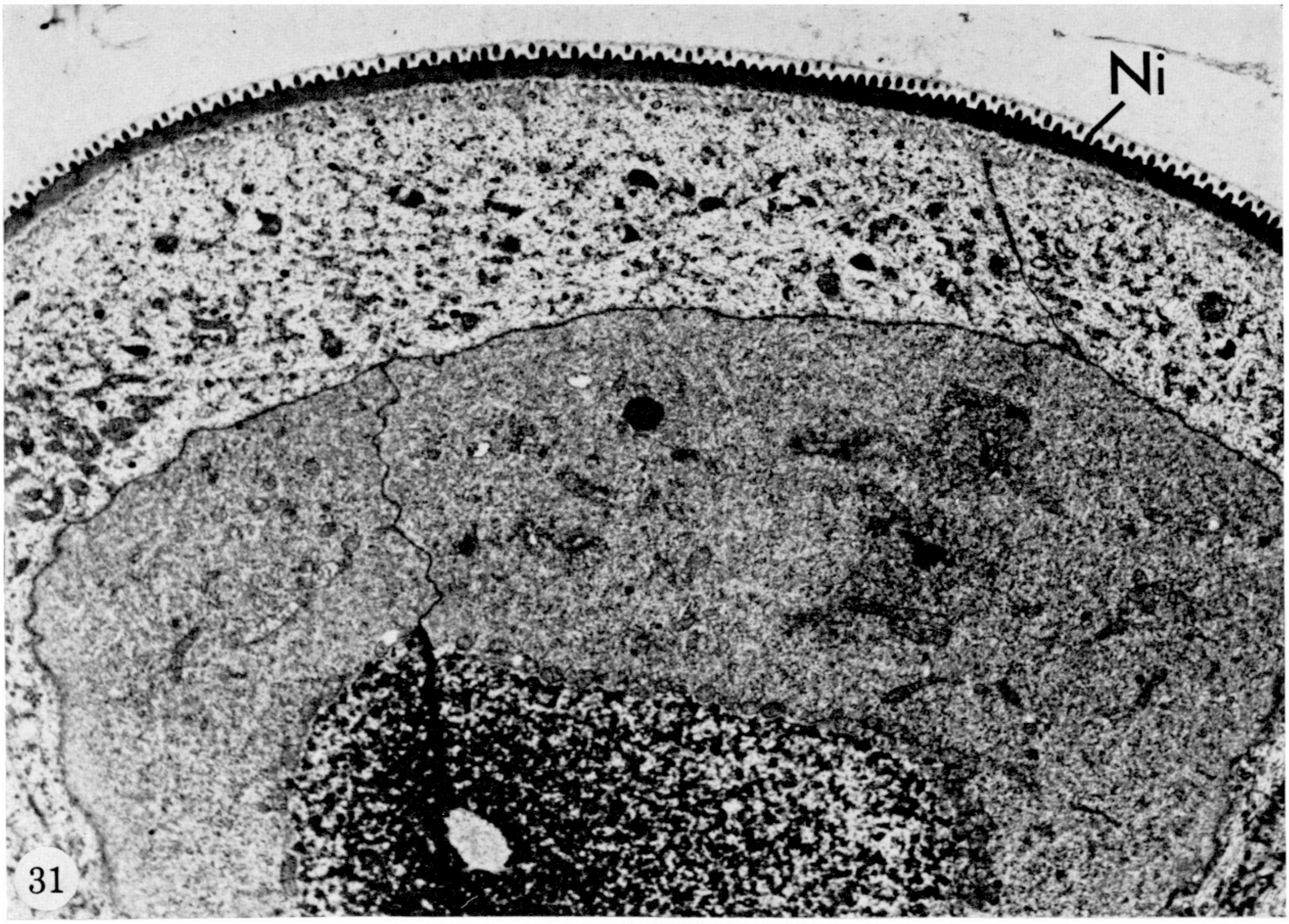

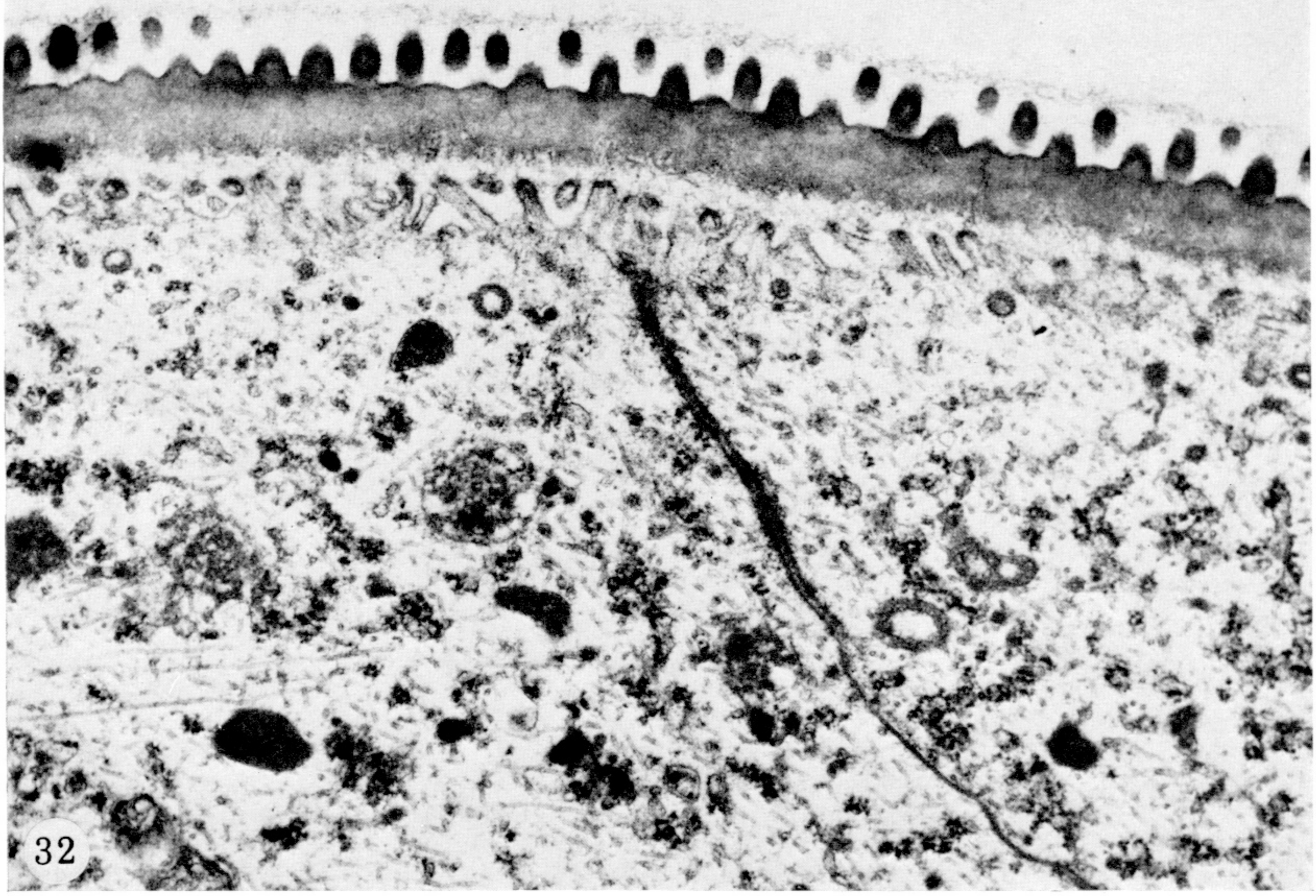

FIGURES 31, 32. Survey electron micrographs of a section through the eye anlage of *Manduca* pupae about $7\frac{1}{2}$ days after pupation. In both pictures, a thin cornea is seen carrying on its surface an array of regularly arranged nipples (Ni) with a tip-to-tip distance of about 200 nm. In figure 32 it can be seen that the regularity in the arrangement of the corneagenous cell microvilli persists also after the completion of the nipple morphogenesis. Figure 31, × 7600; 32, × 28800.

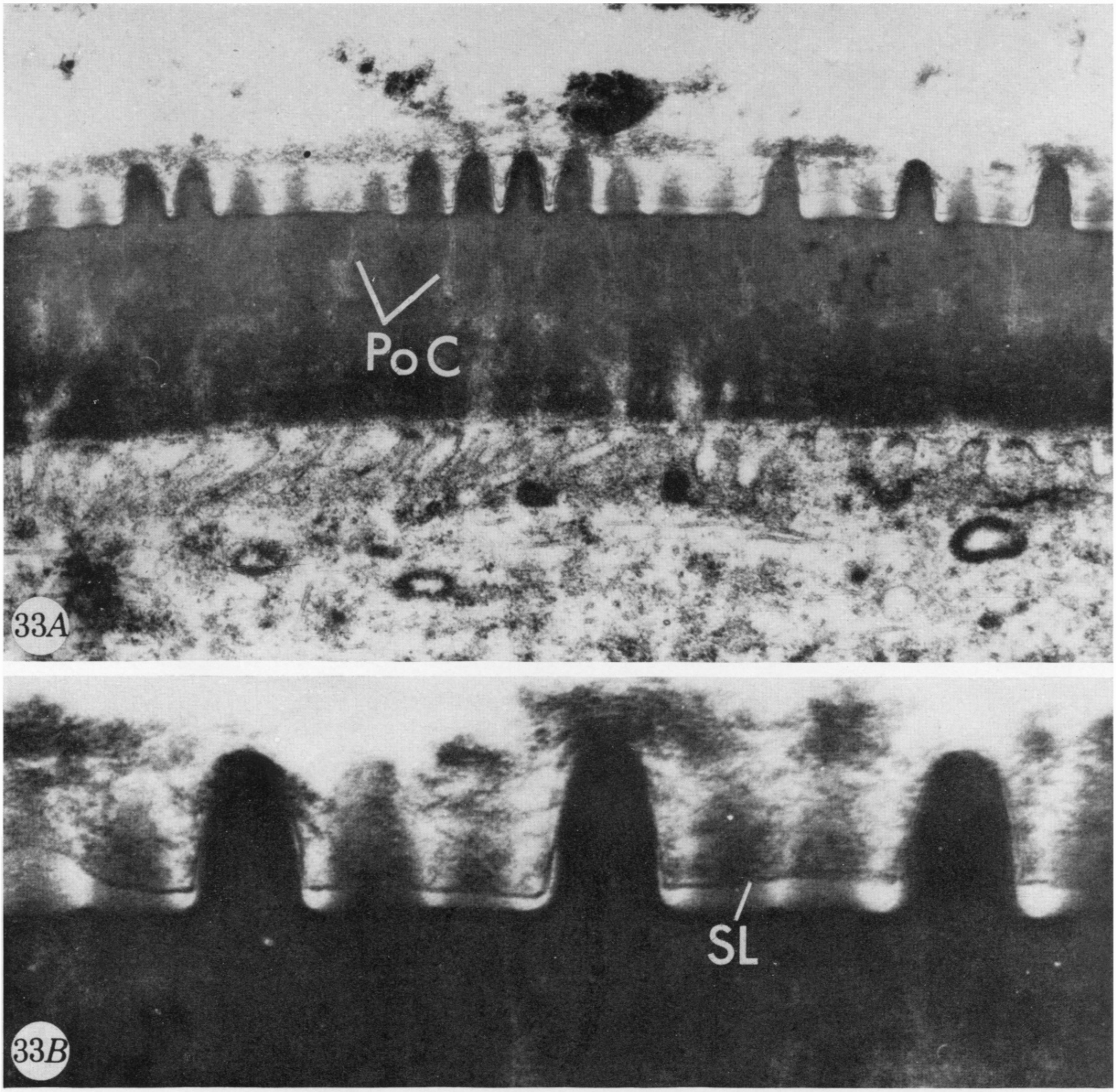

FIGURES 33 and 34. For legends see facing page

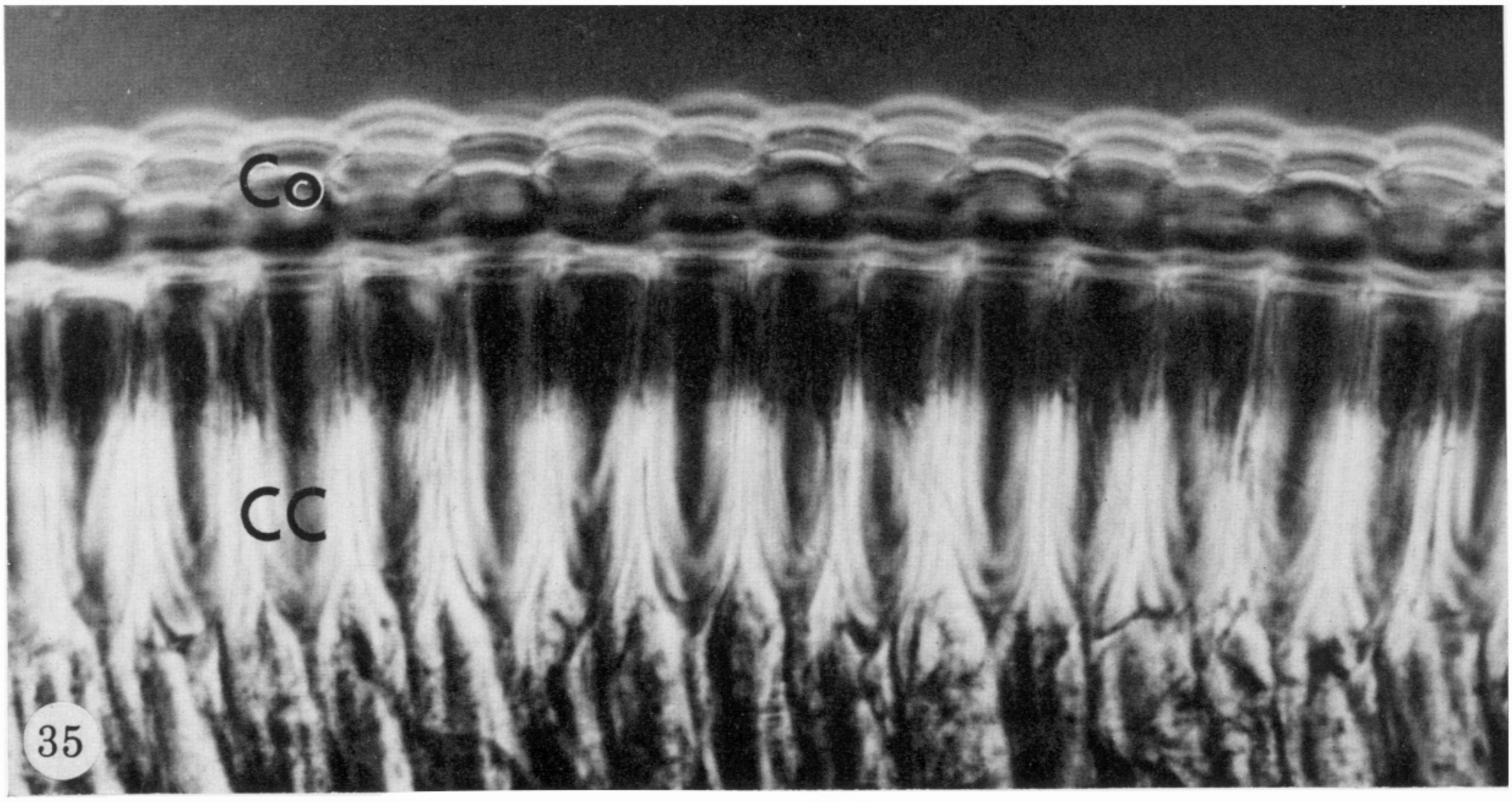

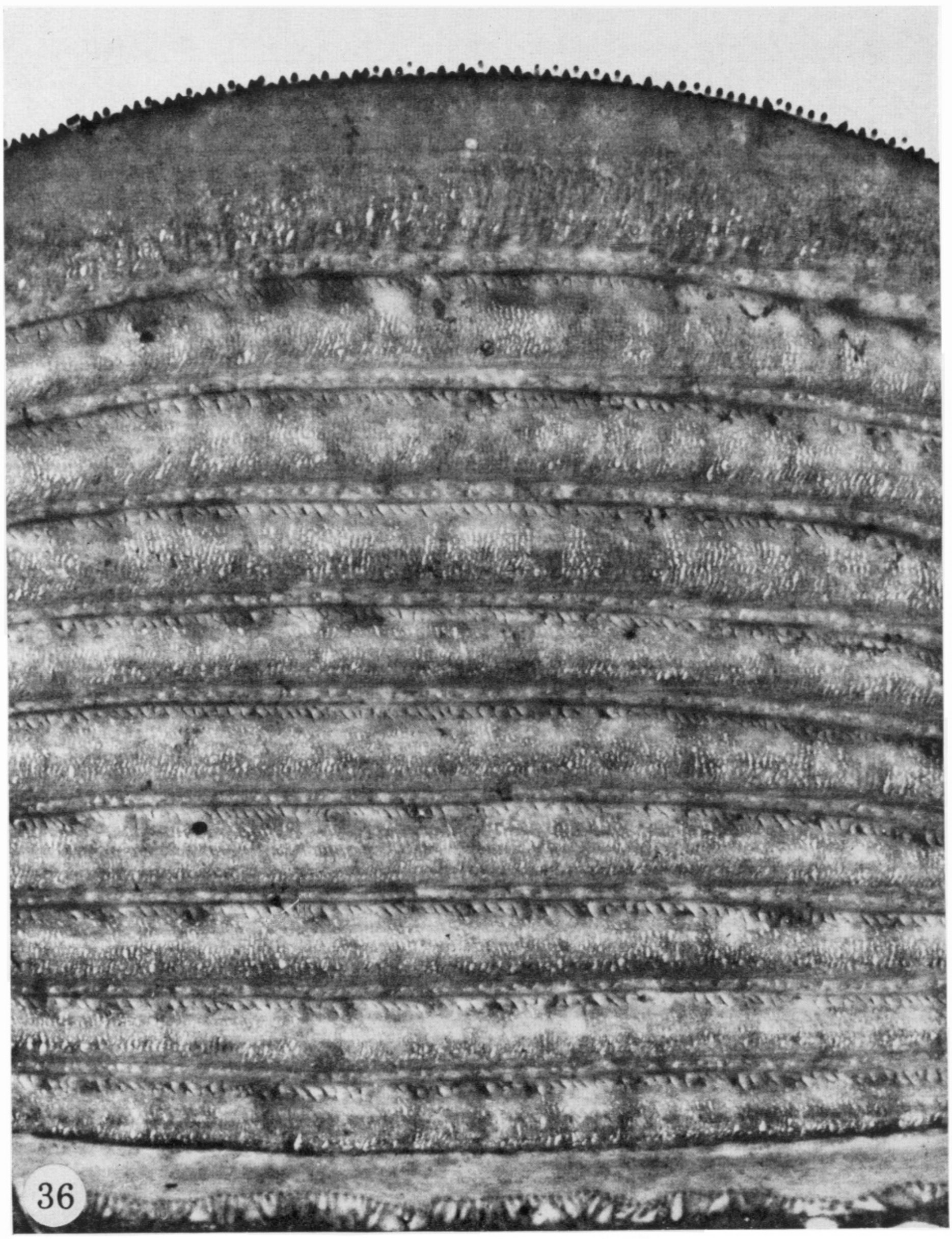

FIGURES 35 and 36. For legends see facing page

37

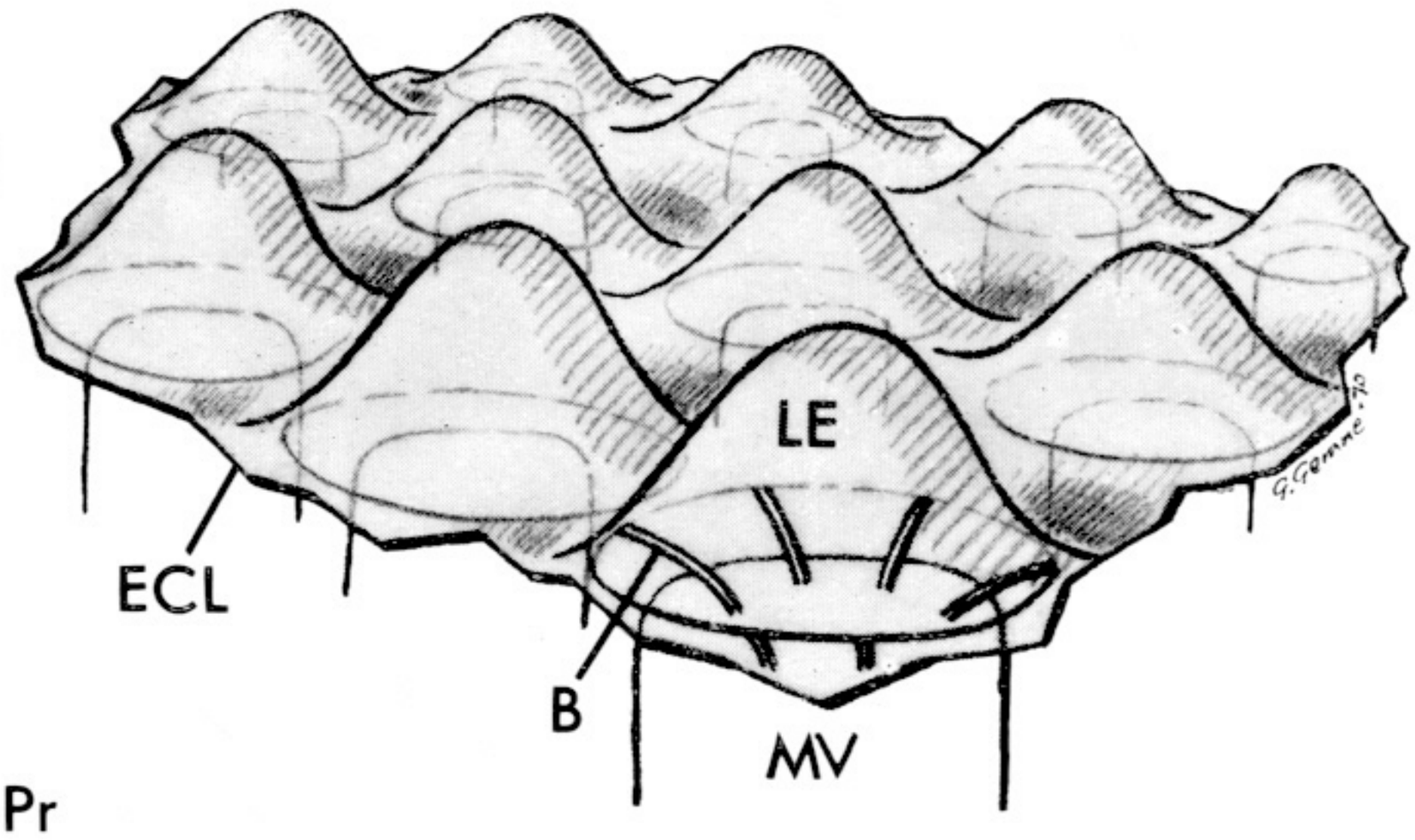

38

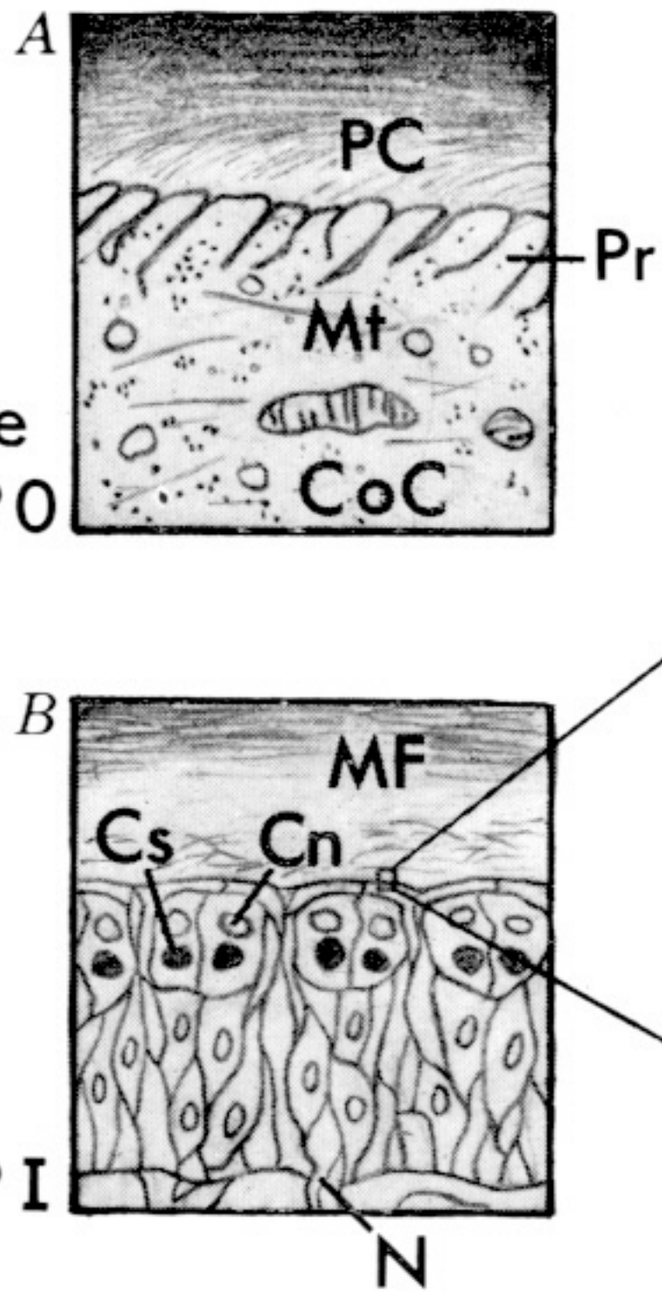

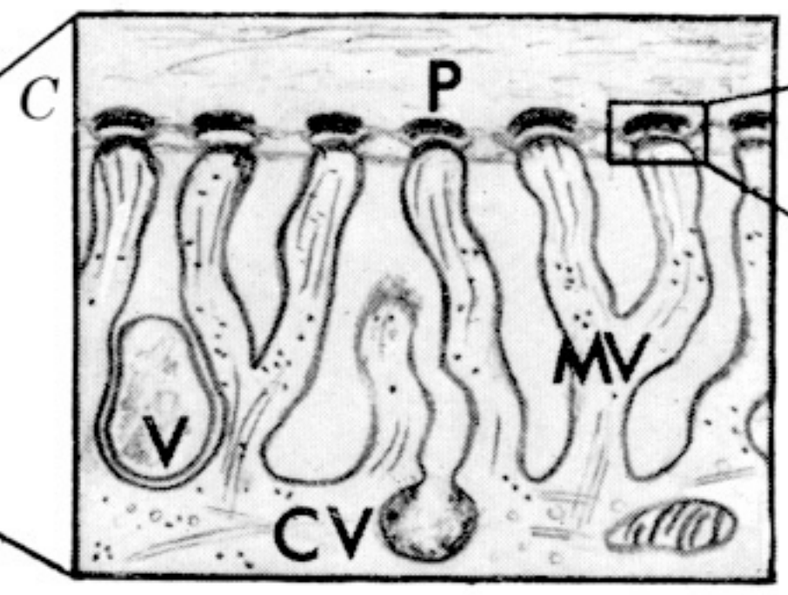

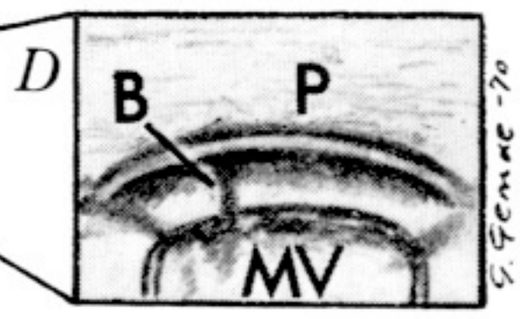

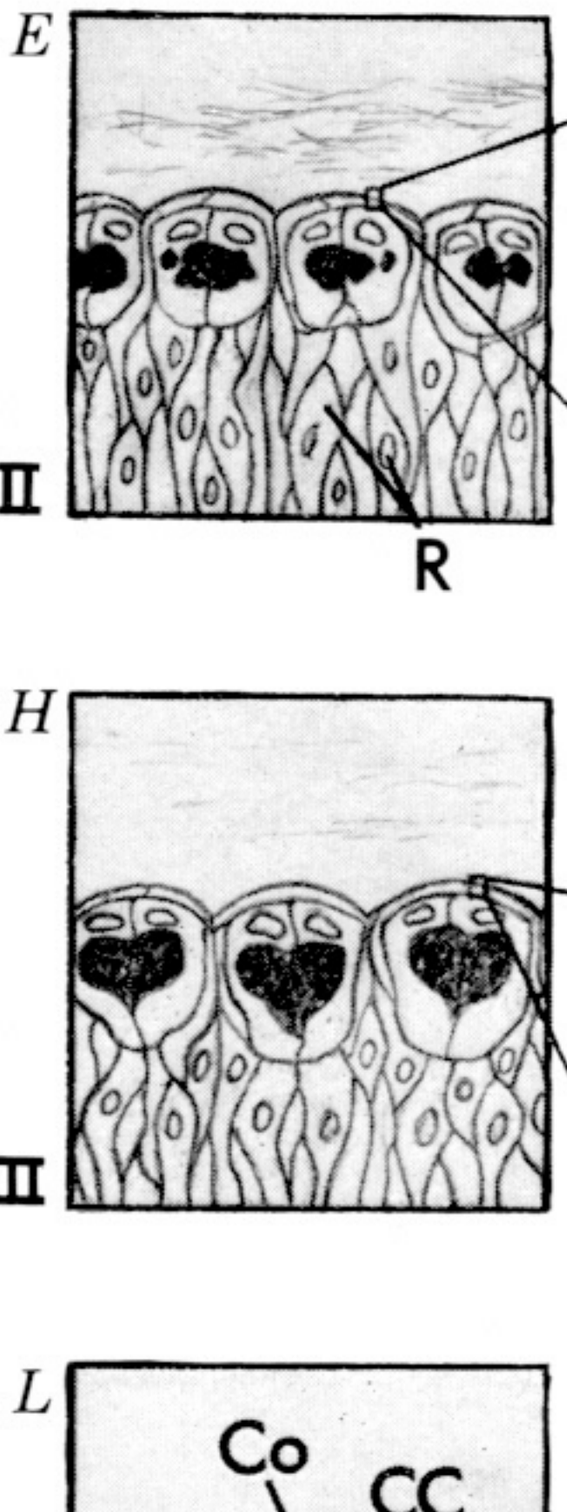

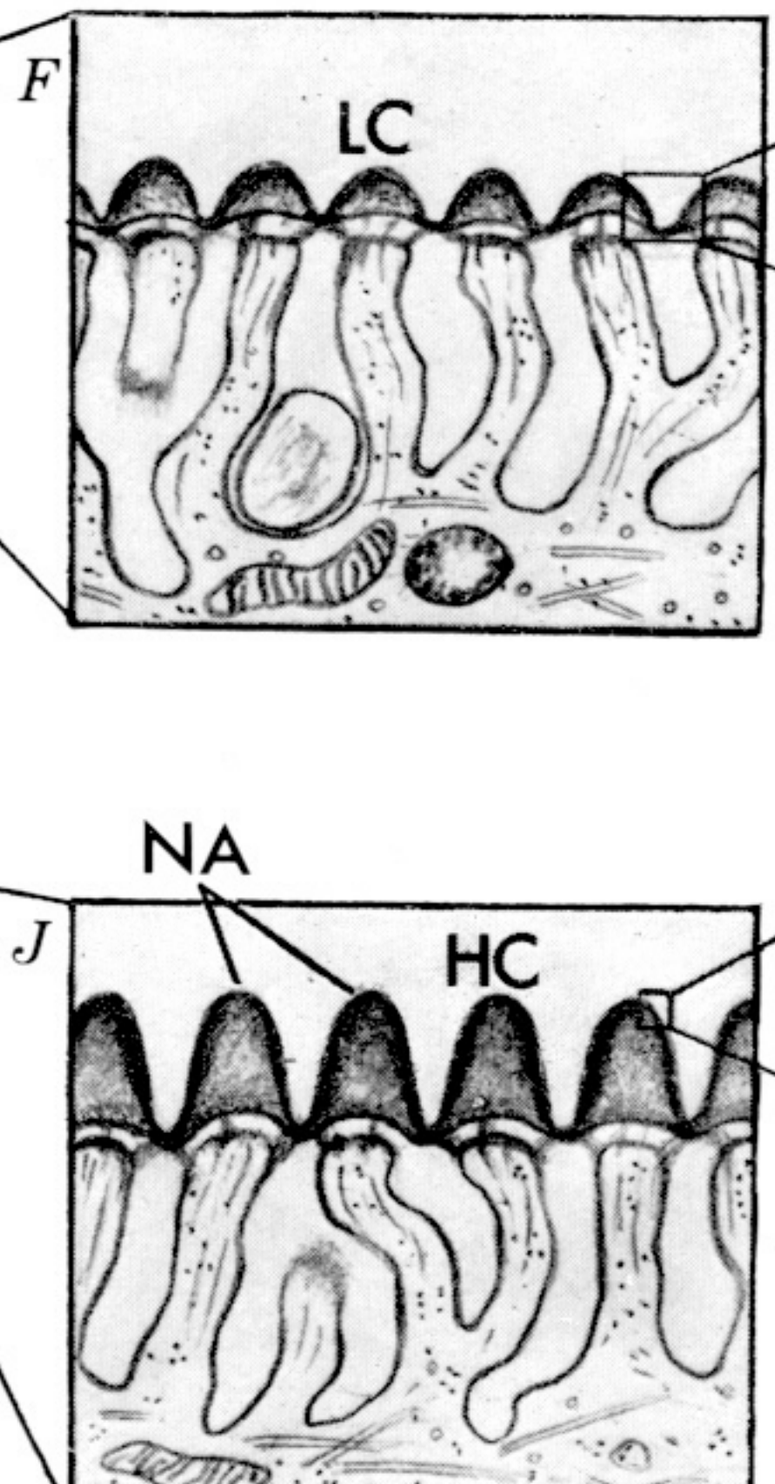

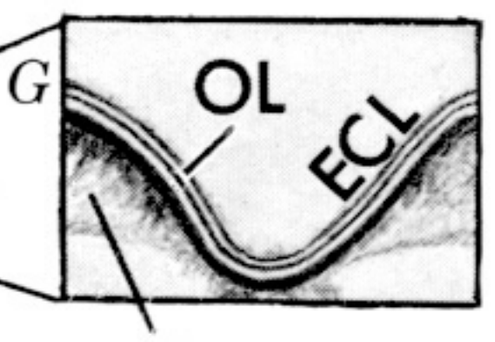

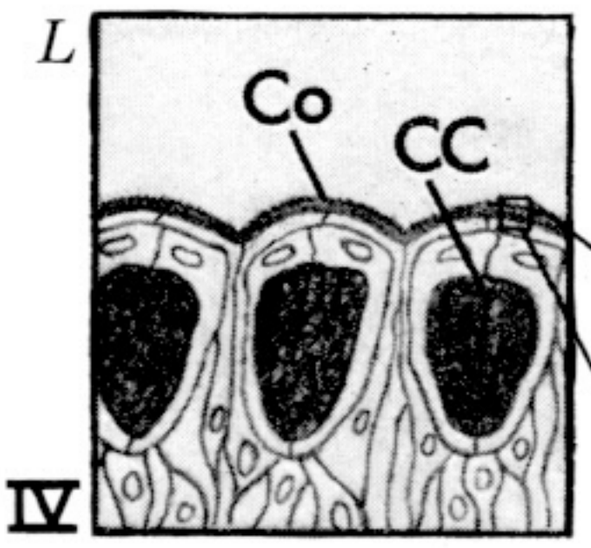

FIGURES 37 and 38. For legends see facing page

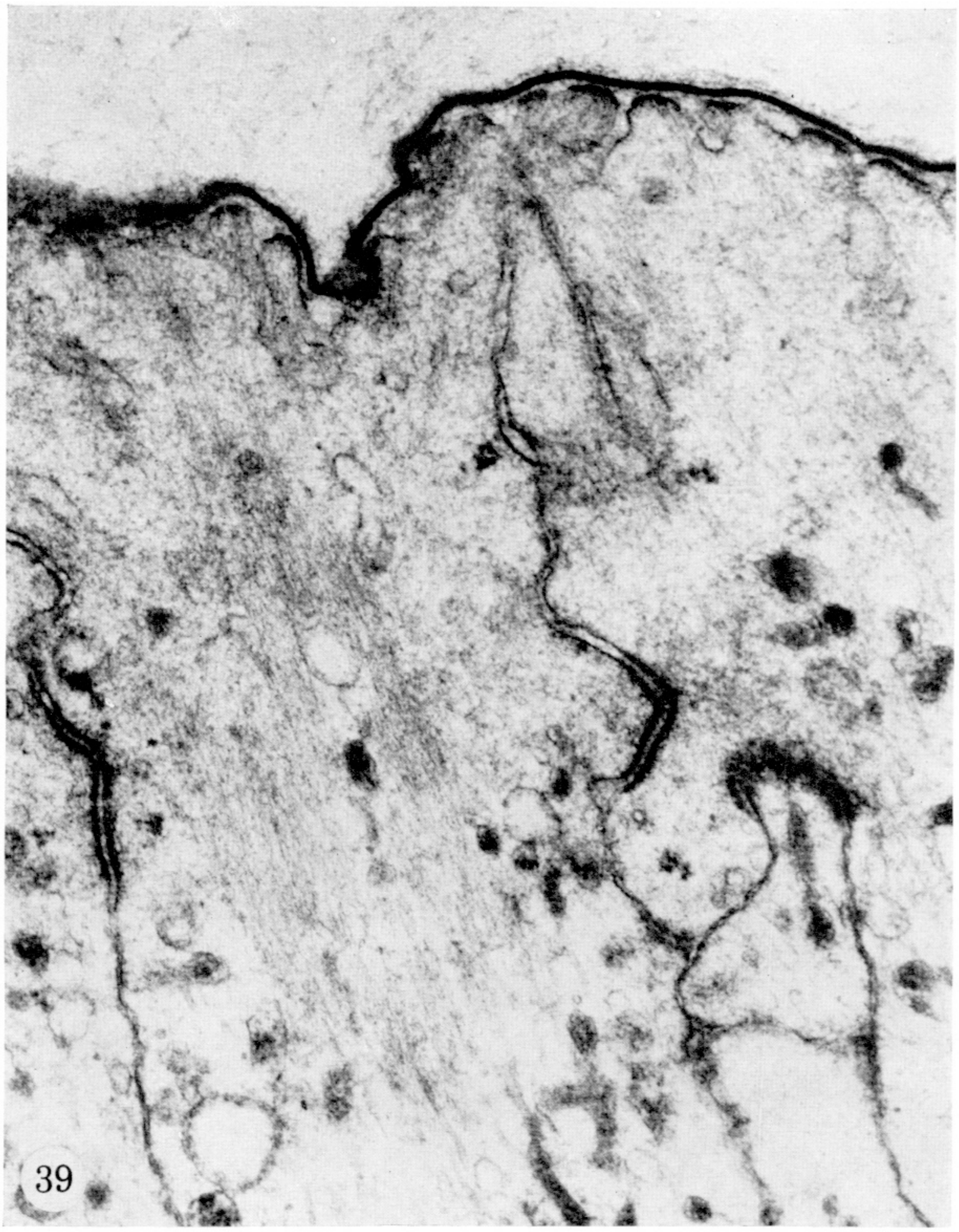

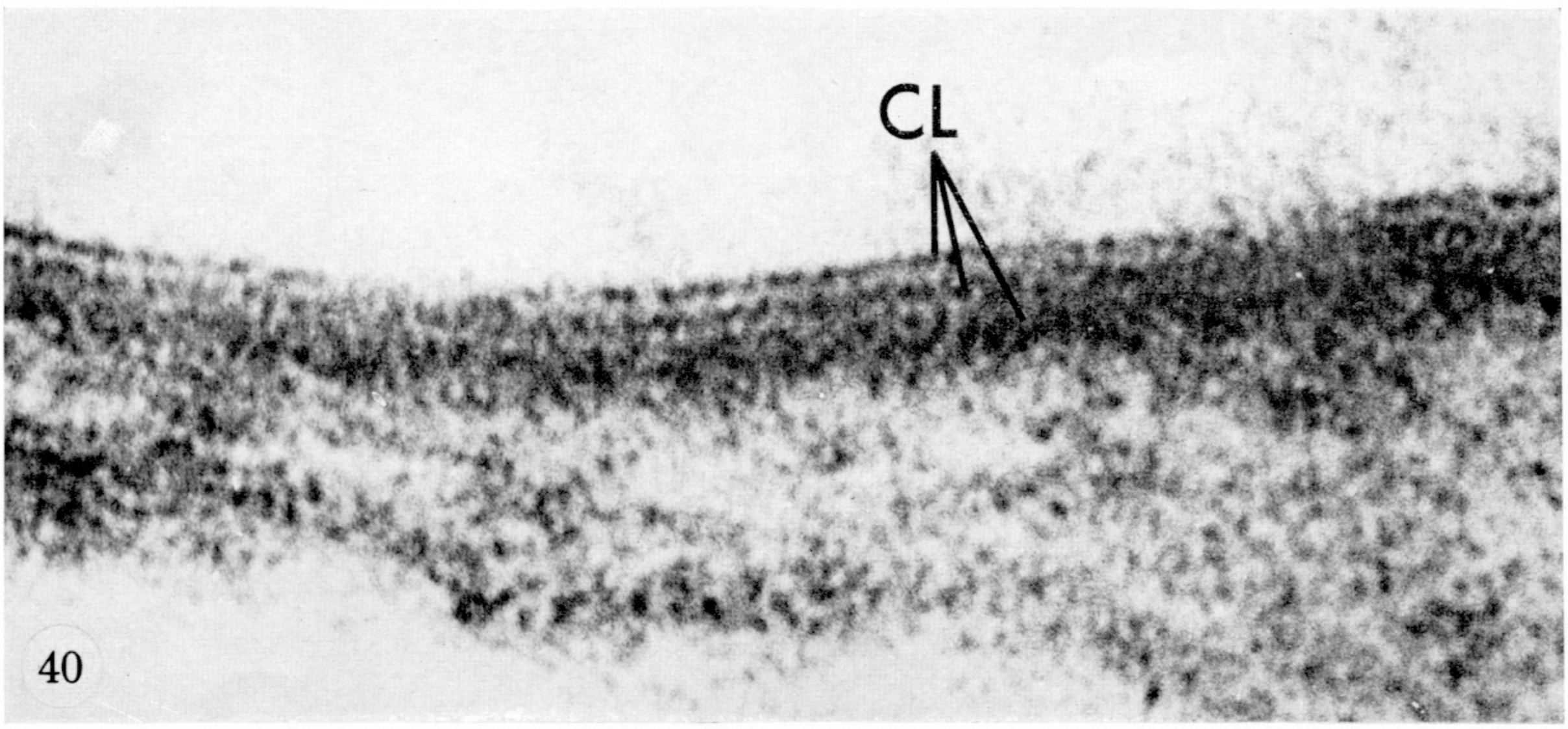

FIGURE 39. Electron micrograph of a perpendicular section through the developing body cuticle about 50 μm from the anterior rim of the eye anlage of a *Manduca sexta* pupa at stage PIII (about 7 days after pupation). The epidermal cells bear short, blunt, irregularly spaced processes. The cuticulin, extending over the tips of the processes, appears continuous in this picture. × 46500.

FIGURE 40. Electron micrograph of a perpendicular section through the cuticulin layer of the body cuticle close to the anterior rim of the eye anlage of the *Manduca* pupa at stage PIII, showing two, possibly three, dense lines, the outer two of which are about 2 nm thick. The two clear spaces are likewise about 2 nm wide. The inner line is ill-defined; its thickness can be estimated to about 10 nm. The total thickness of the extraocular cuticulin at this stage is therefore about 18 nm. × 670000.